

AD-A147 853

THE AFGL (AIR FORCE GEOPHYSICS LABORATORY) ABSOLUTE  
GRAVITY MEASURING SYS. (U) AIR FORCE GEOPHYSICS LAB  
HANSCOM AFB MA R L ILIFF ET AL. 28 OCT 83

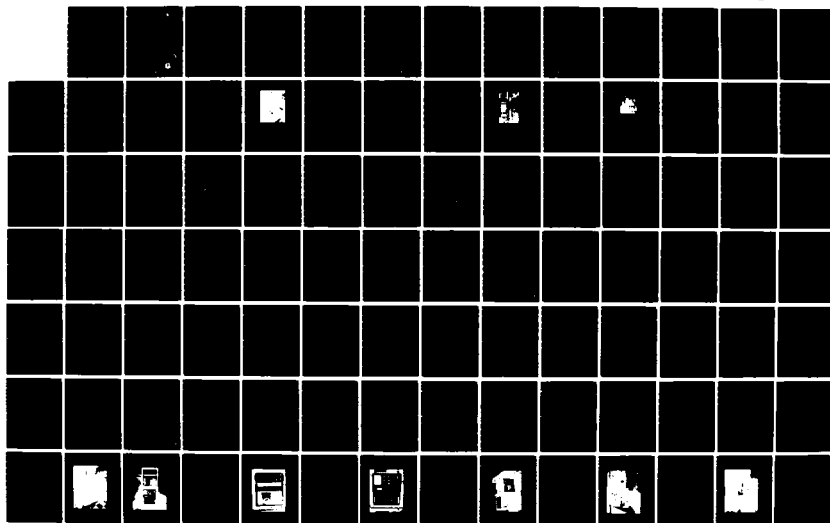
1/2

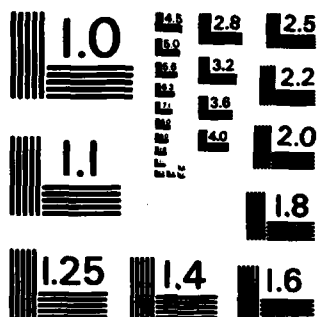
UNCLASSIFIED

AFGL-TR-83-0297

F/G 8/5

NL





MICROCOPY RESOLUTION TEST CHART  
NATIONAL BUREAU OF STANDARDS-1963-A

AFGL-TR-83-0297  
INSTRUMENTATION PAPERS, NO. 321

12



**AD-A147 853**

**The AFGL Absolute Gravity Measuring System  
A Final Report and Operating/Maintenance  
Manual**

**ROBERT L. ILIFF  
ROGER W. SANDS, TSgt, USAF**

**28 October 1983**

Approved for public release; distribution unlimited.

DTIC FILE COPY

**EARTH SCIENCES DIVISION  
AIR FORCE GEOPHYSICS LABORATORY  
HANSCOM AFB, MASSACHUSETTS 01731**

**PROJECT 7600**

DTIC  
ELECTE  
NOV 28 1984  
A

**AIR FORCE SYSTEMS COMMAND, USAF**




**54 11 06 088**

IN-HOUSE REPORTS

This technical report has been reviewed and is approved for publication.

FOR THE COMMANDER

  
THOMAS P. ROONEY  
Chief, Geodesy & Gravity Branch

  
DONALD H. ECKHART  
Director  
Earth Sciences Division

This document has been reviewed by the ESD Public Affairs Office (PA) and is releasable to the National Technical Information Service (NTIS).

Qualified requestors may obtain additional copies from the Defense Technical Information Center. All others should apply to the National Technical Information Service.

If your address has changed, or if you wish to be removed from the mailing list, or if the addressee is no longer employed by your organization, please notify AFGL/DAA, Hanscom AFB, MA 01731. This will assist us in maintaining a current mailing list.

Unclassified

SECURITY CLASSIFICATION OF THIS PAGE (When Data Entered)

REPORT DOCUMENTATION PAGE		READ INSTRUCTIONS BEFORE COMPLETING FORM
1. REPORT NUMBER AFGL-TR-83-0297	2. GOVT ACCESSION NO. AD A147 853	3. RECIPIENT'S CATALOG NUMBER
4. TITLE (and Subtitle) THE AFGL ABSOLUTE GRAVITY MEASURING SYSTEM. A FINAL REPORT AND OPERATING/MAINTENANCE MANUAL		5. TYPE OF REPORT & PERIOD COVERED Scientific. Final
7. AUTHOR(s) Robert L. Iliff Roger W. Sands, TSgt, USAF		6. PERFORMING ORG. REPORT NUMBER IP, No. 321
9. PERFORMING ORGANIZATION NAME AND ADDRESS Air Force Geophysics Laboratory (LWG) Hanscom AFB Massachusetts 01731		8. CONTRACT OR GRANT NUMBER(s)
11. CONTROLLING OFFICE NAME AND ADDRESS Air Force Geophysics Laboratory (LWG) Hanscom AFB Massachusetts 01731		10. PROGRAM ELEMENT, PROJECT, TASK AREA & WORK UNIT NUMBERS 62101F 76000606
14. MONITORING AGENCY NAME & ADDRESS (if different from Controlling Office)		12. REPORT DATE 28 October 1983
		13. NUMBER OF PAGES 161
		15. SECURITY CLASS. (of this report) Unclassified
		15a. DECLASSIFICATION/DOWNGRADING SCHEDULE
16. DISTRIBUTION STATEMENT (of this Report)  Approved for public release; distribution unlimited.		
17. DISTRIBUTION STATEMENT (of the abstract entered in Block 20, if different from Report)		
18. SUPPLEMENTARY NOTES		
19. KEY WORDS (Continue on reverse side if necessary and identify by block number)  Absolute gravity Gravity Interferometer Free-fall		
20. ABSTRACT (Continue on reverse side if necessary and identify by block number)  A multiyear program at the Air Force Geophysics Laboratory (AFGL) has produced an instrument for absolute gravity measurements accurate to eight decimal places. This transportable instrument has been used to measure gravity at a calibration line through the central part of the United States, as well as at Hanscom AFB, Mass., Vandenberg AFB, Calif., Lick Observatory, Calif., and at the National Bureau of Standards at Gaithersburg, Md. Results are:		

DD FORM 1 JAN 73 1473 EDITION OF 1 NOV 65 IS OBSOLETE

Unclassified

SECURITY CLASSIFICATION OF THIS PAGE (When Data Entered)

Unclassified

SECURITY CLASSIFICATION OF THIS PAGE(When Data Entered)

20. Abstract (Contd)

Hanscom AFB, Mass.	980378.685 ± 0.010 mgal
NBS, Gaithersburg, Md.	980103.257 ± 0.009 mgal
McDonald Observatory, Tex.	978828.655 ± 0.008 mgal
Holloman AFB, N. Mex. (CIGTF)	979139.600 ± 0.008 mgal
Trinidad, Colo.	979330.370 ± 0.010 mgal
Denver, Colo.	979598.277 ± 0.010 mgal
Mt. Evans, Colo.	979256.059 ± 0.008 mgal
Boulder, Colo. (JILA site)	979608.601 ± 0.010 mgal
Casper, Wyo.	979947.244 ± 0.025 mgal
Sheridan, Wyo.	980208.964 ± 0.010 mgal
Great Falls, Mont.	980497.367 ± 0.320 mgal
Vandenberg AFB, Calif.	979628.190 ± 0.017 mgal
Lick Observatory, Calif.	979635.503 ± 0.010 mgal
BIPM, Sevres, France	980926.617 ± 0.010 mgal

The final version of the equipment is described. Data processing procedures, corrections applied, and the determination of these corrections are given. The report also gives operation and maintenance procedures for the apparatus. Also included in the report is a history of the development of the absolute-gravity measuring apparatus, including development of the first prototype instrument, experiments with an apparatus incorporating a falling chamber-within-a-chamber, the ideas behind this approach, and the shortcomings that caused a return to the single-chamber approach.

Unclassified

SECURITY CLASSIFICATION OF THIS PAGE(When Data Entered)

## Preface

The authors thank the following persons in support of this report: Walter G. Spita of the Geodetic Survey Squadron, DMAHTC, F. E. Warren AFB, Wyo., for his dedicated support and reconnaissance in field-site selection, gravity gradient measurements, and invaluable knowledge in the field of geodetic surveying. His efforts greatly enhanced the success of the field measurements; and Jeanne M. McPhetres of the Earth Sciences Division, AFGL, for her dedicated efforts, superior secretarial skills, and proficient knowledge of scientific terminology in the fields of geodesy and gravity for preparation of this report.



Accession For	
NTIS GRA&I	<input checked="checked" type="checkbox"/>
ERIC TAB	<input type="checkbox"/>
Unannounced	<input type="checkbox"/>
Justification	
By	
Distribution/	
Availability Codes	
Dist	Avail and/or Special
A1	

## Contents

1. INTRODUCTION	9
1.1 Definitions	10
1.2 Units	10
1.3 Gravity Variations	10
2. MEASUREMENT METHODS STUDIED	11
3. THEORY OF MEASUREMENT	13
4. PROTOTYPE OF SELECTED SYSTEM	16
5. FIELD MEASUREMENTS	25
5.1 Station Descriptions	26
5.2 Gravity Values	41
6. DESCRIPTION OF ORIGINAL EQUIPMENT	44
7. CHAMBER-WITHIN-A-CHAMBER	48
REFERENCES	51
BIBLIOGRAPHY	53
APPENDIX A: COMPUTER PROGRAM	57
APPENDIX B: SET-UP PROCEDURE	75
APPENDIX C: MAINTENANCE PROCEDURES	153
APPENDIX D: COMMERCIAL EQUIPMENT	157
APPENDIX E: TYPICAL SHIPPING LIST	159



## Illustrations

1. Air Force Geophysics Laboratory Absolute Gravity Measurement System	17
2. Gravity Correction as a Function of Pressure	19
3. Gravity Correction as a Function of Laser Wavelength Change in Time	20
4. Original Gravity Measuring System	21
5. Absolute Gravity Measuring Instrument With the Isolating Seismometer, Super Spring, Installed	23
6. Gravity Residuals (Angstroms) vs Distance After Drop (cm)	24
7. Gravity Residuals (Angstroms) vs Distance After Drop (cm)	24
8. Sites of Absolute Gravity Measurements	27
9. Gravity Station Description: Boston A	28
10. Gravity Station Description: Washington AA	29
11. Gravity Station Description: Vandenberg AA	30
12. Gravity Station Description: Lick Observatory	31
13. Gravity Station Description: Boulder D	32
14. Gravity Station Description: Great Falls AA	33
15. Gravity Station Description: Sheridan AA	34
16. Gravity Station Description: Casper AA	35
17. Gravity Station Description: Mt. Evans AA	36
18. Gravity Station Description: Denver H	37
19. Gravity Station Description: Trinidad AA	38
20. Gravity Station Description: Holloman A	39
21. Gravity Station Description: McDonald AA	40
22. Laser Interferometer Absolute Gravity Instrument	49
B1. Overview of Absolute-gravity Measurement Equipment	87
B2. Overview of Electronics Racks Nos. 1 and 2	89
B3. Electronics Rack No. 1	91
B4. Electronics Rack No. 2	93
B5. Electronics Rack No. 3 Plus Peripherals	95
B6. View of Chamber With Vacuum Sleeve Removed	97
B7. Close-up View of Dropped Object and Robot	99
B8. Guides and Catching Mechanism	101
B9. Lower Structure	103
B10. Top View of Inner Hat	105
B11. View of Dropped Object in Uppermost Position	107
B12. View of Robot in Uppermost Position	109

## Illustrations

B13. View of Robot and Dropped Object Package in Near Seated Position	111
B14. View of Robot	113
B15. Optics Box	115
B16. Optics Box With Reference Reflector Removed	117
B17. Interior View of Optics Box	119
B18. Interior View of Optics Box	121
B19. Moveable Turning Mirror	123
B20. Robot Controls	125
B21. Ion Pump	127
B22. Ion Pump External Evacuation Port and Shutoff Valve	129
B23. Vacuum Gauges and Roughing Pump Connector Valve	131
B24. External Alignment Laser	133
B25. Optics-box Leveling Screw	135
B26. Reference Reflector in Mounting	137
B27. Alignment Microscope	139
B28. Vacuum Chamber Top Hat	141
B29. View of Vacuum Chamber Top Hat With Solenoid Removed	143
B30. Bottom View of Top Hat	145
B31. View of Vacuum Chamber Optical Entrance/Exit Window	146
B32. Mercury Pool	147
B33. Simplified Diagram of the Light Path for Verticality	148
B34. Simplified Diagram of Beam Position and Angle Adjusting Optics	148
B35. Simplified Diagram of Verticality and Beam Positioning	149
B36. Diagram of Vacuum Chamber Window Tilt (Exaggerated)	149
B37. Center-of-mass Optical Center Alignment Set-up	151

## Tables

1. Summary of AFGL Absolute Gravity Measurements	41
2. Published Values of Absolute Gravity Measurements at Collocated Sites (11), (12), and (13)	43

# **The AFGL Absolute Gravity Measuring System A Final Report and Operating/Maintenance Manual**

## **1. INTRODUCTION**

Gravity, as defined by Webster, is the "... force that tends to draw all bodies in the earth's sphere toward the center of the earth...". There is, in actuality, a mutual attraction for all bodies to be drawn to the center of their respective masses – but in practice, the amount the earth moves toward another body is so negligible it is considered nonexistent.

Interest in gravity comes from three general disciplines: (1) the use of the acceleration of gravity as a standard force in the laboratory; (2) knowledge of the gravity field and its local variations; and (3) attempts to discover geophysical or cosmological laws. As stated by A. V. Astin, former director of the National Bureau of Standards:<sup>1</sup>

"The determination of the absolute value of the acceleration due to gravity ... provides a base which, together with the standard of mass, establishes the derived standard of force. The standard of force, in turn, is a necessary quantity in the assignment of values to the electrical units of current and voltage. The acceleration due

---

(Received for publication 27 October 1983)

1. Astin, A. V. (1968) Acceleration due to gravity at the National Bureau of Standards, J. Res. Natl. Bur. Std. 72C (foreword to NBS Monograph 107 by D. R. Tate).

to gravity is also an important factor in the accurate pressure determinations needed for the thermodynamic temperature scale and the establishment of the International Practical Temperature Scale.

An absolute measurement of the acceleration due to gravity is of particular interest to the science of geodesy. Rapid advances have recently been made toward the completion of a world gravity network which will establish reliable gravity values at a large number of base points located strategically over the earth."

Although, generally, the science of geodesy requires differences in gravity from site-to-site (relative gravity), it is also important to have many sites with absolute gravity determinations to serve as calibration points for the relative instruments.

### 1.1 Definitions

This paper utilizes the following definitions:

**Absolute Gravity** – The magnitude of the local acceleration of gravity at a particular location;

**Relative Gravity** – The difference in the value of the gravitational acceleration from one location to another; and

**Tidal Gravity** – The variation in gravity due to the effects of the changing positions of the sun and the moon.

### 1.2 Units

The most common unit of measurement is the milligal (mgal)

$$1 \text{ mgal} = 10^{-3} \text{ gal} = 10^{-3} \text{ cm/sec}^2$$

$$g, \text{ then, is about } 10^6 \text{ mgal } (10^3 \text{ cm/sec}^2) \text{ .}$$

With the precision now being reached, the microgal is coming more into common usage.

### 1.3 Gravity Variations

Variations in gravity also need to be considered:

<u>Variation in g</u>	<u>Causes</u>	<u>Magnitude</u>
Elevation	Free air and Bouguer gradients	0.3 mgal to 0.2 mgal/m
Latitude	Earth-flattening and centrifugal acceleration	approx. 85 mgal/degree
Time	Gravity tides, earth tides, weather, and other phenomena	up to 0.2 mgal
Location	Local geology	varies

[Local geology such as mountainous regions and subterranean anomalies can be severe enough to cause deflection of the vertical – a subject in its own right.]

## 2. MEASUREMENT METHODS STUDIED

Approaches to improving the design of instrumentation for the measurement of absolute gravity have included both classical and new methods.

Several methods for measuring absolute gravity that have been carried out and pushed to their practical limits include: (1) the pendulum of various configurations, (2) the charged particle experiment in which a particle is repelled upward by a measured force equal to the downward force of gravity, and (3) the free-fall method in various forms. The pendulum and free-fall methods are well-known and numerous papers written on them are readily available, while reports on the investigations and experimentation with the charged particle gravimeter (as it is called by one author) is rather limited.<sup>2,3</sup> This approach showed promise and was pursued in the 1960s.

During the analysis of the approach to be taken for the development of an absolute-gravity measuring device, it was concluded that the charged particle approach was not worthy of pursuit because of cost, requirements for the advancement of technology, and the determination that a simpler, more direct approach could satisfy the present and foreseeable future requirements.

With the development of the reversible pendulum came the advantage of a definite length measurement as well as the ability to take advantage of long timing periods for averaging timing errors. Ideally, the reversible pendulum could

2. Cunningham, R.A., and Stalder, J.J. (1965) Charged Particle Gradiometer Research, Final Report, AD No. 614681, Martin Marietta Aerospace, Orlando, Fla.
3. Inderwiesen, F.H. (1971) Charged Particle Gravity Meter Research, Final Report, AD No. 783313, Martin Marietta Aerospace, Orlando, Fla.

produce high precision but, in practice, the action and wear of the supporting points (knife edges, for example) and the flexure of the pendulum presented complications that limited their precision and accuracy to about 1 mgal. A more complete discussion of the history of precise gravity measurements with these methods can be found elsewhere.<sup>4-6</sup>

The advances in electronic technology started in the 1940s made measurements of short time-intervals practical. This new technology made the free-fall gravity measurement approach practical since short time-interval determination had been one of the limiting factors for measuring absolute gravity by this method. A variety of different methods for free-fall measurements have been made. The two most general are (1) symmetrical free motion and (2) direct free-fall. In the symmetrical free motion the object is catapulted upward and its travel is timed while it rises and falls and the value of gravity is computed from both directions of travel. Direct free-fall involves dropping an object and measuring the time required to fall given distances and then calculating its acceleration during its fall.

Obviously missing from the discussion so far is the other important quantity-length. In most previous measurements, the object was timed as it crossed marks of known separation. The marks varied from inscribed lines to passing through (thus interrupting) a light beam directed to a photodiode or other optical sensor. Another method was to photograph the trajectory using a strobe light flashing at known intervals as it passed distance marks. These length measurements were adequate as long as accuracy was limited by the timing uncertainties. With the increased timing accuracy a more precise method for the measurement of length was needed to be incorporated into the measurement scheme. The standard of length is based on the wavelength of light and was, therefore, chosen.

Although white light fringes were formed in a two-beam interferometer by Faller<sup>7</sup> to make the first practical application of direct interferometry in an absolute measurement of gravity, interferometric measurement of the distance fallen by an object became practical with the advent of the continuous wave laser in the early 1960s. The coherence and directivity (thus brightness) achieved with the HeNe laser made possible the construction of an interferometer in which one

4. Faller, J. E. (1967) The precision measurement of the acceleration of gravity, Science 158:60.
5. Cook, A. H. (1965) The absolute determination of the acceleration due to gravity, Metrologia 1(No. 3):84-114.
6. Lenzen, V. F., and Multhaupt, R. P. (1965) Development of gravity pendulums in the 19th century, U.S. Natl. Museum Bull. 240, paper 44.
7. Faller, J. E. (1963) An Absolute Interferometric Determination of the Acceleration of Gravity, Ph. D. Thesis, Princeton University, Princeton, N.J.

of the reflectors is dropped and the number of optical fringes is counted, thus allowing the distance fallen to be directly measured. The dropped reflector cannot be constrained and, despite all precautions taken in the mechanical construction of the reflector and the dropping mechanism, the reflector will rotate to some degree. The dropped object can be constructed to minimize the rotation, but the reflected beam must return correctly or loss of fringes will occur. To overcome this problem, retordirective cube corner mirrors are used. This solution however, introduces the possibility of changes in the optical path length, due to rotation, yielding an incorrect value of gravity  $g$ . The remedy for this problem is discussed below.

### 3. THEORY OF MEASUREMENT

For two time-intervals  $t_1$  and  $t_2$ , and their two corresponding measured distances  $x_1$  and  $x_2$ , the initial velocity  $v_0$ , and the acceleration of gravity  $g$ , the relationship is:

$$\begin{aligned} x_1 &= v_0 t_1 + \frac{1}{2} g t_1^2 \\ x_2 &= v_0 t_2 + \frac{1}{2} g t_2^2 \end{aligned} \quad (1)$$

Solving for  $g$  and converting distance to wavelength of light,  $\lambda$  [each fringe corresponds to one-half wavelength of light], this is rewritten:

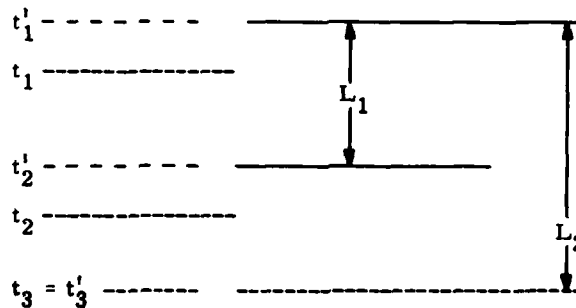
$$g = \lambda \frac{n_2 - \frac{t_2}{t_1} n_1}{t_2^2 - t_1 t_2}, \quad (2)$$

where  $n_1$  and  $n_2$  are the number of fringes counted in their respective time intervals,  $t_1$  and  $t_2$ .

This relationship is not strictly true because the velocity of light is finite. There are two considerations for the velocity of light corrections, (1) the actual velocity and (2) the Doppler effect due to the movement of the dropped object.

The actual velocity of light,  $c$ , is dependent on the index of refraction of the medium in which it travels and a correction must be made to account for any discrepancy due to chamber pressure.

The second consideration for the finitude of the velocity of light results in a correction to the time intervals.<sup>8,9</sup> The calculation considers a moving object (accelerating in this case) and the measurement of the position of the object at  $n$  times (three times,  $t_1$ ,  $t_2$ , and  $t_3$  are given here for simplicity). The following explanation is given by considering the measurements being made by interferometry and using the diagram below:



If the detector is considered at the location of the object at time  $t_3$ , the distances  $L_1$  and  $L_2$  are not given by the positions at times  $t_1$  and  $t_2$ , but at  $t_1'$  and  $t_2'$  which are given by

$$t_1' = t_1 - \frac{L_2}{c}$$

and

$$t_2' = t_2 - \frac{(L_2 - L_1)}{c} \quad (3)$$

The object is seen interferometrically at an earlier time due to the finite velocity of light.

8. Hammond, J. A. (1970) A Laser-Interferometer System for the Absolute Determination of the Acceleration of Gravity, Joint Institute for Laboratory Astrophysics (JILA) Report No. 103, February.
9. Zumberge, M. A. (1981) A Portable Apparatus for Absolute Measurement of the Earth's Gravity, Ph. D. Thesis, University of Colorado.



The actual time intervals are:

$$\begin{aligned}
 T'_1 &= t'_2 - t'_1 = t_2 - \frac{L_2 - L_1}{C} - \left( t_1 - \frac{L_2}{C} \right) \\
 &= t_2 - t_1 + \frac{L_1}{C} = T_1 + \frac{L_1}{C} \\
 T'_2 &= t'_3 - t'_1 = t_3 - \left( t_1 - \frac{L_2}{C} \right) = T_2 + \frac{L_2}{C} .
 \end{aligned} \tag{4}$$

Let  $\lambda$  be the wavelength of the light used,  $N_1$  and  $N_2$  be the number of fringe counts for two distances, and  $T_1$  and  $T_2$ , the appropriate time intervals:

the measured value of  $g$  is given by

$$g_{\text{meas}} = \lambda \frac{N_2 - (T_2/T_1) N_1}{T_2^2 - T_1 T_2}$$

and

the actual value of  $g$  is given by

$$g_{\text{actual}} = \lambda \frac{N_2 - (T'_2/T'_1) N_1}{T'^2_2 - T'_2 T'_1} .$$

Then setting  $\Delta_2 = L_2/C$  and  $\Delta_1 = L_1/C$ ,  $T'_2$  and  $T'_1$  become

$$T'_1 = T_2 + \Delta_2$$

$$T'_2 = T_1 + \Delta_1$$

and, solving:

$$g_{\text{actual}} = \frac{L(M_2 - [(T_2 + \Delta_2)/(T_1 + \Delta_1)] M_1)}{(T_2 + \Delta_2)^2 - (T_1 + \Delta_1)(T_2 + \Delta_2)} .$$

Expanding and neglecting terms of order 2 and higher in the  $\Delta$ 's, this becomes

$$g_{\text{actual}} = \frac{L \left( M_2 - \frac{T_2}{T_1} M_1 \right)}{T_2^2 - T_1 T_2} \left( 1 - \frac{2T_2 \Delta_2 - T_2 \Delta_1 - T_2 \Delta_2}{T_2^2 - T_1 T_2} - \frac{M_1}{M_2} - \frac{T_2}{T_1} M_1 \left( \frac{\Delta_2 T_1 - \Delta_1 \Delta_2}{T_1^2} \right) \right).$$

resulting in the relationship

$$g_{\text{actual}} = g_{\text{measured}} (1 + \Delta g/g).$$

#### 4. PROTOTYPE OF SELECTED SYSTEM

The present version (Figure 1) of the absolute-gravity measuring system utilizes the same conceptual approach as the original system: (a) a freely falling mirror as one arm of a Michelson interferometer, (b) use of the wavelength of light from a stabilized HeNe laser as the standard of length, (c) use of a rubidium frequency oscillator as a time standard, and (d) a single vacuum chamber for dropping the freely falling reflector.

Although the general concept is the same, many modifications and improvements have been made both mechanically and electronically. The improvements made in the electronics have led to the incorporation of on-line corrections, heretofore made separately, and on-line calculations not possible with the original equipment. The final program and an explanation of the various steps are given in Appendix A. The improved computer capabilities allow an earth tide program to be stored and with the real-time information; tide corrections are made for each measurement. The tide program used is a shortened form by D. H. Eckhardt of the program developed by Cabaniss and Eckhardt.<sup>10</sup>

The data that are acquired with the improved system are 500 time measurements that relate to the position of the object during the fall of about 65 cm — a large improvement over the three-position determination of the original system. A least-squares analysis is made of the times for each drop to fit a parabola to

10. Cabaniss, G. H., and Eckhardt, D. H. (1973) The AFGL Earth Tide Program, AFGL-TR-73-0084, AD 762275.

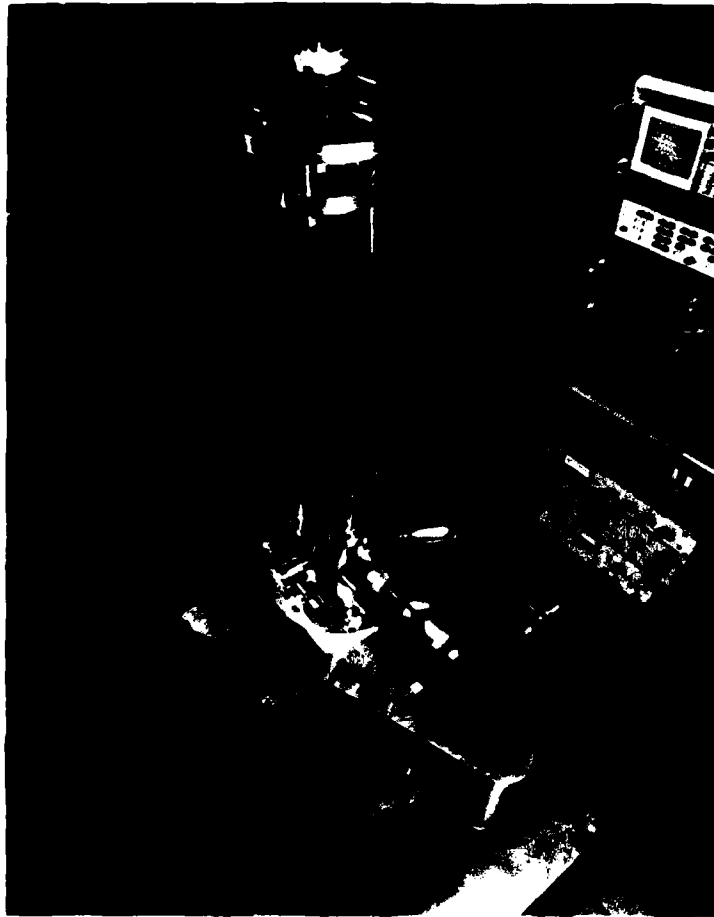


Figure 1. Air Force Geophysics Laboratory Absolute Gravity Measurement System

obtain  $g$  and the initial velocity [440 of these data points are used and along with other data processing and corrections, the computer time required to perform these computations limits the rapidity that data can be taken, thus the 30-sec lower limit mentioned in the robot/controller remarks].

This measurement technique allows a unique method of determining the value of two important corrections: (1) the vertical gradient of gravity, and (2) the effect of the finite velocity of light. [The original system took this into account for only three points.]

Errors are introduced when the calculation assumes uniform acceleration that is not exact in the case of a gradient. A spatial gradient is time dependent because the falling body is moving in space and a time-averaged value is obtained

with the least-squares method. The points at which acceleration is measured are the time-averaged positions of the falling object.

Although the points can be determined in an analytical manner by computing an integral, an essentially numerical method is used in our procedure to determine the effective measuring points. Calculations are made to synthesize time values using the formula:

$$t = (2X/g_0)^{1/2} - 5/12 A (2X/g_0)^{3/2} ,$$

where  $A$  is the gravity gradient,  $X$  is the distance the object has fallen, and  $g_0$  is the value of gravity at the top of the chamber. This expression may be derived by solving the differential equation describing the motion of a body in a uniform gradient field and expanding the result assuming the gradient change is small compared with the magnitude of  $g$ . The result of fitting these time values is to produce a measured value of  $g_m$  that is different from  $g_0$ . That difference can be used to calculate the effective measuring point  $X_m$ :

$$X_m = (g_m - g_0)/A .$$

The present program is set up so that the object falls 7.5 cm before the approximate 60-cm measurement interval begins, resulting in an effective height of the measurement of about 32 cm from the top of the chamber. [Note that the leveling screws can cause about 3 cm of top-of-chamber difference, which necessitates measurement of the leveled instrument.]

Corrections to the time values that depend on the location of the dropped object in the chamber are required since the velocity of light is finite. A set of corrected time values is calculated and analyzed by the least-squares computation that determines the effect on the measured value of  $g$ . This is a much more detailed calculation than the three-position correction described in the original equipment section.

Other corrections that must be made include: (1) the effect of air resistance on the falling body caused by residual air in the vacuum chamber and (2) the difference between the assumed wavelength of the laser light used as a standard of length and its actual value. The correction for air resistance is determined empirically and is generally checked, periodically, in the pressure range of about  $10^{-7}$  to  $5 \times 10^{-4}$  mm Hg. Figure 2 is a graph over the extended range of about  $10^{-7}$  to  $10^{-3}$  mm Hg. Since most of the gravity measurements are made in the range of  $10^{-7}$  to  $10^{-6}$  mm Hg, the correction is, roughly, from 1 to 10  $\mu$ gal. In spite of this relatively small change in the correction, the new system monitors, on line, the vacuum chamber pressure in order to correct and evaluate

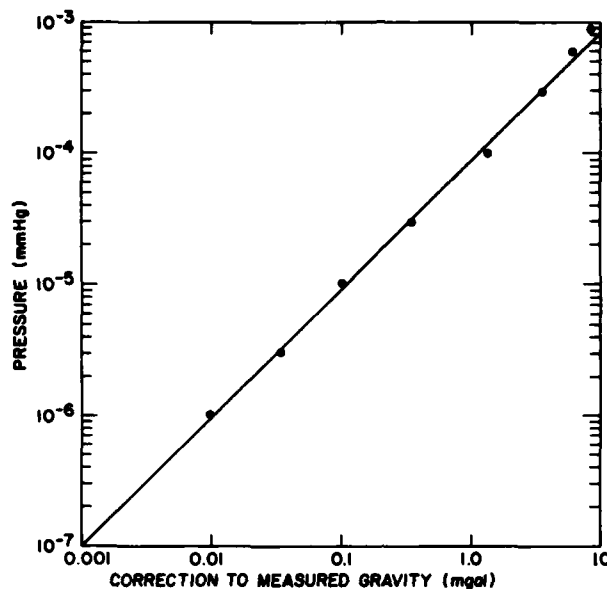


Figure 2. Gravity Correction as a Function of Pressure

individual drops. It is also noted that the correction for the change in the velocity of light due to the medium in which it travels [in this case, the fact that it is not travelling in absolute vacuum] is absorbed in this empirically determined correction.

The wavelength of the stabilized laser is checked, periodically, against an iodine-stabilized laser developed by the NBS. The Spectra Physics Model 119 stabilized laser has been in use with this system since its inception and has been checked against two different NBS-developed laser wavelength standards and the typical wavelength shift of about one part in  $10^8$  per year has been observed. The observed wavelength change, converted to the correction to the measured value of  $g$  vs time, is plotted in the graph below (Figure 3).

Several mechanical improvements have been made. In addition, some trial modifications were discarded because they did not meet expectations. These modifications include: (1) stabilization of the reference reflector and (2) positioning mechanisms that included more friction-free release and pick-up of the dropped object.

The isolation system used in the earlier version to isolate the reference reflector from the disturbing effects of seismic noise was a long period commercial seismometer. Aside from the bulk required to incorporate this system, as seen in Figure 4 (2), [in part due to the necessity of placing it as far as

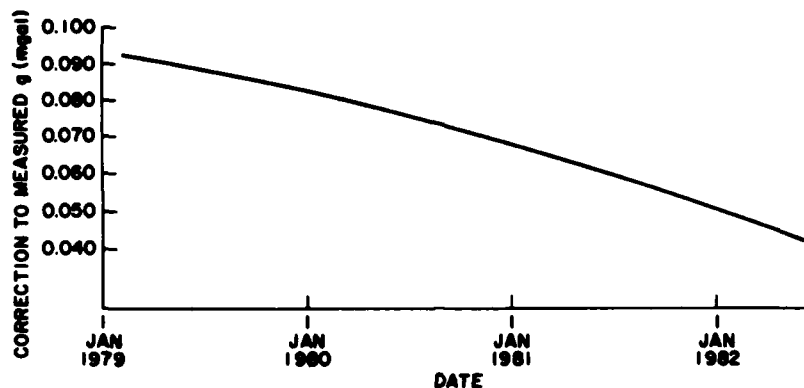


Figure 3. Gravity Correction as a Function of Laser Wavelength Change in Time

possible from the disturbing effects of the gravity measuring equipment], the seismometer suspension system was one area of concern as had been reported earlier.<sup>8</sup>

Since the mechanical configuration had been changed in the final version, it was concluded that a new, more compact seismometer could be used and still be physically far enough away from the disturbing magnetic fields set up by the gravity apparatus. A new commercial seismometer was modified to retrofit the reference reflector [by removing material from the suspended mass to compensate for the mass of the retroreflector as well as making physical space for the cube-corner reflector] and to allow the light beam access to the reflector [by installing a plane parallel window in the seismometer enclosure].

Attempts to remove disturbing magnetic effects included: (1) demagnetizing as many parts of the system as was practical, (2) changing the size of the ION pump thereby reducing the necessary magnetic field of the pump, (3) physically removing the ION pump magnet just before each drop, (4) setting up the ION pump as far away as possible using long tubing (which, not surprisingly, was detrimental to the achievable vacuum in the main chamber), and (5) shielding various parts of the system with mu-metal. Although the trial solutions were somewhat beneficial, none reduced the effects sufficiently to warrant continued use of this particular seismometer. This seismometer was, however, useful in determining the general seismic background noise and showed that different times of the day or week were quieter due to cultural noise. It showed, for example, that the most reliable times for taking data at some sites were nights and/or weekends.

The main difficulty encountered thus far in isolating the reference reflector has been magnetic fields. A commercial seismometer has, by design, magnetic

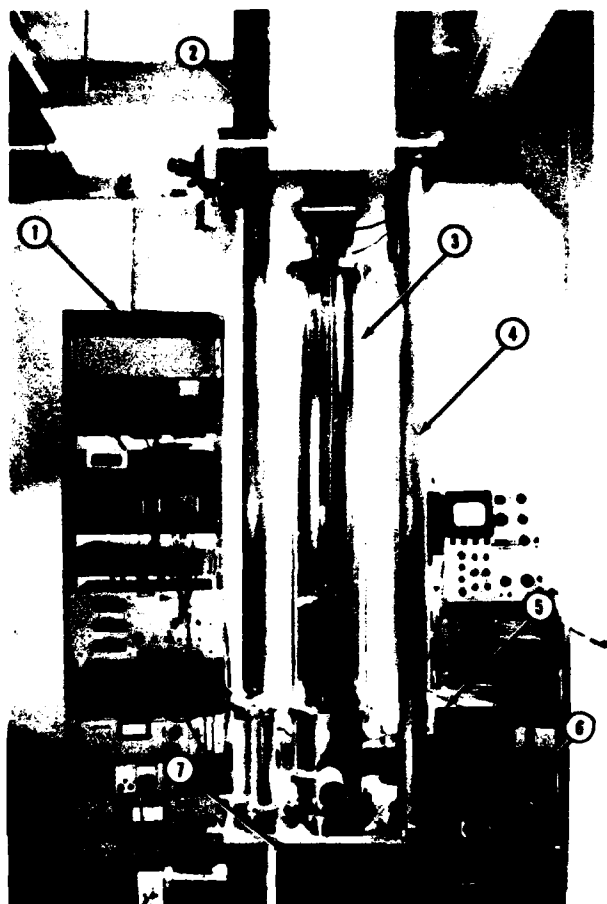


Figure 4. Original Gravity Measuring System

Legend

1. Electronics Rack
2. Seismometer
3. Vacuum Chamber
4. Support Pillars
5. ION Pump
6. Laser
7. Optics Base

materials, since it functions as a transducer. Our design for the absolute-gravity measuring equipment incorporates an electromagnet to hold the object until release. The collapse of the field, at release, is fast and timing of the free-fall does not start until after the field has collapsed thereby eliminating any measurable effects on the dropped object — the seismometer mass, however, is set in motion and, although critically damped, is still in motion during the drop.

There are two obvious solutions to this problem: (1) remove the electromagnet from the gravity apparatus by using, for example, a purely mechanical dropping mechanism or (2) design a seismometer that is unaffected by outside fields. Some thought was given to solution (1), but it was dropped in favor of the second approach.

This decision was made because a purely mechanical dropping system that would release the object without imparting forces causing rotation or lateral velocity (to the repeatable precision required) appeared to be extremely complex. Also laboratory funding for the development of a very long period isolator, designed for this specific use, was already underway with the Joint Institute for Laboratory Astrophysics (JILA), of the NBS. The result of this long period isolator is a synthesized spring in a 1-m long housing along with the electronics and servo system that makes the spring appear to be 1 km long. The super spring can be seen on the gravity apparatus in Figure 5. The natural period of this relatively short spring is made to look like a very long spring by electronically measuring the distance from the suspension point to the mass and servoing the suspension point to make the total system think it has a 1 km length spring. A more detailed mechanical description of this system can be found in the literature.<sup>9</sup>

The prototype super-spring isolator, as received, showed promise but did have some electronic problems, which are still being resolved. At seismically noisy sites the isolator reduced the scatter of the data by a factor of 10 or more, but it also introduced a bias. However at seismically quiet sites the scatter was not improved very much (as would be expected), but there was no bias. Electronics is suspected to be the cause of this heretofore unexplained problem and is still being investigated. Until this "bias when noisy — no bias when quiet" mystery is solved it was decided to not use the super spring and rely on statistics to obtain a gravity value, that is, the resulting error is proportional to the inverse square of the number of measurements. During the checkout/use of the super spring there appeared to be no bias caused by the electromagnet on the gravity measuring equipment verifying the antimagnetic design of the super spring.

Although the ideal isolating seismometer should remove all seismically induced noise, including cultural disturbances induced by the equipment itself, that is, recoil. When the object is dropped it is no longer part of the mass of the





Figure 5. Absolute Gravity Measuring Instrument With the Isolating Seismometer, Super Spring, Installed

earth-fixed system and, upon release, the remaining portion of the system will recoil as a result of this loss of mass. If the reference reflector is not isolated from this reaction, the result is a systematic source of error since the drop and recoil are related. The effects of the vibrations set up by recoil are evident in Figure 6.

All system improvements in isolating the reference reflector up to this point had been concentrated on the reference reflector itself. Then, a new approach to isolating the system from the recoil problem emerged. This new approach involved isolating, as much as possible, a massive portion of the system that was necessary to the total system but not involved in the actual measurement – the whole vacuum/dropping chamber. The vacuum chamber and the Vac ION pump with a mass of approximately 130 kgm, was attached to the optical system, that is, the Michelson interferometer – the actual measuring portion of the system.

In spite of the fact that the first attempts to isolate the vacuum chamber/dropped object portion of the system was very crude, the results were extremely promising. Next, an isolation tripod was constructed and off-the-shelf shock mounts were purchased for further isolation. The final mechanical configuration can be seen in Figure B1.

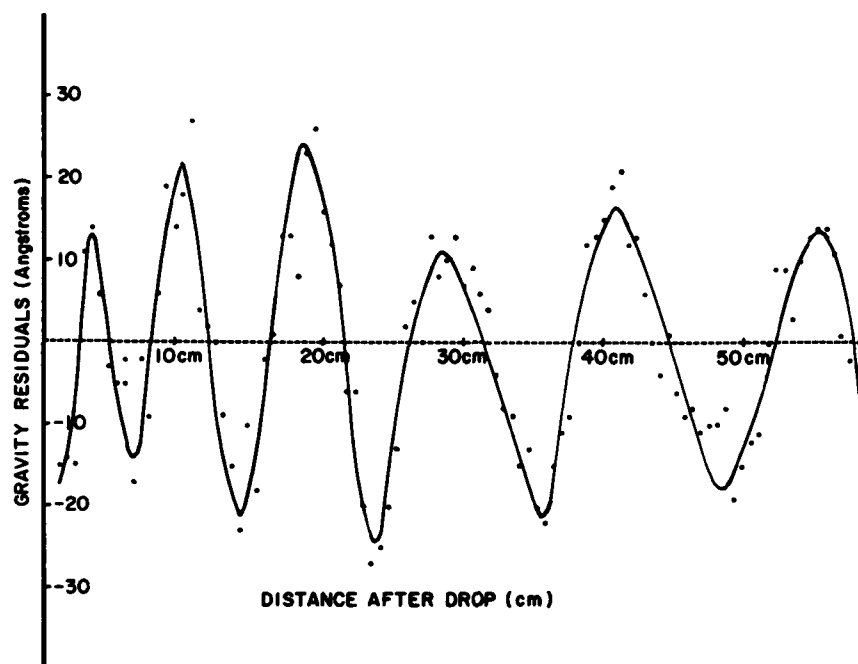


Figure 6. Gravity Residuals (Angstroms) vs Distance After Drop (cm)

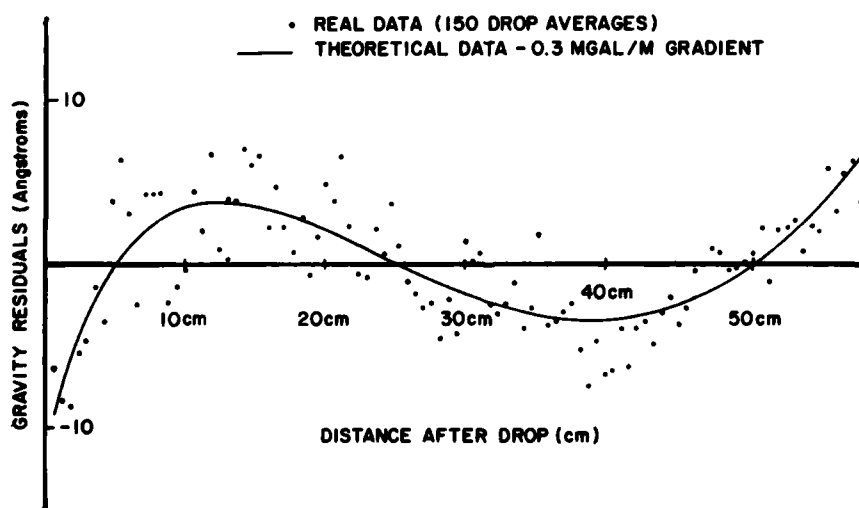


Figure 7. Gravity Residuals (Angstroms) vs Distance After Drop (cm)

The data plotted in Figure 7 shows the results of the tripod isolation. The plot also shows the theoretically expected residuals due to a gradient — theory and data follow very closely as a result of this isolation. Also note the difference in scale when comparing Figure 6 with Figure 7.

Another area of concern, from a mechanical and maintenance point-of-view, which had plagued the system from the onset,<sup>8</sup> was the mechanical, pre-drop positioning mechanism. The dropped object package is mechanically repositioned prior to each drop by a three ball and groove positioning mechanism. The dropped object package (Figure B7(2)) has three positioning balls (Figures B7(6), B13(7)) that are positioned into their respective V grooves (Figure B13(3)), thus assuring that the dropped object has the same pre-drop position. The physical problem with this system was the eventual cohesive sticking of the balls and grooves under vacuum conditions. In spite of the precaution taken of using like metals (stainless steel) in the ball and groove configuration in order to avoid contact differential potential to eliminate static charge, the cohesion of the contacts eventually increased to the point of imparting rotation of the dropped object because of unequal sticking at the three ball and groove contact points. Although burnishing the contact points with molybdenum disulfide increased the life of the contacts, that is, time between system teardown and cleaning, the loss of time in a system breakdown/repair/reevacuation was still excessive for field equipment.

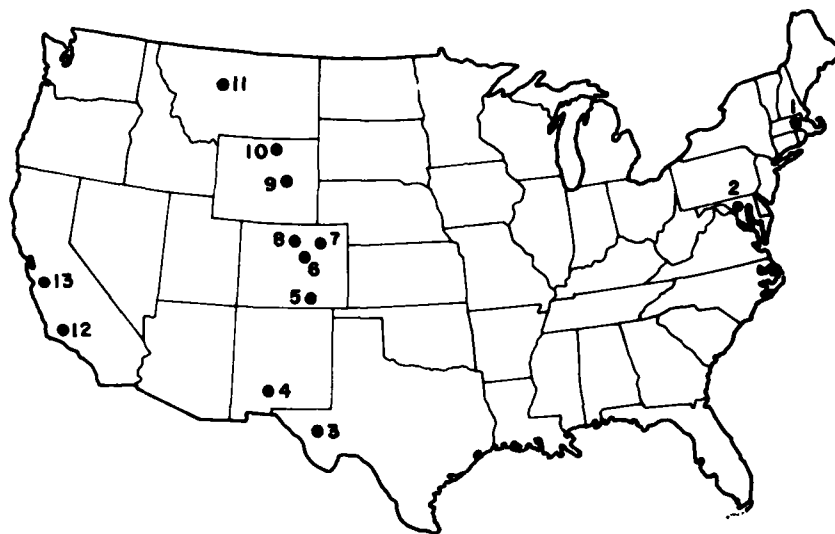
In efforts to eliminate, or at least reduce the problem to an acceptable level, the ball material was the most likely candidate as opposed to the V grooves because of the minimum amount of modification required if unlike materials were to be used. The two main areas of concern in the use of dissimilar or different materials were introduction of static charge and outgassing within the vacuum chamber. It was found that delcron is a commonly used material in vacuum systems, with negligible outgassing at  $10^{-7}$  mm Hg and no noticeable charge is set up. Since balls of this material were incorporated (nearly two years) there has been no need to open the vacuum chamber because of ball-groove sticking.

## 5. FIELD MEASUREMENTS

The results obtained from the field measurements that have been made are the rewards for the laboratory measurements and experimentation, modifications, and improvements. Measurements were made at several sites of interest to various government agencies.

### 5.1 Station Descriptions

One important aspect of the measurement process is the site selection. The general geographical location of a calibration line through the central part of the United States was presented to the Geodetic Survey Squadron (GSS), DMAHTC, F.E. Warren AFB, Wyo., who, in turn, accepted the responsibility of locating specific sites at these geographical locations. The expertise and liaison provided by GSS personnel has been invaluable in the measurement process. GSS generally provided AFGL with three sites at each location from which to choose the most suitable for measurement purposes. For example, one of the sites made available at Sheridan, Wyo., was a reasonably quiet site, a root cellar. This particular site was excellent from a gravity measuring point-of-view, but the equipment would have needed to be taken into the site in pieces. Therefore, one of the other sites provided was chosen for the measurement. The liaison provided by GSS made the site occupation go smoothly. The measurements that have been made include the following sites: Hanscom AFB, Mass. (our home base), the National Bureau of Standards in Gaithersburg, Md.; Vandenberg AFB, Calif.; Lick Observatory, Calif.; NBS-JILA in Boulder, Colo.; sites in Great Falls, Mont.; Sheridan, Wyo.; Casper, Wyo.; Mt Evans, Colo.; Denver, Colo.; Trinidad, Colo.; Holloman AFB, N. Mex., and McDonald Observatory, Tex. The geographical locations of these stations are shown in Figure 8. These last eight sites (Figures 9-21) form a calibration line with a total gravity difference of about 1600 mgal. Several of the sites have been occupied by more than one absolute instrument. Descriptions of these sites (as provided by DMAHTC/GSS) are given in the following pages.



- |                               |                          |                              |
|-------------------------------|--------------------------|------------------------------|
| 1. HANSCOM AFB, MASS. (AFGL)  | 6. DENVER, COLO.         | 10. SHERIDAN, WYO.           |
| 2. GAITHERSBURG, MD. (NBS)    | 7. MT. EVENS, COLO.      | 11. GREAT FALLS, MONT.       |
| 3. MCDONALD OBSERVATORY, TEX. | 8. BOULDER, COLO. (JILA) | 12. VANDENBERG AFB, CALIF.   |
| 4. HOLLOMAN AFB, N. MEX.      | 9. CASPER, WYO.          | 13. LICK OBSERVATORY, CALIF. |
| 5. TRINIDAD, COLO.            |                          |                              |

Figure 8. Sites of Absolute Gravity Measurements

GRAVITY STATION DESCRIPTION		STATION TYPE	STATION DESIGNATION
		Absolute Site	Boston A
COUNTRY	USA	STATE/PROVINCE	Massachusetts
CITY	Bedford		
LATITUDE	42° 27.1 N	LONGITUDE	71° 16.3W
ELEVATION	66 meters		
GRAVITY STATION MARK	brass disk	AGENCY/SOURCE	DMA
INSCRIPTION	Gravity Base		
POSITION REFERENCE	Map	POSITION SOURCE	USGS 7½'
SOURCE DESIGNATION	Concord, Mass.	1958	
ELEVATION REFERENCE	Map	ELEVATION SOURCE	USGS 7½'
SOURCE DESIGNATION	Concord, Mass.	1958	
POSITION/ELEVATION REMARKS			
CI = 10 feet			
DESCRIPTION The station is south of Bedford at the southern part of Hanscom Air Force Base, at the south end of Grenier Street, in the Haskell Seismic- Gravity Observatory (Building IIII). Observations were made in Room 1 (the northernmost room at the center of the easternmost concrete pier (Pier 1). The disk is at the southeast corner of the pier.			
IGB Code: 15221A			
W.G. Spita		AGENCY	DMATC/GSS
		DATE	December 1977

Figure 9. Gravity Station Description: Boston A

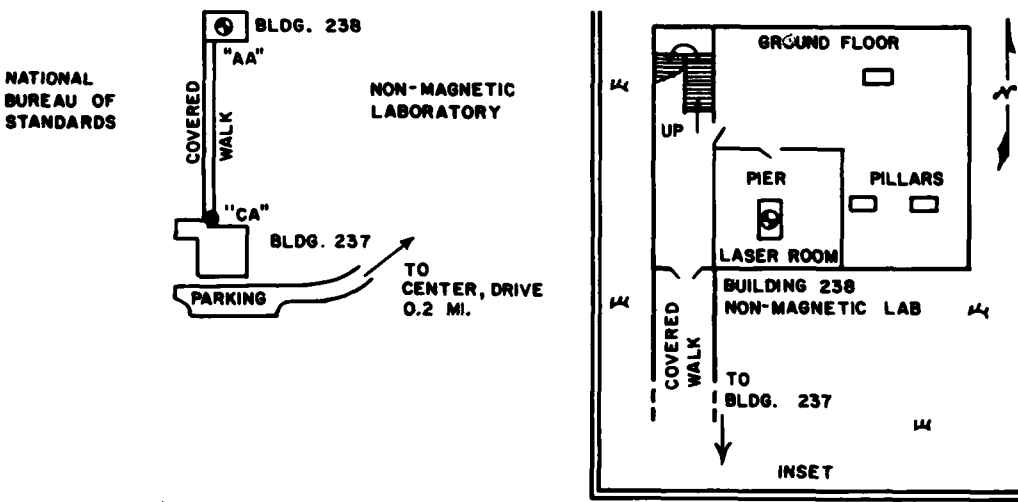
GRAVITY STATION DESCRIPTION	STATION TYPE Absolute Site	STATION DESIGNATION Washington AA
COUNTRY USA	STATE/PROVINCE Maryland	CITY Gaithersburg
LATITUDE 39° 07.' 6N	LONGITUDE 77° 13.' 3W	ELEVATION 123.3 meters
GRAVITY STATION MARK None	AGENCY/SOURCE	INSCRIPTION
POSITION REFERENCE Map	POSITION SOURCE IISGS 7 1/2'	SOURCE DESIGNATION Gaithersburg, Md 1971
ELEVATION REFERENCE Site Plan	ELEVATION SOURCE NBS	SOURCE DESIGNATION
POSITION/ELEVATION REMARKS		
CI=4 feet		
DESCRIPTION The station is about 1 1/2 miles southwest of Gaithersburg at the National Bureau of Standards (NBS). To reach from the Quince Orchard Rd. interchange of Interstate 270, go south on Quince Orchard Rd. (Maryland Route 124) 1.2 miles to the NBS Gate 4. Turn left and go east through the gate 0.3 miles on South Drive to Center Drive. Turn right on Center Drive and go south 0.3 miles to Bldg. 235. Turn right and go southwest 0.2 miles to the end of the driveway and the Non-Magnetic Laboratory area. The station is in Bldg. 238, ground floor, in the Laser Room, at the center of the 1m x 1.5m concrete pier which is flush with the floor. GSS Code: 116B01		
		
DATE OF PHOTO		
DESCRIBED BY W. G. Spita	AGENCY DMAHTC/GSS	DATE March 1980

Figure 10. Gravity Station Description: Washington AA

<b>GRAVITY STATION DESCRIPTION</b>	<b>STATION TYPE</b> ABSOLUTE <b>GRAVITY SITE</b>	<b>STATION DESIGNATION</b> VANDENBERG AA 121A03
<b>COUNTRY</b> USA	<b>STATE/PROVINCE</b> California	<b>CITY</b> Lompoc
<b>LATITUDE</b> 34°46' 14" N	<b>LONGITUDE</b> 120°30' 16" W	<b>ELEVATION</b> 246 m
<b>GRAVITY STATION MARK</b> None	<b>AGENCY/SOURCE</b> USAF/AFGL	<b>INSCRIPTION</b>
<b>POSITION REFERENCE</b> Station SAND	<b>POSITION SOURCE</b> National Geodetic Survey	<b>SOURCE DESIGNATION</b>
<b>ELEVATION REFERENCE</b> Station SAND	<b>ELEVATION SOURCE</b> National Geodetic Survey	<b>SOURCE DESIGNATION</b>
<b>POSITION/ELEVATION REMARKS</b>		
<b>DESCRIPTION</b> Station is approximately 1.5 miles north/northeast of the Vandenberg AFB Main Gate near the Western Space and Missile Center Command Transmitter No. 1 (Bldg. 21200). The absolute station is located along the northwest wall just southwest of the theodolite base within the Vandenberg AFB Azimuth Laying Set Facility (Bldg. 21205).		
<p>The diagram illustrates the layout of the gravity station. A 'FREE FALLING ABSOLUTE GRAVITY METER' is connected via a tube to a 'VACUUM PUMP'. The meter is positioned near a 'THEODOLITE BASE' and 'WINDOWS'. A 'CONCRETE PIER' is shown to the right. Below the meter is a 'COMPUTER &amp; ELECTRONIC EQUIPMENT' unit, which is connected to a 'COMPUTER PRINTER'. 'PRISONS' are indicated near the computer equipment. A north arrow points towards the top right of the diagram.</p>		
<b>DESCRIBED/RECOVERED BY</b> W. E. Smith	<b>AGENCY</b> DMAHTC GSS Detachment 1	<b>DATE</b> 2 SEP 80

Figure 11. Gravity Station Description: Vandenberg AA



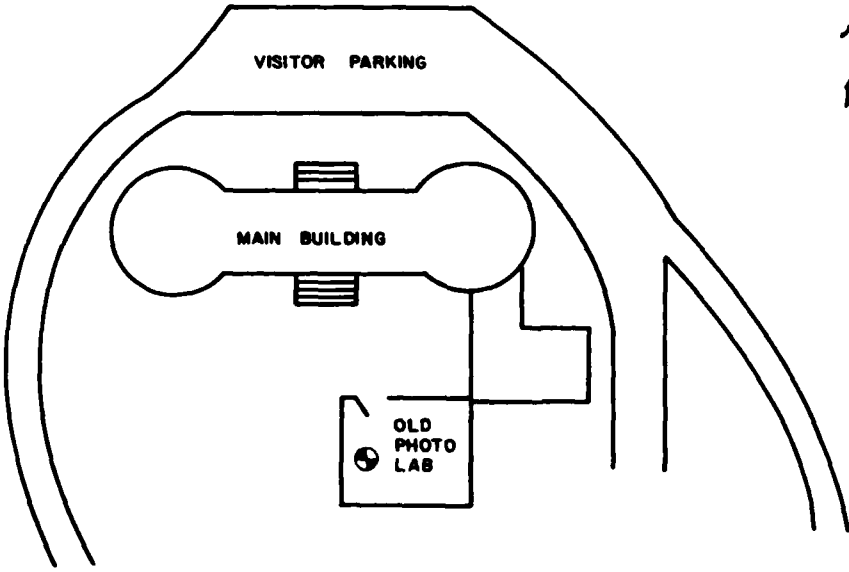
GRAVITY STATION DESCRIPTION		STATION TYPE	STATION DESIGNATION
COUNTRY	USA	STATE/PROVINCE	CITY
		CALIFORNIA	
LATITUDE	37° 20' 52"N	LONGITUDE	ELEVATION
		121° 38' 49"W	4213 ft
GRAVITY STATION MARK	AGENCY/SOURCE	INSCRIPTION	
POSITION REFERENCE	POSITION SOURCE	SOURCE DESIGNATION	
ELEVATION REFERENCE	ELEVATION SOURCE	SOURCE DESIGNATION	
POSITION/ELEVATION REMARKS			
<p>DESCRIPTION</p> <p>The station is located approximately 13 miles east of Alum Rock at the Lick Observatory on top of Mt. Hamilton. From Alum Rock, take H.W.Y 130 (Mt. Hamilton Road) to Lick Observatory. The station is located in the old photo lab, 5'7" from the west wall and 10'1" from the north wall, between the 40" reflector telescope and the 36" refractor telescope.</p> <p>ICB Code: 121A02</p>			
<p>DIAGRAM/PHOTOGRAPH</p> 			
DATE OF PHOTO			
DESCRIBED/RECOVERED BY		AGENCY	DATE

Figure 12. Gravity Station Description: Lick Observatory

GRAVITY STATION DESCRIPTION	STATION TYPE	STATION DESIGNATION
	Absolute Site	Boulder D
COUNTRY USA	STATE/PROVINCE Colorado	CITY Boulder
LATITUDE 40° 00.'5 N	LONGITUDE 105° 16.'1 W	ELEVATION 1633 meters
GRAVITY STATION MARK Brass disk	AGENCY/SOURCE USAF	INSCRIPTION Gravity Station
POSITION REFERENCE Map	POSITION SOURCE USGS 7 1/2'	SOURCE DESIGNATION Boulder, Colo 1966
ELEVATION REFERENCE Map	ELEVATION SOURCE USGS 7 1/2'	SOURCE DESIGNATION Boulder, Colo 1966
POSITION/ELEVATION REMARKS		
<p>DESCRIPTION The station is in the southern part of Boulder at the University of Colorado, 0.5 miles west of 28th Street, south of Colorado Avenue and Folsom Stadium, in the Joint Institute for Laboratory Astrophysics (JILA) building. Observations were made in the sub-basement in Room B0017 (the Spectroscopy Lab) near the northwest corner, 1.5 meters south of the north wall, 2.0 meters east of the west wall, on the tile floor.</p> <p>ICB Code: 15505D</p>		
<p>DATE OF PHOTO May 1980</p> <p>RECOVERED BY W.G. Spita</p> <p>AGENCY DMAHTC/GSS</p> <p>DATE May 1980</p>		

Figure 13. Gravity Station Description: Boulder D

GRAVITY STATION DESCRIPTION	STATION TYPE Absolute Site	STATION DESIGNATION Great Falls AA
COUNTRY U.S.A.	STATE/PROVINCE Montana	CITY Great Falls
LATITUDE 47° 28.'7 N	LONGITUDE 111° 21.'6 W	ELEVATION 1120 Meters
GRAVITY STATION MARK Brass Disk	AGENCY/SOURCE DMA	INSCRIPTION
POSITION REFERENCE Map	POSITION SOURCE USGS 7 1/2'	SOURCE DESIGNATION 1965 Southwest Great Falls, MT
ELEVATION REFERENCE Map	ELEVATION SOURCE USGS 7 1/2'	SOURCE DESIGNATION 1965 Southwest Great Falls, MT
POSITION/ELEVATION REMARKS  CI = 20 Feet		
<p>DESCRIPTION The station is at the west side of Great Falls on Gore Hill, south of the airport and at the south side of the intersection of Avenue C and Second Street, at the CPT William W. Galt US Army Reserve Center. Observations were made near the south side of the building in the firing range, northeast end, 1.5 meters southwest of the middle firing stall (also 1.5 meters from edge of carpet). The station is midway between the northwest and southeast walls, 2.0 meters southeast of the disk, on the concrete floor.</p> <p>GSS Code: 156E05</p>		
<p>July 1979 DESCRIBED BY W.G. Spita</p> <p>AGENCY DMAHTC/GSS</p> <p>DATE July 1979</p>		

Figure 14. Gravity Station Description: Great Falls AA

GRAVITY STATION DESCRIPTION	STATION TYPE	STATION DESIGNATION
	Absolute Site	Sheridan AA
COUNTRY U.S.A.	STATE/PROVINCE Wyoming	CITY Sheridan
LATITUDE 44° 45.'6 N	LONGITUDE 106° 58.'1 W	ELEVATION 1205 Meters
GRAVITY STATION MARK Brass Disk	AGENCY/SOURCE DMA	INSCRIPTION
POSITION REFERENCE Map	POSITION SOURCE USGS 7 1/2'	SOURCE DESIGNATION Sheridan, Wyo 1968
ELEVATION REFERENCE Map	ELEVATION SOURCE USGS 7 1/2'	SOURCE DESIGNATION Sheridan, Wyo 1968
POSITION/ELEVATION REMARKS CI= 20 feet		
<p>DESCRIPTION</p> <p>The station is about 2.5 miles south of the center of Sheridan, west of Wyoming Highway #333, at the Wyoming State Girls School, in Stolt Hall (Administration Building). Observations were made in the basement, east of the boiler room, near the northeast corner of the large room used for arts and crafts, in a small storage room. The station is 1.1 meters north of the south wall of the room and 0.9 meters west of the brass disk and east wall (which is also the east wall of the building) on the concrete floor.</p> <p>GSS Code: 155V03</p> <p>The diagram includes an inset map of the Wyoming State Girls School and Stolt Hall, showing a driveway and parking area. The main map shows the basement of Stolt Hall, with a boiler room, arts and crafts room, and a walkway leading to the station. The station is marked with a dot and labeled 'AA'.</p>		
Walter G. Spita	DMAHTC/GSS	July 1979

Figure 15. Gravity Station Description: Sheridan AA

GRAVITY STATION DESCRIPTION	STATION TYPE Absolute Site	STATION DESIGNATION Casper AA
COUNTRY USA	STATE/PROVINCE Wyoming	CITY Casper
LATITUDE 42°51.'0 N	LONGITUDE 106° 19.'4 W	ELEVATION 1558 Meters
GRAVITY STATION MARK Brass Disk	AGENCY/SOURCE DMA	INSCRIPTION
POSITION REFERENCE Map	POSITION SOURCE USGS 7 1/2'	SOURCE DESIGNATION Casper, Wyo. 1961
ELEVATION REFERENCE Bench Mark	ELEVATION SOURCE NGS	SOURCE DESIGNATION B18 Reset 1971
POSITION/ELEVATION REMARKS Station is north of and 3 meters below BM.		
DESCRIPTION The station is in Casper at the southeast corner of East First Street and South Wolcott Street in the Federal Building - US Court House (former Post Office), in the basement level. Observations were made in Room B1 (GSA Storage Room) which is the northwestern most room, about 4 meters west of the entrance and 0.7 meters west of a supporting pillar. The station is 0.7 meters west of the disk, on the concrete floor.		
GSS Code: 155V01		
<p>The map shows the layout of the basement of the Federal Building U.S. Court House. East First Street runs horizontally across the top, and South Wolcott Street runs vertically along the left side. The building footprint is a large rectangle. Inside, Room B1 is in the northwest corner. To its east is a Lobby, and further east is RM B21. A Hall connects these areas. A Freight Elevator is located near the southeast corner of the building. A Loading Dock is outside the building, accessible via Steps. A Bench Mark (BM) is located on the exterior wall of the building. The gravity station 'AA' is marked with a dot in Room B1. A driveway is shown on the right side of the map.</p>		
BY: CHIEF D. Spita	AGENCY DMAHTC/GSS	DATE July 1979

Figure 16. Gravity Station Description: Casper AA

GRAVITY STATION DESCRIPTION	STATION TYPE	STATION DESIGNATION
	Absolute Site	Mt. Evans AA
COUNTRY U.S.A.	STATE/PROVINCE Colorado	CITY Idaho Springs
LATITUDE 39° 39.'3 N	LONGITUDE 105° 35.'6 W	ELEVATION 3247 meters
GRAVITY STATION MARK Brass Disk	AGENCY/SOURCE DMA	INSCRIPTION
POSITION REFERENCE Map	POSITION SOURCE USGS 7 1/2'	SOURCE DESIGNATION Idaho Springs, Colo 1957
ELEVATION REFERENCE Map	ELEVATION SOURCE USGS 7 1/2'	SOURCE DESIGNATION Idaho Springs, Colo 1957
POSITION/ELEVATION REMARKS		
CI=40 feet		
DESCRIPTION The station is 13 miles southwest of Idaho Springs on Mt. Evans, 0.1 miles south-east of the intersection of Colorado Highways 103 and 5, at the Inter-University High Altitude Lab. Observations were made at the southwest part of the Lab complex in the Lab building, western room, 4.1 meters east of the west wall of the building and 1.8 meters south of the north wall. The station is 1.5 meters east of the disk (which is at the west end of the wooden partition) on the concrete floor.		
GSS Code: 119C03		
<p>TO IDAHO SPRINGS TO BERGEN PARK TO MT. EVANS DIRT ROAD PAVILLION GARAGE RED TANK "AA" LAB INTER-UNIVERSITY HIGH ALTITUDE LAB INSET "AA" SINK DARK ROOMS</p>		
DESCRIBED BY W.G. Spita	AGENCY DMAHTC/GSS	DATE July 1979

Figure 17. Gravity Station Description: Mt. Evans AA

<b>GRAVITY STATION DESCRIPTION</b>	<b>STATION TYPE</b> Absolute Site	<b>STATION DESIGNATION</b> Denver H
<b>COUNTRY</b> USA	<b>STATE/PROVINCE</b> Colorado	<b>CITY</b> Denver
<b>LATITUDE</b> 39° 40.'5 N	<b>LONGITUDE</b> 104° 57.'8 W	<b>ELEVATION</b> 1634 meters
<b>GRAVITY STATION MARK</b> Brass Disk	<b>AGENCY/SOURCE</b> DMA	<b>INSCRIPTION</b> Gravity Base
<b>POSITION REFERENCE</b> Map	<b>POSITION SOURCE</b> USGS 7 1/2'	<b>SOURCE DESIGNATION</b> Englewood, Colo 1965
<b>ELEVATION REFERENCE</b> Map	<b>ELEVATION SOURCE</b> USGS 7 1/2'	<b>SOURCE DESIGNATION</b> Englewood, Colo 1965
<b>POSITION/ELEVATION REMARKS</b>  CI=10 feet		
<b>DESCRIPTION</b> The station is in southern Denver at the University of Denver, southeast of the intersection of East Iliff Avenue and South Race Street, in the Boettcher Building complex. Observations were made in the west wing (Boettcher West), ground floor, in Room 13 (physics lab). The station is about 3 meters east of the west wall, 1.4 meters north of the south wall and disk, on the concrete floor, at a bolt imbedded in the floor.		
IGB Code: 11994H		
<b>NAME</b> M. Watters	<b>AGENCY</b> DMATC/GSS	<b>DATE</b> May 1978

Figure 18. Gravity Station Description: Denver H

GRAVITY STATION DESCRIPTION	STATION TYPE	STATION DESIGNATION
	Absolute Site	Trinidad AA
COUNTRY U.S.A.	STATE-PROVINCE Colorado	CITY Trinidad
LATITUDE 37° 10.'4 N	LONGITUDE 104° 30.'8 W	ELEVATION 1849.6 Meters
GRAVITY STATION MARK Brass Disk	AGENCY/SOURCE DMA	INSCRIPTION
POSITION REFERENCE Map	POSITION SOURCE USGS 7 1/2'	SOURCE DESIGNATION Trinidad, Colo 1951
ELEVATION REFERENCE Bench Mark	ELEVATION SOURCE Trinidad State Jun. Coll.	SOURCE DESIGNATION BM #1
POSITION ELEVATION REMARKS  Station is NW of BM and at same elevation.		
DESCRIPTION The station is in the west side of Trinidad at Trinidad State Junior College, southwest of the intersection of Pine Street and Prospect Street in the Davis (Science) Building. Observations were made on the ground floor, near the southwest corner of the building, in Room 130 (the Civil Engineering Technology Lab). The station is near the northwest corner of the room, 1.4 meters east of the west wall, 1.0 meters south of the center of the door to the storeroom, and 1.2 meters SSE of the disk, on the concrete floor. GSS Code: 119C01		
W.G. Spita	DMAHTC/GSS	DATE July 1979

Figure 19. Gravity Station Description: Trinidad AA



<b>GRAVITY STATION DESCRIPTION</b>	<b>STATION TYPE</b> Absolute Site	<b>STATION DESIGNATION</b> Holloman A
<b>COUNTRY</b> USA	<b>STATE/PROVINCE</b> New Mexico	<b>CITY</b> Alamogordo
<b>LATITUDE</b> 32° 53' .5N	<b>LONGITUDE</b> 106° 06.0' W	<b>ELEVATION</b> 1250 meters
<b>GRAVITY STATION MARK</b> Brass Disk	<b>AGENCY/SOURCE</b> DMA	<b>INSCRIPTION</b> Gravity Base
<b>POSITION REFERENCE</b> Map	<b>POSITION SOURCE</b> USGS 15'	<b>SOURCE DESIGNATION</b> Holloman, N.M. 1948
<b>ELEVATION REFERENCE</b> Map	<b>ELEVATION SOURCE</b> USGS 15'	<b>SOURCE DESIGNATION</b> Holloman, N.M. 1948
<b>POSITION/ELEVATION REMARKS</b>  contour interval = 25 feet		
<b>DESCRIPTION</b> The station is about 8 miles west of Alamogordo at the north side of Holloman Air Force Base in the Advanced Inertial Test Laboratory (Building 1256). Observations were made in the basement level in Room 10 (the northeastern most room of the basement), on the round concrete pier, midway between the center and the south edge of the pier.		
ICB Code: 11926A		
DATE OF PHOTO <b>November 1977</b> CHECKED BY <b>W. G. Spita</b>		
AGENCY <b>DMATC/GSS</b>		DATE <b>November 1977</b>

Figure 20. Gravity Station Description: Holloman A

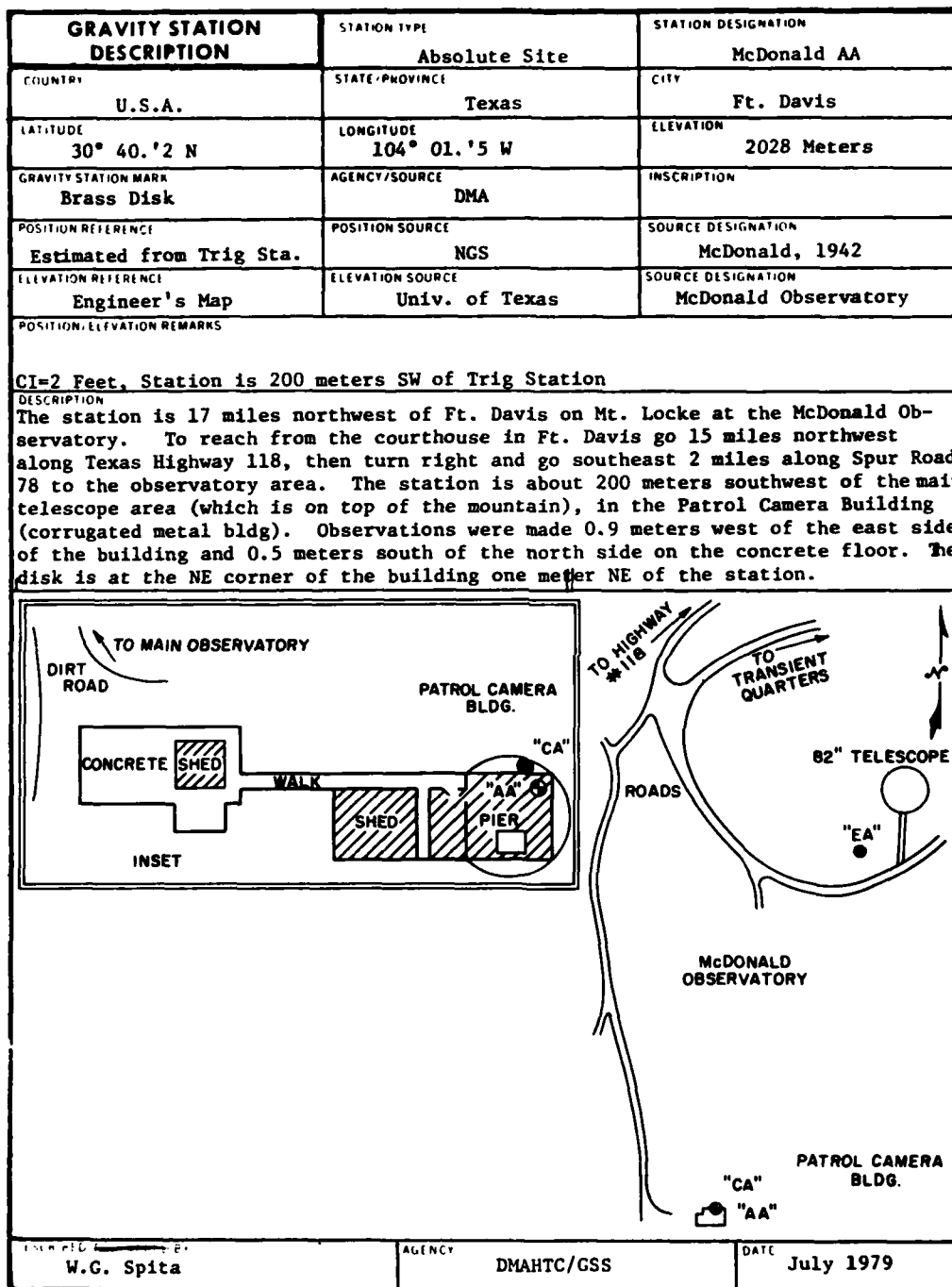


Figure 21. Gravity Station Description: McDonald AA

## 5.2 Gravity Values

Table 1 is a tabulation of the AFGL absolute gravity measurements. The values given are reduced to the pier (or floor) level and do not contain the Honkasalo correction. The table also includes the AFGL value obtained in 1981 at the Bureau International des Poids et Mesures (BIPM) in Sevres, near Paris, France.

The gravity value determined in 1970 with the original gravimeter design at the Hanscom AFB site (8) was  $980378.69 \pm 0.05$  mgal and the average value for the years 1978 to 1980 (Table 1) is  $980378.685 \pm 0.005$  mgal. Not only does this show that the original value was extremely good, but the confidence level has increased tenfold as well, and the stability of the site is excellent. Some of the reoccupied sites in Table 1 show relatively large differences in the measured values, and it is not known at this time if there was an actual change in gravity, a variable not fully accounted for, or systematic errors in the instrument not yet recognized.

Table 1. Summary of AFGL Absolute Gravity Measurements  
(Values in milligal reduced to floor (1.198 m), no Honkasalo correction)

	Absolute Value (mgal)	Gradient (mgal/m)
<u>Hanscom AFB, Mass. (Boston, Mass.)</u>		
27 Sep to 6 Oct 78	980378.678 ± 0.007	0.302
14 Aug 79 to 7 Sep 79	980378.687 ± 0.010	
20 Nov 79 to 6 Dec 79	980378.689 ± 0.010	
5 & 6 May 80	980378.688 ± 0.010	
7 Jul 80	980378.681 ± 0.010	
<u>NBS, Gaithersburg, Md. (new absolute site in non-magnetic laboratory)</u>		
13-14 Mar 80	980103.257 ± 0.009	0.325
<u>McDonald Observatory, Tex.</u>		
3-4 Jul 79	978828.655 ± 0.008	0.414
<u>Holloman AFB, N. Mex. (CIGTF)</u>		
6 Jul 80	979139.600 ± 0.010	0.285
14 & 31 May 80	979139.600 ± 0.008	
<u>Trinidad, Colo.</u>		
10-11 Jul 79	979330.370 ± 0.010	0.296
25-26 Oct 80	979330.393 ± 0.010	

Table 1. Summary of AFGL Absolute Gravity Measurements  
(Values in milligal reduced to floor (1.198 m), no Honkasalo  
correction) (Contd)

	Absolute Value (mgal)	Gradient (mgal/m)
<u>Denver, Colo.</u>		
27-29 Apr 79	979598.277 $\pm$ 0.010	0.292
<u>Mt Evans, Colo.</u>		
12-13 Jul 79	979256.059 $\pm$ 0.008	0.288
<u>Boulder, Colo. (JILA Site)</u>		
18-23 Oct 80	979608.601 $\pm$ 0.010	0.228
<u>Casper, Wyo.</u>		
15-17 Jul 79	979947.244 $\pm$ 0.025	0.263
<u>Sheridan, Wyo.</u>		
18-19 Jul 79	980208.912 $\pm$ 0.010	0.232
13-16 Oct 80	980208.964 $\pm$ 0.010	0.244
<u>Great Falls, Mont.</u>		
21-22 Jul 79	980497.311 $\pm$ 0.010	0.320
9-11 Oct 80	980497.367 $\pm$ 0.010	
<u>Vandenberg AFB, Calif.</u>		
3-4 Jun 80	979628.190 $\pm$ 0.017	0.321
<u>Lick Observatory, Calif.</u>		
6-8 Jun 80	979635.503 $\pm$ 0.010	0.415
<u>BIPM, France</u>		
18-30 Oct 81	980926.617 $\pm$ 0.010	0.251

Table 2 is a listing of absolute gravity values obtained from two different absolute gravity measuring systems at the collocated sites: Our system (AFGL) which, as described in the text, is a direct free-fall system; (Table 1) the JILA system which, as described in Reference 9, is a Chamber-Within-A-Chamber direct free-fall system; and the Istituto de Metrologia "G. Colonnetti" (IMGC) system, which is a symmetrical free-fall system [the object is catapulted

upward and its travel is timed as it rises and falls]. This system is described in more detail in References 11 and 12.

Table 2. Published Values of Absolute Gravity Measurements at Collocated Sites (References 11, 12, and 13). Values (reduced to the floor) are in milligal

Station	Instrument and Date			
	JILA		IMGC	
	1981	1982	1977	1980
Holloman AFB, N. Mex.		979139.615		979139.584
Vandenberg AFB, Calif.		979628.137		
Lick Observatory		979635.503		
Boulder, Colo. (JILA)	979608.568	979608.565		979608.498
Sheridan, Wyo.		980208.952		980209.007
Gaithersburg, Md. (NBS)		980103.259		
Hanscom AFB, Boston, Mass.		980378.697	980378.659	
Denver, Colo.	979598.322	979598.302	979598.268	
McDonald Obs., Tex.				978820.097
Great Falls, Mont.				980497.412

11. Marson, I., and Alasia, F. (1978) Absolute Gravity Measurements in the United States of America, AFGL-TR-78-0126, AD 057136.
12. Marson, I., and Alasia, F. (1980) Absolute Gravity Measurements in the United States of America, AFGL-TR-81-0052, AD A099017.
13. Zumberge, M. A., Faller, J. E., and Gschwind, J. (1983) Results from an absolute gravity survey in the United States, J. Geophys. Res. 88(No. B9).

## 6. DESCRIPTION OF ORIGINAL EQUIPMENT

The original configuration, shown in Figure 4, does not differ greatly in principle from the final version. It consists of a vacuum chamber containing the dropped object or more descriptively, the moving mirror in the Michelson interferometer. Also visible in the figure is the rack of electronics that includes the counting and timing electronics, data processor, power supplies, and robot control. Also shown is the isolating seismometer on top of the vacuum chamber. [Figure 4 (2) and the supporting pillars Figure 4 (4)].

The original system was a Michelson interferometer with two cube corner reflectors – one held stationary as the reference reflector, the other being dropped. The interference fringe pattern between the two was converted to electrical signals with a photomultiplier, and then counted electronically-yielding distance in terms of the wavelength of light. An electronic scaler was gated ON and OFF, and the number of fringes during the predetermined ON time was counted. The ON/OFF time was preset on a precision time standard. This method required interpolation of the fractional part of the fringe interval and also had an ambiguity of  $1/2$  wavelength of the light.<sup>8</sup> The average velocity was then determined by knowing the time interval and the measured distance.

Some features have been continued in the present apparatus. The data processor accepted the data and performed the necessary calculations for determining the value of gravity  $g$ . The processor was not capable of performing all of the corrections. The data were examined manually to determine if they were in error by  $1/2$  wavelength (the ambiguity mentioned previously) and a correction was then applied to correct this deficiency.

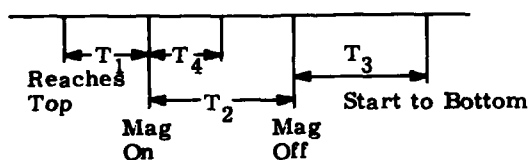
The robot controller is responsible for controlling the mechanical operation of the dropped object. The robot and controller performs the following operations:

1. Pick up the dropped object from its resting position.
2. Bring it to the top of the chamber.
3. Position it into the V grooves.
4. Turn on the solenoid to hold the dropped object in place.
5. Back-down to pull the fingers out of the way.
6. Turn off the solenoid to release the object for its free-fall.
7. Return to bottom of the chamber for the next cycle.

The timing of these operations are adjustable by front panel controls (see Figure B4). This procedure can be repeated continuously at variable rates of once every 30 sec to once every three minutes. These time intervals can be changed using different time-delay relays.

The speed of the robot is controlled by the Carriage Robot Speed Control [Figure B4, (3)] and the timing of the various functions are controlled by the setting of the front panel controls,  $T_1$ ,  $T_2$ ,  $T_3$ , and  $T_4$  [Figure B4, (5), (6), (7), (8)] and the Slow control [Figure B4, (10)]. The times ( $T_N$ ) are explained with reference to the following diagram and Figure B4.

#### Relay Timing



$T_4$  must be less than  $T_2$ .

$T_1$  [Figure B4, (5)] = The time from when the carriage reaches the top of the chamber until the solenoid turns ON: variable from 1 to 10 sec. [Full CCW to full CW position.]

$T_2$  [Figure B4, (6)] = The time from solenoid ON to solenoid OFF: variable from 1 to 10 sec. [Full CCW to full CW position.]

$T_3$  [Figure B4, (7)] = The time from solenoid OFF (drop of object) to start of robot to return to bottom to pick up dropped object: variable from 1 to 10 sec.

$T_4$  [Figure B4, (8)] = Time from solenoid ON until carriage backs down (to remove fingers from the path of the dropped object). Note that  $T_4$  must be less than  $T_2$ .

Slow [Figure B4, (10)] = The time the carriage backs off. Since this is a timing function, the distance travelled during this time is dependent on the carriages speed, which is controlled by the Speed Control [Figure B4, (3)]. Because of the mechanical design, the distance the carriage backs off is somewhat critical, so  $T_4$  must be adjusted in conjunction with the speed control.

As previously noted, one reflector is dropped inside of a vacuum chamber. This is done for two reasons: (1) the object would flutter as a result of differential air drag causing loss of signal and (2) slowing of the dropped object due to air drag, both of which give erroneous results. Loss of signal due to flutter [flutter could be eliminated or sufficiently reduced by aerodynamic design of the dropped object] obviously produces faulty values in the data, while incorrect data caused

by slowing of the dropped object could be corrected for, if it was a consistent error (bias). It was shown Reference (8) that in the range of  $10^{-3}$  mm of Hg "... the effect is quite closely proportional to pressure...", and at this pressure the effect is about 15 mgal. Even if the effective correction was calibrated, the precision with which the pressure would need to be known (at the time of each drop) would be unreasonable in field equipment — especially at the level of precision expected from this system. The differential pressure within the dropping chamber [which was considered in Reference 8] and the difference in turbulence from drop-to-drop necessitates a vacuum chamber to reduce these effects as much as possible. The data taken with this system were at a pressure of about  $10^{-6}$  mmHg, yielding a theoretical correction<sup>8</sup> of +0.007 mgal, which was used as a correction throughout this phase of development.

As stated above, in the Michelson interferometer approach, one reflector is dropped with the other held stationary — stationary with respect to what? If the reflector is held stationary to the earth's surface it is not stationary with respect to the earth's center-of-mass due to seismic disturbances, both natural and cultural. This movement of the fixed reflector introduces noise or scatter in the data both during an individual measurement (drop) and from measurement to measurement. The higher frequency microseisms cause the fixed reflector to move during a single drop and the longer period seismic noise causes the reflector to be in a different position from one drop to another resulting in different values. If the seismic noise is random, a sufficient number of measurements could be taken to arrive at the correct value. Two disturbing aspects of this approach are: (1) it may not be random and (2) the noise may be so high in some areas that a sufficiently large number of measurements is impractical. Seismic noise can be either corrected for, or eliminated, or at least reduced to a satisfactory level. Ideally, it would be best to eliminate all disturbing sources causing the reference reflector to move with respect to the earth's center of gravity. The method chosen was to affix the reference reflector to the stabilized mass of a long period seismometer. Although it would be desirable to have a period sufficiently long to eliminate even the effects of tidal gravity changes (these effects will be discussed later), the minimum acceptable condition is to reduce the effects of the high-frequency seismic disturbances — those on the order of 10 Hz, which cause the reference reflector to move during a single measurement (drop), which takes about 0.2 sec.

Ideally, the seismometer approach should eliminate the shaky earth-surface problem, but due to (magnetic) materials used in off-the-shelf equipment it was necessary to shield and separate, as much as possible, the seismometer from other parts of the gravity measuring apparatus. The approach and solution to



the problems encountered in the original equipment are given in more detail in Reference 8.

As indicated above, some geographical areas are more seismically active than others so, at seismically quiet sites, some of the data were gathered with the seismometer pinned (not allowed to oscillate) resulting in a slightly higher scatter but with more consistent values.<sup>8</sup> Other modifications to the system to reduce seismic effects are discussed in Section 4, PROTOTYPE OF SELECTED SYSTEMS.

As previously stated, the use of a cube corner reflector can introduce errors due to changes in the optical path length, if the reflector rotates. Therefore constraints, both optical and mechanical, are placed on the dropped object package. Since solid cube corners are used, the quality, or constancy of the index of refraction, of the material used must be of the highest grade.

The three reflecting surfaces must be orthogonal since not only do the deviations in the angles produce two or more divergent beams, but there will also be (1) a displacement of the reflected beam causing transfer and possible loss of the interfering beam, (2) shearing of the two beams resulting in error due to an apparent wavelength shift since the wavefronts have some finite curvature, and (3) a verticality error yielding an incorrect value of  $g$ . As derived in Reference 8 the optical center of the cube corner must coincide with the mechanical center-of-mass of the dropped object package, since it is desirable to keep the effects of rotation to a minimum. It is impractical to remove rotation completely since a rotational velocity of  $10^{-2}$  radian per second represents an error of only one part in  $10^8$  of  $g$ . In practice one can do much better than this if care is taken to make the optical and mass centers coincide. See Appendix C for the method used to place the optical center of the center-of-mass. The optical surface should also be flat to better than  $1/10 \lambda$  (our specifications were  $1/20 \lambda$ ).

As indicated above, verticality is an important factor. If the three reflecting surfaces of the reflector are not orthogonal, the above problems will be encountered due to non orthogonality, but the verticality of the light beam in the interferometer is equally important. Verticality of the light beam entering the free-fall chamber is extremely important since a deviation from the direction of free-fall and light paths results in a cosine error in length measurement. (Free-fall implies that  $g$  is the only force acting on the mass,  $m$ , and therefore the motion is vertical.)

A small deviation from the vertical by an angle  $\theta$  results in an error given by the equation:

$$\Delta g = -g \frac{\theta^2}{2} .$$

Therefore,  $\theta$  should be no greater than about  $10^{-5}$  rad. This can be accomplished very effectively by reflecting the light beam, after reflection from the cube corner in the dropping chamber, from a mercury pool, and adjusting the light path such that it returns through the spatial filter (see Figure B33) thus ensuring verticality. For a detailed vertical alignment procedure see Appendix B.

## 7. CHAMBER-WITHIN-A-CHAMBER

The first generation system described above utilized a long dropping path in order to reduce length measurement uncertainty, that is, a length measurement error (fixed error) results in a larger proportion of a short length than a long length. The long dropping path also required a large volume (required diameter being equal) to evacuate. This in turn required a large, and massive vacuum pump to achieve and maintain the required vacuum to reduce errors introduced by air drag at higher pressures. Figure 22 depicts the size difference of the original and chamber-within-a-chamber systems. In an effort to reduce the high vacuum requirement and thereby reduce pressure dependent errors, a chamber-within-a-chamber approach was conceived, constructed, and tested. This approach entailed allowing the dropped object to be in free-fall inside a chamber, which was separated from the dropped object but also in free-fall inside another vacuum chamber, thus carrying residual air molecules along with it (Figure 22). This approach was to have the advantage of operating at a higher pressure ( $10^{-3}$  to  $10^{-4}$  mmHg) without concern of introducing air drag errors and was to have the added advantage of a less massive vacuum pump and chamber, which would make the system more manageable for a portable system. It is also noted that advancements in timing electronics and computer capabilities had also allowed a shorter dropping path, which was also advantageous to reducing the vacuum chamber volume, allowing the design of a less massive and bulky system.

One of the problems encountered with this system was the separation of the falling chamber from the dropped object of interest. Experiments were made to determine if the dropped object and falling chamber were actually separating. Pictures were taken using a strobe light to obtain stop-motion at various positions during the drop. These experiments revealed that separation was taking place but the separation distance was not constant during the fall, nor was it repeatable from drop-to-drop. [If the separation distance had been repeatable, the results would be a biased value with low scatter, which was not the case.] Although a higher vacuum tended to give more consistent results with lower scatter, the separation distance still was not constant, indicating that drag forces inside the falling chamber were present due to a relative velocity between the two falling

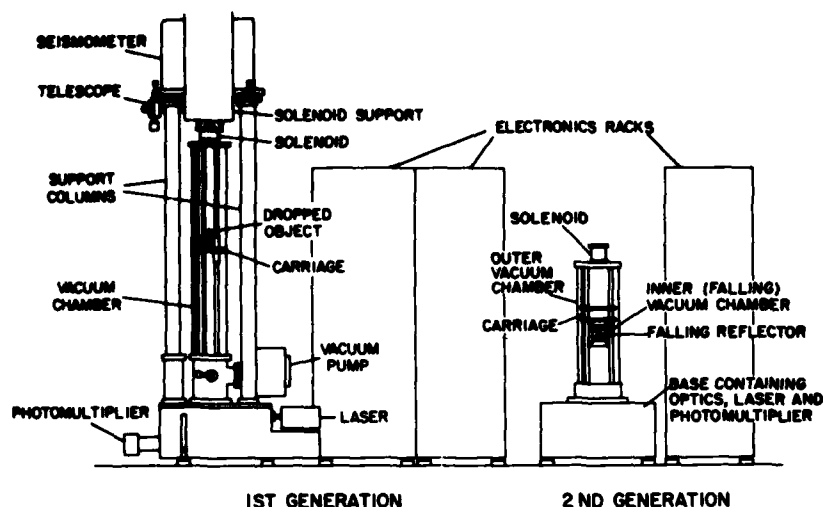


Figure 22. Laser Interferometer Absolute Gravity Instrument

bodies caused by residual air<sup>9</sup> or electrical charge differences between the two bodies and/or residual magnetism. Repeated demagnetization of various components showed little or no improvements. All possible parts of the system were electrically grounded up until the time of release of the objects and, the system was symmetrized as much as possible to minimize the dependence of capacitance on position.

Since a higher vacuum improved system performance, but not to the extent expected, other causes were investigated. One possibility was varying changes in the optical path that could be induced as the light passes through the entrance window of the rotating falling chamber. Although precautions taken into account during the design of the system included specifying and verifying plane parallel windows for all laser entrance/exit paths, error could still be induced if the window rotated. The aforementioned photographs revealed the dropping chamber was indeed rotating. Since it is extremely difficult to assure that the object will not rotate, the plane parallel window was replaced with a pellicle to all but eliminate the path length inside the window. This modification improved system performance considerably but it still failed to meet expectations. Although it was felt that the remaining problems were not unsolvable, the experience gained led to the decision to discard the chamber-within-a-chamber approach. One compelling reason was that the required vacuum was close to that necessary for a less cumbersome, simple dropped object in a conventional vacuum chamber.

## References

1. Astin, A. V. (1968) Acceleration due to gravity at the National Bureau of Standards, J. Res. Natl. Bur. Std. 72C (foreword to NBS Monograph 107 by D. R. Tate).
2. Cunningham, R. A., and Stalder, J. J. (1965) Charged Particle Gradiometer Research, Final Report, AD No. 614681, Martin Marietta Aerospace, Orlando, Fla.
3. Inderwiesen, F. H. (1971) Charged Particle Gravity Meter Research, Final Report, AD No. 783313, Martin Marietta Aerospace, Orlando, Fla.
4. Faller, J. E. (1967) The precision measurement of the acceleration of gravity, Science 158:60.
5. Cook, A. H. (1965) The absolute determination of the acceleration due to gravity, Metrolgia 1(No. 3):84-114.
6. Lenzen, V. F., and Multhauf, R. P. (1965) Development of gravity pendulums in the 19th century, U.S. Natl. Museum Bull. 240, paper 44.
7. Faller, J. E. (1963) An Absolute Interferometric Determination of the Acceleration of Gravity, Ph. D. Thesis, Princeton University, Princeton, N.J.
8. Hammond, J. A. (1970) A Laser-Interferometer System for the Absolute Determination of the Acceleration of Gravity, Joint Institute for Laboratory Astrophysics (JILA) Report No. 103, February.
9. Zumberge, M. A. (1981) A Portable Apparatus for Absolute Measurement of the Earth's Gravity, Ph. D. Thesis, University of Colorado.
10. Cabaniss, G. H., and Eckhardt, D. H. (1973) The AFGL Earth Tide Program, AFGL-TR-73-0084, AD 762275.
11. Marson, I., and Alasia, F. (1978) Absolute Gravity Measurements in the United States of America, AFGL-TR-78-0126, AD 057136.

12. Marson, I., and Alasia, F. (1980) Absolute Gravity Measurements in the United States of America, AFGL-TR-81-0052, AD A099017.
13. Zumberge, M.A., Faller, J.E., and Gschwind, J. (1983) Results from an absolute gravity survey in the United States, J. Geophys. Res. 88(No. B9).

## Bibliography

- (1983) Association International De Geodesie Bureau Gravimetrique International Bulletin D'Information No. 52.
- Baer, T., Kowalski, F.V., and Hall, J.L. (1980) Frequency stabilization of a 0.633- $\mu$ m He-Ne longitudinal Zeeman laser, Appl. Opt. 19(No.18):3173-3177.
- Bay, Z., and Luther, G.G. (1968) Locking a laser frequency to the time standard, Appl. Phys. Lett. 13:303.
- Cannizzo, G., Cerutti, G., and Marson, I. (1978) Absolute gravity measurements in Europe, Il Nuovo Cimento 1C(No. 1):39-85.
- Cerutti, G., Cannizzo, L., Sakuma, A., and Hostache, J. (1974) A Transportable Apparatus for Absolute Gravity Measurements, IMEKO Subcommittee, Measurement of Force and Mass, Fourth International Discussion Meeting on Recent Developments in Force Measuring Devices, UDINE.
- Clark, J.S. (1939) An absolute determination of the acceleration due to gravity, Phil. Trans. Roy. Soc. London, Ser. A 238:65-123.
- Cook, A.H. (1967) A new absolute determination of the acceleration due to gravity at the National Physical Laboratory, England, Phil. Trans. Roy. Soc. London, Ser. A 261:211-252.
- Cook, A.H. (1969) Gravity and the Earth, Wykeham Publications (London) Ltd.
- Cook, A.H., and Hammond, J.A. (1969) The acceleration due to gravity at the National Physical Laboratory (Note), Metrologia 5(No. 4):141-142.
- Dryden, H.L. (1942) A reexamination of the Potsdam absolute determination of gravity, J. Res. NBS 29:303-314.
- Egorov, K.N. (1963) Methods of determining the absolute value of gravity by interference measurements of a free-fall length, Izvestia Geophys., Ser. No. 9:1348-1356. Translated by Stephen B. Dresner.
- Faller, J.E. (1965) An absolute interferometric determination of the acceleration of gravity, Bulletin Geodesique, Arnee 1965(No. 77):203-204.

- Hamilton, A.C. (1957) World standards for gravity measurements, R.A.S.C.J. 57(No. 5):199-209.
- Hammond, J.A., and Faller, J.E. (1967) Laser-interferometer systems for the determination of the acceleration of gravity, IEEE J. Quantum Electronics QE-3(No. 11):597-602.
- Hammond, J.A., and Faller, J.E. (1974) A laser interferometer system for the absolute determination of the acceleration due to gravity, Proceedings of the International Conference on Precision Measurement and Fundamental Constants, D.N. Langenburg, and B.N. Taylor, (Editors), NBS Special Publication No. 343, U.S. Govt. Printing Office.
- Hammond, J.A., and Faller, J.E. (1971) J. Geo. Res. 76:7850.
- Faller, J.E., and Hammond, J.A. (1974) A new portable absolute gravity instrument, Bulletin D'Information, International Gravimetric Bureau, No. 35:1-43.
- Hammond, J.A. (1978) Bollettino Di Geofisica Teorica ed Applicata XX.
- Hammond, J.A., and Iliff, R.L. (1979) The AFGL absolute gravity system, Proceedings of the 9th GEOP Conference, October 2-5, 1978, Dept. of Geodetic Science Report No. 280, The Ohio State University, Columbus, Ohio; AFGL-TR-79-0128, AD A070432.
- Harrison, J.C. (1971) New Computer Programs for the Calculation of Earth Tides, Internal Report, Cooperative Institute for Research in Environmental Sciences.
- Jachens, R.C. (1978) Temporal gravity changes as applied to studies of crustal deformation, Proceedings of Conference VII, Stress and Strain Measurements Related to Earthquake Prediction, National Earthquake Hazards Reduction Program, pp. 222-243.
- Larden, D.R. (1980) Some geophysical effects on geodetic levelling networks, Proceedings of the Second International Symposium on Problems Related to the Redefinition of North American Geodetic Networks, Ottawa, Canada, pp. 151-167.
- Monchalín, J., Kely, M.J., Thomas, J.E., Kurnit, N.A., Szoke, A., Javan, A., Zernike, F., and Lee, P.H. (1975) Wavelength comparisons between lasers, Frontiers in Laser Spectroscopy, Balian et al (Editors), Session XXVII, 695-712.
- Prothero, W.W., and Goodkind, J.M. (1972) Earth-tide measurements with the superconducting gravimeter, J. Geophys. Res. 77(No. 5):926-937.
- Rinker, R.L., and Faller, J.E. (1981) Long period mechanical vibration isolator, Proceedings of the Second International Conference on Precision Measurement and Fundamental Constants, NBS, Gaithersburg, Md.
- Sakuma, A. (1970) Recent developments in absolute measurement of gravitational acceleration, NBS Special Publication No. 343, pp. 447-456.
- Schweitzer, W.G., Jr., Kessler, E.G., Jr., Deslattes, R.D., Layer, H.P., and Whetstone, J.R. (1973) Description, performance, and wavelengths of iodine stabilized lasers, Appl. Opt. 12(No. 12):2927-2938.
- Tate, D.R. (1968) Acceleration due to gravity at the National Bureau of Standards, J. Res. NBS, Vol. 72C(No. 1):1-20. (Available as NBS Monograph 107 from the U.S. Govt. Printing Office, Washington, D.C.)

Tate, D.R. (1969) Gravity Measurements and the Standards Laboratory, NBS (U.S.), Tech. Note 491, 10 pages.

Taylor, B.N., Parker, W.H., and Langenberg, D.N. (1969) The Fundamental Constants and Quantum Electrodynamics, Reviews of Modern Physics Monograph, Academic Press, N.Y.

Warburton, R.J., Beaumont, C., and Goodkind, J.M. (1975) The effect of ocean tide loading on tides of the solid earth observed with the superconducting gravimeter, Geophys. J. Roy. Astro. Soc. 43:707-720.

Warburton, R.J., Beaumont, D., and Goodkind, J.M. (1977) The influence of barometric-pressure variations on gravity, Geophys. J. Roy. Astro. Soc. 48:281-292.

Whitcomb, J.H., Wolfgang, O.F., Given, J.W., Pechman, J.C., and Ruff, L.J. (1980) Time-dependent gravity in Southern California, May 1974 to April 1979, J. Geophys. Res. 85(No. B8):4363-4373.



## Appendix A

### Computer Program

The on-line computer used with the present absolute-gravity measuring instrument is the Hewlett Packard 9825B and, therefore, uses HPL programming. The following pages give a listing of the program used and then the program, along with a step-by-step explanation of the functions of the programs. Some functions are self-explanatory and, therefore, have no comments. The Computer Device Codes and their Functions, as used in the program, and the Special Function keys, as presently programmed, are also given.

#### A1. PROGRAM LISTING

File 0

```
0: dsp "I like the way you turn me on!"  
1: trk 0;ldk 3;ldp 5  
*27681
```

File 1

```

0: fxd 3;wti 0,10;wti 6,3
1: ent "approx. starting data file",V;0+r31
2: dim E$(92),B$(92),C$(92);buf "axes",B$,1;buf "grid",C$,1;buf "data",E$,1
3: trk r31;fdf V;idf V,A,B,C;if A>0;V+1+V;gto +0
4: dim R(440),S$(15),L$(20),L(2),D$(12),P(7),V(20),A$(11),Y$(4),V$(13)
5: 2.59273306112e15/1.024+L;0+I+R+r30;1982+Y;" set summary"+S$
6: dim M$(36);"JanFebMarAprMayJunJulAugSepOctNovDec"+M$
7: "Hanscom AFB,MA "→L$;dsp L$;42.45→L(1);-71.26→L(2)
8: dsp L$,L(1),L(2);wait 4000;fxd 0
9: cll /clock;C+D/60→U
10: M$(A*3-2,A*3)→D$(1);str(B)→D$(4);str(Y)→D$(6+min(int(B/10),.95))
11: dim T(500),Q(500),G(91);980378.5+G(91);dsp "date",D$
12: dim T$(2516);buf "ti",T$,3
13: for J=1 to 90;0+G(J);next J;0+R+I;for J=1 to 440;0+R(J);next J
14: fmt 8," ",c," ",f6.0;wrt 10.8,D$,int(U)*100+frc(U)*60
15: fxd 0;ppt D$,int(U)*100+frc(U)*60;fxd 3
16: 2.53196588e15+L;wti 0,10;wti 6,3;red 723,V$;wrt 703,"tb1"
17: wrt 703,"FN1GT1SS3MD2SA2S02AR1"
18: dsp "ready",G;buf "ti"
19: tfr 703,"ti",2500
20: if rds("ti")<0;gto +0
21: dsp "data xfer over"
22: val(V$(1,6))*10+val(V$(8,9))*-2.39+r30;if r30<2;r30*10+r30
23: cll /clock;A+M;C+D/60→U;fxd 0;str(B)→D$(4,6);gsb "tide"
24: for J=1 to 2490 by 5
25: num(T$(J+4))*256+num(T$(J+5))+N
26: 1+Q
27: if bit(5,num(T$(J+1)))=0;-1+Q
28: band(num(T$(J+1)),3)*65536+num(T$(J+2))*256+num(T$(J+3))+B
29: if B>131072;B-262144+B
30: (B/256+N*Q)*5+T(J/5+1)
31: if abs(T(J/5+1))>2.01e4;J+1+J
32: next J
33: 53+N;0+P+0;fxd 3
34: N+M;0+1+0;if 0>10;wait 17000;gto 16
35: -T(60)→Q(P+1);N*20000-T(61)→Q(P+2)
36: 3+J
37: Q(J-1)+T(J+58)+M*20000-T(J+59)→Q(J)
38: gto 44
39: (1/(Q(3)-Q(2)))-1/(Q(2)-Q(1)))/(Q(3)-Q(1))+X;if X<0;gto +5
40: if abs(N-53)>5;wait 15000;gto 16
41: X*L+X;dsp X,N;if abs(X-9.8)>.2;N+sgn(X-9.8)+N;gto 34
42: if abs(N-53)>4;wait 17000;gto 16
43: gto 48
44: Q(J)-2Q(J-1)+Q(J-2)→Q
45: if Q<-20000;M+1+M;gto 37
46: if Q>0;M-1+M;gto 37
47: gto 39
48: 1+N;0+A+B+C+D+E+F+H
49: for J=P+4 to P+439
50: Q(J-1)+T(J+58)+M*20000-T(J+59)→Q(J)
51: Q(J)-2Q(J-1)+Q(J-2)→Q

```

```

52: if Q<-20000;M+1+M;gto -2
53: if Q>0;M-1+M;gto -3
54: next J
55: Q[180]+Q
56: for K=1 to 439
57: Q[K]-Q+Q[K]
58: A+Q[K]Q[K]+A
59: B+KQ[K]Q[K]+B
60: C+Q[K]Q[K]+C
61: D+Q[K]Q[K]Q[K]+D
62: E+Q[K]Q[K]Q[K]Q[K]+E
63: F+Q[K]+F
64: H+N+H
65: N+1+N
66: next K
67: N-1+N
68: A-FH/N+H;B-HC/N+H;C+P;C-FF/N+H;D-PF/N+H;E-PP/N+H
69: (BC-AD)/(CE-DD)+G;(AE-BD)/(CE-DD)+V;(H-VF-GP)/N+S
70: L*G+1e5+G;prt G;beep;if abs(G-G[91])>1;gto 16
71: V*L/2e9+V;S*L/2e18+S
72: for J=1 to 439
73: Q[J]/1e9+Q
74: J*L/2e18-G/1e5*Q+2/2-V*Q-S+Q;if Q*1e10>10000;stp
75: Q*1e10+R[J]+R[J]
76: next J
77: if abs(G-G[91])>1;gto 16
78: I+1+I;G+V[I]
79: G-int(G[91]/10)*10+G
80: G[1]+G+G[1]
81: G[2]+G+G[2]
82: G[6]+G[5]+G[6]
83: if I<2;gto +2
84: G[1]/I+G[3];r(I/(1-I)*(G[2]/I-(G[1]/I)+2))+G[4];G[6]/I+G[7]
85: r30+Z+Z;if I<20;gto 16
86: R+1+R;0+I
87: fmt 1,6x,"set",2x,"time",4x,"g(avg)",3x,"TIDE",5x,"g(corr)",3x,"S.D.",z
88: fmt 3,f8.0,f7.0,f9.3,f6.1,e9.1,f6.0
89: fmt 2,3x,"wgt",3x,"pres",5x,"file",/
90: if R>1;gto +2
91: wrt 10.1;wrt 10.2
92: int(U)*100+frc(U)*60+G[25+R]+J
93: 1/(G[4]+2*100)+W
94: trk r31;idf V,A;if A>0;fdf V+1;gto +0
95: fxd 0;wrt 10.3,R,J,G[3],G[7],G[3]+G[7],G[4],W,Z*1e-7/20,V
96: J+P[1];G[3]+P[2];G[7]+P[3];G[3]+G[7]+P[4];G[4]+P[5];W+P[6];Z*1e-7+P[7]
97: mrk 1,236;rcf V,D$,P[*],V[*]
98: fxd 0;prt "set #",R,"time",int(U)*100+frc(U)*60;fxd 3
99: prt "g(avg)=",G[3],"s.d.",G[4],"tide=",G[7];flt 1;prt "P=",Z*1e-7/20
100: G[3]+G[10+R];fxd 3
101: G[4]+G[40+R];G[7]+G[70+R];0+G[2]+G[1]+G[6]+Z
102: if R<15;wait 25000;gto 16
103: "summary":uti 0,10;uti 6,3;fxd 0;str(R)+S$[1,4]
104: fmt 5,"",c,"",c,f6.0,"",c
105: wrt 10.5,S$,D$,G[26],L$
106: for J=60 to 65;0+G[J];next J;0+G[90]
107: for J=1 to 15
108: if G[10+J]=0;gto +7
109: 1/(G[J+40]+2*100)+G[62]
110: G[60]+G[10+J]+G[62]+G[60]
111: G[61]+G[10+J]+2*G[62]+G[61];G[90]+G[70+J]+G[62]+G[90]
112: G[63]+G[62]+G[63];G[64]+1+G[64]
113: prt
114: next J;fxd 0;prt "time",G[24+J];fxd 3
115: fxd 3;G[60]/G[63]+G[60];G[90]/G[63]+G[90]
116: r((G[61]-G[63]+G[60]+2)/(G[63]-1))+G[65]
117: fmt 6,6x,"Weighted Avg=",f6.3," Avg Tide Corr.",f6.3," Sum Wgt's=",f4.1

```

```

118: wrt 10.6,G[60],G[90],G[63]
119: fxd 1
120: fnt 7,"      Corrected Value=",f12.3," mgal  s.e.=",f6.3
121: int(G[91]/10)*10+G[60]+G[90]+G
122: wrt 10.7,G,G[65]/rG[64]
123: G[26]+P[1];G[60]+P[2];G[90]+P[3];G[63]+P[4];G+P[5];G[65]/rG[64]+P[6]
124: trk r31;idf V,A;if A>0;fdf V+1;gto +0
125: 0+P[7];gto +2;trk r31;fdf V;mrk 1,3664;rcf V,R[*],S$,L$,L[*],D$,P[*]
126: fnt 8,"File # ",f4.0;wrt 10.8,V
127: wtb 10,10,10,10
128: trk 0;ldf 2
129: "time":icll 'clock'
130: fxd 0;dsp A,B,C,D,E;wait 10;gto 129
131: "clock":wrt 704,"C";red 704,A;fxd 0;str(A)+A$
132: val(A$[1,2])+A;val(A$[3,4])+B;val(A$[5,6])+C;val(A$[7,8])+D;val(A$[9])+E
133: net
134: "time9":wrt 9,"R";red 9,A,B,C,D,E;dsp B,A,C,D,E;gto +0
135: "tide":deg;fxd 3
136: (Y-1900)365+int((Y-1901)/4)+int(int(Y/4)/(Y/4))int(min(1,M/3))+A
137: A+(M-1)30+int((M+int((M-1)/8))/2)-2+2(int(2/M)-int(1/M))+B+D
138: L[1]+N;L[2]+E
139: D-.5+U/24+T
140: N-.1921sin(2N)+P
141: -360frc(-.719953+.000147094228T)+r1
142: 360frc(.822513+.036291645685T)+r2
143: 360frc(.995766+.002737778519T)+r3
144: 360frc(.031252+.036748195692T)+r4
145: 360frc(.974271+.033863192198T)+r5
146: r1+r4+r6
147: r6-r5+r7
148: 1.0047+.1644'cs'(1,0,0,0)+.0315'cs'(1,0,0,-2)+.0266'cs'(0,0,0,2)+A
149: A+.0134'cs'(2,0,0,0)+.0042'cs'(1,0,0,2)+r8
150: 1+.0502'cs'(0,1,0,0)+r9
151: 6.289'sn'(1,0,0,0)-1.274'sn'(1,0,0,-2)+.658'sn'(0,0,0,2)+A
152: A+.214'sn'(2,0,0,0)-.185'sn'(0,1,0,0)-.115'sn'(0,0,2,0)+r6+r10
153: 1.917'sn'(0,1,0,0)+r7+r11
154: 5.128'sn'(0,0,1,0)+.281'sn'(1,0,1,0)-.278'sn'(-1,0,1,0)+A
155: A-.173'sn'(0,0,1,-2)+r12
156: 2.486sin(2r7)-1.797cos(r7)-.408sin(r7)+r13
157: E+15U+r7+180+r14
158: r13+r14-r7+r15
159: asn(.3979sin(r11))+r16
160: 'fox'(r16,P,r15)+r17
161: cos(r12)cos(r10)+r19
162: 'fox'(r12,-23.45,90-r10)+r20
163: if r19=0;jmp 3
164: atn(r20/r19)+r21
165: jmp 2
166: 0+r21
167: if r19<0;180+r21+r21
168: 'fox'(r12,66.55,90-r10)+r22
169: asn(r22)+r23
170: r14-r21+r24
171: 'fox'(r23,P,r24)+r25
172: 1.16(25.25r9(3r17+2-1)+54.99r8(3r25+2-1+.025(5r25+3-3r25)))/1000+G[5]
173: net
174: stp
175: "cs":
176: net cos(p1+r2+p2+r3+p3+r4+p4+r5)
177: "sn":
178: net sin(p1+r2+p2+r3+p3+r4+p4+r5)
179: "fox":
180: net sin(p1)sin(p2)+cos(p1)cos(p2)cos(p3)
181: tlist
*14354

```

File 2

```

0: wtb 701,12
1: fxd 3;wtb 701,10,27,"0n126c8d8e8f8g8h8i8j8k73142m28n80"
2: fxd 0;fmt 1,18x,f3.0," sets, File number",f4.0," ",",c;wrt 701.1,R,V,D$
3: wrt 701
4: 9.8+.000002*rnd(W)+G
5: 2.53196588e-3+L;1.25e-7+A;.015489796+D
6: fxd 0
7: for J=1 to 440
8: D+J*L/G+B
9: rB-rD-A(rB+r3-rD+r3)+Q[J]
10: next J
11: 1+N;0+A+B+C-D+E+F+H
12: for K=1 to 440
13: A+NQ[K]+A
14: B+NQ[K]Q[K]+B
15: C+Q[K]Q[K]+C
16: D+Q[K]Q[K]Q[K]+D
17: E+Q[K]Q[K]Q[K]Q[K]+E
18: F+Q[K]+F
19: H+N+H
20: N+1+N
21: next K
22: N-1+N
23: A-FH/N+A;B-HC/N+B;C+P;C-FF/N+C;D-PF/N+D;E-PP/N+E
24: (BC-AD)/(CE-DD)+G;(AE-BD)/(CE-DD)+V;(H-VF-GP)/N+S
25: fxd 5;L+G+G;V*L/2+V;S*L/2+S
26: for J=1 to 440
27: J*L/2-G+Q[J]*Q[J]/2-V*Q[J]-S+T[J];T[J]*1e10+T[J]
28: next J
29: buf "data";buf "axes";buf "grid"
30: wtb 701,27,"&a30C",27,"1",13
31: wtb 701,9,"Residuals-(Angstroms)",13,10,27,"3"
32: for J=1 to 76;wtb "data",0;wtb "axes",255;wtb "grid",0;next J
33: buf "grid"
34: for J=1 to 46
35: char(2*(7-int(J*1.65*8)mod8))+C$(int(J*1.65),int(J*1.65))
36: next J
37: buf "data";buf "axes";buf "grid"
38: 5+H;0+P
39: for T=1 to 429
40: for J=T to T+10;C+R[J]+C;next J;C/(R*200)+C;fxd 0
41: (C+20)*1.65+r1;(T[T]+20)*1.65+r2;cll 'plt'(r1,r2)
42: buf "data";buf "axes";buf "grid"
43: if T=90;wtb 701,27,"&l0S";wrt 701," Position (CM) ",char(126)
44: wtb 701,27,"&l12S"
45: 0+C;next T
46: ldf 1,0,13
47: "plt";T*100*L/2+Q
48: wtb "data",27,"*b70W";wtb "axes",27,"*b70W";wtb "grid",27,"*b70W"
49: if T>1;gto +3
50: fmt 1,"-20",15x,"-10",18x,"0",17x,"10",17x,"20";wrt 701.1
51: for J=1 to 3;wtb 701,C$;next J;wtb 701,B$
52: int(p1)+r3;frc(p1)+r4;int(p2)+r5;frc(p2)+r6
53: if int(Q+.6)*M or P#0;gto 57
54: fmt 1,36x,f2.0;wtb 701,27,"&l0S";wrt 701.1,M
55: wtb 701,27,"&l12S";1+P
56: gto 58
57: char(32)+E$(41,41);char(0)+E$(40,40)
58: if r3+8#41;gto 60
59: 32+N
60: char(ion(N,2*(7-int(r4*8))))+E$(r3+8,r3+8)

```

```

61: char(ion(num(E$(r5+8,r5+8)),2↑(7-int(n6*8))))→E$(r5+8,r5+8]
62: if int(Q)=M;char(1)→E$(40,40];char(252)→E$(41,41];M+5→M
63: utb 701,E$
64: char(0)→E$(r3+8,r3+8]→E$(r5+8,r5+8];char(32)→E$(41,41]
65: 0→N
66: if int(Q)=M-4;0→P
67: ret
*32535

```

File 4

```

0: "CLOCK DATE/TIME SET-UP 59309-16002 rev A":
1: dim D[12],T$[20]
2: 0→D[1];31→D[2];59→D[3];90→D[4];120→D[5];151→D[6]
3: 181→D[7];212→D[8];243→D[9];273→D[10];304→D[11];334→D[12]
4: 704→C;1→M→D→H→N;0→S
5: 731→B
6: dsp "MONTH",M;ent "",M
7: dsp "DAY",D;ent "",D
8: dsp "HOUR",H;ent "",H
9: dsp "MINUTES",N;ent "",N
10: dsp "SECONDS",S;ent "",S
11:
12: cmd C,"RP"
13: for I=1 to D[M];utb B,68;next I
14: for I=1 to D-1;utb B,68;next I
15: for I=1 to H;utb B,72;next I
16: for I=1 to N;utb B,77;next I
17: for I=1 to S;utb B,83;next I
18: dsp "PRESS CONTINUE TO START CLOCK";stp
19: cmd C,"T"
20: fnt ;red C,T$
21: dsp "THE TIME IS ",T$
22: gto -2
*27367

```

File 5

```

0: utb 701,27,"&n92c30g16h16j48k16L",13,10
1: utb 701,27,"&n94c8f28g42h8i8j8k8L",13,10
2: utb 701,27,"&n125c8g4h62i4j8k",13,10
3: ldp 1
*10846

```

## A2. EXPLANATION OF PROGRAM

### Main Program (HPL for the 9825B Computer)

File 0:

File 0: This is an introductory file that also loads the remaining programs.

```
0: dsp "I like the way you turn me on!"
1: trk 0;ldk 3;ldp 5
```

### Main Program

File 1

Lines 0, 1: Allows fast forward to data file.

```
0: fxd 3;uti 0,10;uti 6,3
1: ent "approx. starting data file",V;0+r31
```

Line 2: Dimensions plot buffers.

```
2: dim E$(92),B$(92),C$(92);buf "axes",B$,1;buf
    "grid",C$,1;buf "data",E$,1
```

Line 3: Finds First empty data file.

```
3: trk r31;fdf V;idf V,A,B,C;if A>0;V+1+V;gto +0
```

Line 4: Dimensions the following:

```
4: dim R[440],S$(15),L$(20),L[2],D$(12),P[7],V[20],A$(11),Y$(4),V$(13)
```

R[440] = the residuals from the least squares fit.

S\$(15) = "% set summary" used in the plot program.

L\$(20) = the name of the site [REM statement].

L[2] = the latitude and longitude of the site.

D\$(12) = date and time.

P[7] = data for recording on tape.

V[20] = 20 values of gravity for a 20 drop set.

Line 5: Defines the following variables:

```
5: 2.59273306112e15/1.024+L;0+I+R+r30;1982+Y;"    set summary"+S$
```

L = wavelength value:  $\times 4000 \times 10^{18}$

=  $6.3299147 \times 10^{-7}$  meters  $\times 4096/1.024 \times 10^{18}$

[ $10^{18}$  is required since times are in nanoseconds]

I = counter ← number of drops.

R = counter ← number of 20 drop sets.

r30 = counter ← number of total drops.

Line 6: Dimensions the following:

```
6: dim M$(36); "JanFebMarAprMayJunJulAugSepOctNovDec" → M$
```

M\$(36) = month abbreviations

Line 7: Loads site, latitude, and longitude. (Must be changed for each site.)

```
7: "Hanscom AFB, MA " → L$; dsp L$; 42.45 → L[1]; -71.26 → L[2]
```

Line 8: Display to allow checks.

```
8: dsp L$, L[1], L[2]; wait 4000; fxd 0
```

Lines 9, 10: Loads date and time.

```
9: cll 'clock'; C → D/60 → U
```

```
10: M$(A*3-2, A*3) → D$(1); str(B) → D$(4); str(Y) → D$(6+min(int(B/10), .95))
```

Line 11: Dimensions the following:

```
11: dim T(500), Q(500), G(91); 980378.5 → G[91]; dsp "date", D$
```

T(500) = residuals plotted as a smooth curve.

Q(500) = time values used in least squares.

Array G(91) = various g values (line 100).

Value G(91) = approximate value of g in milligals.

Line 12: Dimensions the following:

```
12: dim T$(2516); buf "ti", T$, 3
```

T\$(2516) = buffer for data from counter.

Lines 13, 14: Writes data and time on computer terminal.

```
13: for J=1 to 90; 0 → G[J]; next J; 0 → R → I; for J=1 to 440; 0 → R[J]; next J
```

```
14: fmt 8, " ", "c, " ", f6.0; wrt 10.8, D$, int(U)*100+frn(U)*60
```

Line 15: Print command for date and time.

```
15: fxd 0; prt D$, int(U)*100+frn(U)*60; fxd 3
```

Lines 16-19: Reads 5370A (clock) when data are being transferred.

```
16: 2.53196588e15 → L; wti 0, 10; wti 6, 3; red 723, V$; wrt 703, "tb1"
```

```
17: wrt 703, "FN1GT1SS3MD2SA2S02AR1"
```

```
18: dsp "ready", G; buf "ti"
```

```
19: tfr 703, "ti", 2500
```



Lines 20-22: Loads pressure value.

```
20: if rds("ti")<0; goto +0
21: dsp "data xfer over"
22: val(Vs[1,6])*10+val(Vs[8,9])*-2.39+r30; if r30<2;r30*10+r30
```

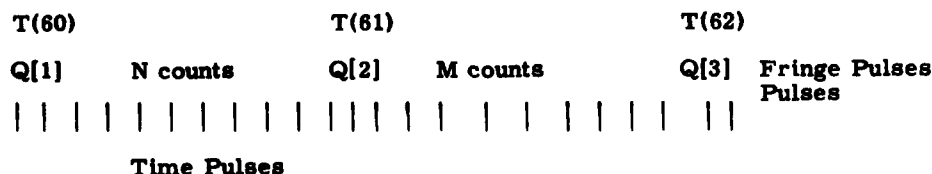
Line 23: Reads clock and goes to tide subroutine.

```
23: cll 'clock'; A+M; C+D/60+; :xd 0; str(B)+D$[4,6]; gsb "tide"
```

Lines 24-32: Unpacks string T\$, which is a buffer for data sent from 5370A [routine from 5370A Manual].

```
24: for J=1 to 2490 by 5
25: num(T$[J+4])*256+num(T$[J+5])*N
26: 1+Q
27: if bit(5,num(T$[J+1]))=0;-1+Q
28: band(num(T$[J+1]),3)+65536+num(T$[J+2])*256+num(T$[J+3])*B
29: if B=131072;B-262144+B
30: (B/256+M+Q)*5+T[J/5+1]
31: if abs(T[J/5+1])>2.01e4;J+1+J
32: next J
```

Lines 33-47: Routine to determine the number of clock pulses occurring between the first three fringe pulses - starts at 53:



Q[1] is the 60th time value obtained by the 5370A (T[60]). Starts with 53 for both N and M. Then attempts to calculate a reasonable value for g by using the three short time values and N and M.

$$Q[1] = - T[60]$$

$$Q[2] = N \times 20000 - T[61]$$

$$Q[3] = M \times 20000 + Q[2] + T[61] - T[62]$$

Lines 44, 45, and 46 prevents differences of Q[1]'s from being larger than 20000 nsec (20000 nsec is time between clock pulses).

As noted, the routine starts with 53 for both N and M, then attempts to calculate a reasonable value for g using the three short-time values and N and M. The Q[1]'s are times measured from the arbitrary starting time of the first clock pulse following the 60th fringe after the object is released.

At line 43 the program goes to line 48 when everything is as it should be, that is, the N and M for the first two intervals give a value for  $G = 0.2 \text{ M/sec}^2$  (or less) from  $9.8 \text{ m/sec}^2$ . The "if" statements with "wait"s in them send the program back to a ready mode if the data yield an unreasonable value for g.

```

33: 53+N;0+P+0;f*d 3
34: N+M;0+1+0;if 0>10;wait 17000;gto 16
35: -T[60]+Q[P+1];N*20000-T[61]+Q[P+2]
36: 3+J
37: Q[J-1]+T[J+58]+M*20000-T[J+59]+Q[J]
38: gto 44
39: (1/(Q[3]-Q[2]))-1/(Q[2]-Q[1]))/(Q[3]-Q[1])*X;if X<0;gto +5
40: if abs(N-53)>5;wait 15000;gto 16
41: X*L+X;dsp X,N;if abs(X-9.8)>.2;N+sgn(X-9.8)*N;gto 34
42: if abs(N-53)>4;wait 17000;gto 16
43: gto 48
44: Q[J]-2Q[J-1]+Q[J-2]+Q
45: if Q<-20000;M+1+M;gto 37
46: if Q>0;M-1+M;gto 37
47: gto 39

```

Lines 48-54: This section goes through the rest of the time values assigning values to Q[I] based on the assumption that the time between successive fringe pulses decreases but does not change by more than 20000 nsec in each interval. It must allow for the fact that the number of pulses may increase even though the total time between fringes is always decreasing.

```

48: 1+N;0+A+B+C+D+E+F+H
49: for J=P+4 to P+439
50: Q[J-1]+T[J+58]+M*20000-T[J+59]+Q[J]
51: Q[J]-2Q[J-1]+Q[J-2]+Q
52: if Q<-20000;M+1+M;gto -2
53: if Q>0;M-1+M;gto -3
54: next J

```

Lines 55-71: Least square fit of the distance dropped (proportional to K) as quadratic function of time (Q[K] - Q[180]). The Q(I) are from lines 35, 37, and 50 and the distances are N times the interval between fringe pulses ( $\frac{L}{10^{18}}$ ). Remember, L has a factor of  $10^{18}$  because the times at this point are in nanosec. Line 70 computes g in milligal ( $10^{-5} \times \text{m/sec}^2$ ). Line 71 computes initial velocity and starting position.

```

55: Q[180]+Q
56: for K=1 to 439
57: Q[K]-Q+Q[K]
58: A+KQ[K]+A
59: B+KQ[K]Q[K]+B
60: C+Q[K]Q[K]+C
61: D+Q[K]Q[K]Q[K]+D
62: E+Q[K]Q[K]Q[K]Q[K]+E
63: F+Q[K]+F
64: H+N+H
65: N+1+N
66: next K
67: N-1+N
68: A-FH/N+H;B-HC/N+H;C+P;C-FF/N+C;D-PF/N+D;E-PP/N+E
69: (BC-AD)/(CE-DD)+G;(AE-BD)/(CE-DD)+V;(H-VF-GP)/N+S
70: L*G*1e5+G;prt G;beep;if abs(G-G[91])>1;gto 16
71: V*L/2e9+V;S*L/2e18+S

```

Lines 72-76: Computes residuals that are the difference between the real data (position determined by using the number of fringes times the distance between fringes. The residual at each position for a drop is totaled with the residuals for that position in previous drops in line 75. Line 74 computes the residual for a particular position ( $J \times L/2e18$ ) using the  $g$ ,  $v$ , and  $s$  from the least squares calculation. That is the parabola that best fits the data is described by:  $x = s + vt + \frac{1}{2}gt^2$  by using the real  $t$ 's ( $Q[I]$ ) and the least-squares determined  $s$ ,  $v$  and  $g$ .

An estimated  $x$  value is calculated and compared with the real position. These residual differences are summed for a number of drops so averages can be determined (to observe systematic effects). Residuals from individual drops are not retained.

```
72: for J=1 to 439
73: Q[J]/1e9+Q
74: J*L/2e18-G/1e5+Q*2/2-V*Q-S+Q;if Q*1e10>10000;stp
75: Q*1e10+R[J]+R[J]
76: next J
```

Line 77: Defines the following:

```
77: if abs(G-G[91])>1;gto 16
```

If calculation of  $g > 1$  mgal from assumed local  $g$ , program resets. This can be changed if scatter is high.

Lines 78-85: Line 78 increments drop counter and loads  $g$  into  $V[I]$ . Line 79 converts  $g$  to smaller value by subtracting  $g(41)$  rounded to 10 milligal from calculated  $g$ . Lines 80-82 sums  $g$  and  $g^2$ , and line 85 keeps average, S.D., sum of tide correction ( $g[5]$ ). Line 85 instructs that if  $I$  (number of drops in current set) is less than 20 go back to take more data.

```
78: I+1;G+V[I]
79: G-int(G[91]/10)*10+G
80: G[1]+G+G[1]
81: G[2]+GG+G[2]
82: G[6]+G[5]+G[6]
83: if I<2;gto +2
84: G[1]/I+G[3];r(I/(I-1)*(G[2]/I-(G[1]/I)+2))+G[4];G[6]/I+G[7]
85: r30+2+2;if I<20;gto 16
86: R+1;R;0+1
87: fmt 1,6x,"set",2x,"time",4x,"g(avg)",3x,"TIDE",5x,"g(corr)",3x,"S.D.",z
88: fmt 3,f8.0,f7.0,4f9.3,f6.1,e9.1,f6.0
89: fmt 2,3x,"ugt",3x,"pres",5x,"file",/
90: if R>1;gto +2
91: wrt 10.1;wrt 10.2
92: int(U)*100+frn(U)*60+G[25+R]+J
```

Line 93: Computes weight  $\left(\frac{1}{(SD) 100}\right)$ . this relative weight is used to combine data with different scatter in a statistically correct manner.

93:  $1/(G[4]+2*100)+W$

Lines 94-96: Loads current data into array for recording on tape.

```
94: trk r31;idf V,A;if A>0;fdf V+1;gto +0
95: fxd 0;wrt 10.3,R,J,G[3],G[7],G[3]+G[7],G[4],W,Z*1e-7/20,V
96: J+P[1];G[3]+P[2];G[7]+P[3];G[3]+G[7]+P[4];G[4]+P[5];W+P[6];Z*1e-7+P[7]
```

Lines 97-98: Print on 9825 printer.

```
97: wrk 1,236;rcf V,D$,P[*],V[*]
98: fxd 0;prt "set #",R,"time",int(U)*100+frc(U)*60;fxd 3
```

Lines 99-101: Loads data from current set into array G[I]. Array G[I] (91 dimension) is used to hold a number of different data (for instance G[11]). G(10 + R) holds the average values for sets 1 to R. These are printed and recorded when getting a set summary or when 15 sets are obtained.

```
99: prt "g(avg)=",G[3],"s.d.=",G[4],"tide=",G[7];flt 1;prt "P=",Z*1e-7/20
100: G[3]+G[10+R];fxd 3
101: G[4]+G[10+R];G[7]+G[10+R];0+G[2]+G[11]+G[6]+Z
```

Lines 102-127: This section performs data summary. Line 125 is for recording on tape.

```
102: if R<15;wait 25000;gto 16
103: "summary":wti 0,10;wti 6,3;fxd 0;str(R)+S$[1,4]
104: fnt 5,"      ",c,"      ",c,f6.0,"      ",c
105: wrt 10.5,S$,D$,G[26],L$
106: for J=60 to 65;0+G[J];next J;0+G[90]
107: for J=1 to 15
108: if G[10+J]=0;gto +7
109:  $1/(G[J+40]+2*100)+G[62]$ 
110:  $G[60]+G[10+J]+G[62]+G[60]$ 
111:  $G[61]+G[10+J]+2*G[62]+G[61];G[90]+G[70+J]+G[62]+G[90]$ 
112:  $G[63]+G[62]+G[63];G[64]+1+G[64]$ 
113: prt
114: next J;fxd 0;prt "time",G[24+J];fxd 3
115: fxd 3;G[60]/G[63]+G[60];G[90]/G[63]+G[90]
116:  $r((G[61]-G[63]+G[60]+2)/(G[63]-1))+G[65]$ 
117: fnt 6,6x,"Weighted Avg=",f6.3," Avg Tide Corr.=",f6.3,"
      Sum Wgts=",f4.1
118: wrt 10.6,G[60],G[90],G[63]
119: fxd 1
120: fnt 7,"      Corrected Value=",f12.3," mgal s.e.=",f6.3
121:  $int(G[91]/10)+10+G[60]+G[90]+G$ 
122: wrt 10.7,G,G[65]/rG[64]
123:  $G[26]+P[1];G[60]+P[2];G[90]+P[3];G[63]+P[4];G+P[5];G[65]/rG[64]+P[6]$ 
124: trk r31;idf V,A;if A>0;fdf V+1;gto +0
125: 0+P[7];gto +2;trk r31;fdf V;wrk 1,3664;rcf V,R[*],S$,L$,L[*],D$,P[*]
126: fnt 8,"File # ",f4.0;wrt 10.8,V
127: wtb 10,10,10,10
```

Lines 128-134: Loads File 2: Plots Residuals, Returns (to line 3 of main program).

```
128: trk 0;ldf 2
129: "time"=cll 'clock'
130: fxd 0;dsp A,B,C,D,E;wait 10;gto 129
131: "clock"=urt 704,"C";red 704,A;fxd 0;str(A)>A$
132: val(A$[1,2])>A;val(A$[3,4])>B;val(A$[5,6])>C;val(A$[7,8])>D;
    val(A$[9])>E
133: ret
134: "time9"=urt 9,"R";red 9,A,B,C,D,E;dsp B,A,C,D,E;gto +0
```

Line 135-181: Tide correction subroutine.

```
135: "tide"=deg;fxd 3
136: (Y-1900)365+int((Y-1901)/4)+int(int(Y/4)/(Y/4))int(min(1,M/3))>A
137: A+(M-1)30+int((M+int((M-1)/8))/2)-2+2(int(2/M)-int(1/M))>B+D
138: L[1]+N;L[2]+E
139: D-.5+U/24+T
140: N-.1921sin(2N)>P
141: -360frc(-.719953+.000147094228T)>r1
142: 360frc(.822513+.036291645685T)>r2
143: 360frc(.995766+.00273778519T)>r3
144: 360frc(.031252+.036748195692T)>r4
145: 360frc(.974271+.033863192198T)>r5
146: r1+r4+r6
147: r6-r5+r7
148: 1.0047+.1644'cs'(1,0,0,0)+.0315'cs'(1,0,0,-2)+.0266'cs'(0,0,0,2)>A
149: A+.0134'cs'(2,0,0,0)+.0042'cs'(1,0,0,2)>r8
150: 1+.0502'cs'(0,1,0,0)>r9
151: 6.289'sn'(1,0,0,0)-1.274'sn'(1,0,0,-2)+.658'sn'(0,0,0,2)>A
152: A+.214'sn'(2,0,0,0)-.185'sn'(0,1,0,0)-.115'sn'(0,0,2,0)+r6+r10
153: 1.917'sn'(0,1,0,0)+r7+r11
154: 5.128'sn'(0,0,1,0)+.281'sn'(1,0,1,0)-.278'sn'(-1,0,1,0)>A
155: A-.173'sn'(0,0,1,-2)+r12
156: 2.486sin(2r7)-1.797cos(r7)-.408sin(r7)+r13
157: E+15U+r7+180+r14
158: r13+r14-r7+r15
159: asn(.3979sin(r11))>r16
160: 'fox'(r16,P,r15)>r17
161: cos(r12)cos(r10)+r19
162: 'fox'(r12,-23.45,90-r10)>r20
163: if r19=0;jmp 3
164: atn(r20/r19)>r21
165: jmp 2
166: 0+r21
167: if r19<0;180+r21+r21
168: 'fox'(r12,66.55,90-r10)>r22
169: asn(r22)>r23
170: r14-r21+r24
171: 'fox'(r23,P,r24)>r25
172: 1.16(25.25r9(3r17+2-1)+54.99r8(3r25+2-1+.025(5r25+3-3r25)))/1000+G[5]
173: ret
174: stp
175: "cs":
176: ret cos(p1*r2+p2*r3+p3*r4+p4*r5)
177: "sn":
178: ret sin(p1*r2+p2*r3+p3*r4+p4*r5)
179: "fox":
180: ret sin(p1)sin(p2)+cos(p1)cos(p2)cos(p3)
181: tlist
```

File 2

Lines 0-5: Routine to plot average residuals on 9876A printer.

```
0: wtb 701,12
1: fxd 3;wtb 701,10,27,"&n126c8d8e8f8g8h8i8j8k73142m28n80"
2: fxd 0;fmt 1,18x,f3.0," sets, File number",f4.0," ",c;urt 701.1,R,V,D#
3: urt 701
4: 9.8+.000002*rand(N)+G
5: 2.53196588e-3+L;1.25e-7+A;.015489796+D
```

Lines 6-10: Subroutine for computing artificial time values using an assumed gravity gradient.

```
6: fxd 0
7: for J=1 to 440
8: D+J*L/G+B
9: rB-rD-A(rB+3-rD+3)+Q[J]
10: next J
```

Lines 11-24: This section performs a least-squares calculation on the just computed time values. When a plot of the residuals is made, the T[J]'s make the smooth curve.

```
11: 1+N;0+A+B+C+D+E+F+H
12: for K=1 to 440
13: A+NQ[K]+A
14: B+NQ[K]Q[K]+B
15: C+Q[K]Q[K]+C
16: D+Q[K]Q[K]Q[K]+D
17: E+Q[K]Q[K]Q[K]Q[K]+E
18: F+Q[K]+F
19: H+N+H
20: N+1+N
21: next K
22: N-1+N
23: A-FH/N+A;B-HC/N+B;C+P;C-FF/N+C;D-PF/N+D;E-PP/N+E
24: (BC-AD)/(CE-DD)+G;(AE-BD)/(CE-DD)+V;(H-VF-GP)/N+S
```

Lines 25-28: Format for computing residuals.

```
25: fxd 5;L*G+G;V*L/2+V;S*L/2+S
26: for J=1 to 440
27: J*L/2-G+Q[J]*Q[J]/2-V*Q[J]-S+T[J];T[J]*1e10+T[J]
28: next J
```

Lines 29-46: This section initializes plot buffers, prints axis label on 9876A printer, loads grid buffer, performs ten-point average of residuals at 429 points, and scales average residuals and plots them versus time.

Line 46 sends the program back to File 1 (Main Program), loaded at Line 0, and run starting at line 13.

```

29: buf "data";buf "axes";buf "grid"
30: wtb 701,27,"%a30C",27,"1",13
31: wtb 701,9,"Residuals-(Angstroms)",13,10,27,"3"
32: for J=1 to 76;wtb "data",0;wtb "axes",255;wtb "grid",0;next J
33: buf "grid"
34: for J=1 to 46
35: char(2↑(7-int(J*1.65*8)mod8))+C$(int(J*1.65),int(J*1.65))
36: next J
37: buf "data";buf "axes";buf "grid"
38: 5→M;0→P
39: for T=1 to 429
40: for J=T to T+10;C+R[J]→C;next J;C/(R*200)→C;fxd 0
41: (C+20)*1.65→r1;(T[T]+20)*1.65→r2;cll 'plt'(r1,r2)
42: buf "data";buf "axes";buf "grid"
43: if T=90;wtb 701,27,"%10S";urt 701,"    Position (CM)    ",char(126)
44: wtb 701,27,"%112S"
45: 0→C;next T
46: ldf 1,0,13

```

Lines 47-67: The plot subroutine outline is: Loads the buffers that print a line of single dots. Each line has an axis point, a real residual, and a computed residual (from the previous calculation). This subroutine determines where these are printed.

```

47: "plt":T*100+L/2+0
48: wtb "data",27,"%b70W";wtb "axes",27,"%b70W";wtb "grid",27,"%b70W"
49: if T>1;gto +3
50: fmt 1,"-20",15x,"-10",18x,"0",17x,"10",17x,"20";urt 701.1
51: for J=1 to 3;wtb 701,C$;next J;wtb 701,B$
52: int(p1)+r3;fnc(p1)+r4;int(p2)+r5;fnc(p2)+r6
53: if int(Q+.6)≠M or P≠0;gto 57
54: fmt 1,36x,f2.0;wtb 701,27,"%10S";urt 701.1,M
55: wtb 701,27,"%112S";1→P
56: gto 58
57: char(32)→E$(41,41);char(0)→E$(40,40)
58: if r3+8≠41;gto 60
59: 32→N
60: char(ior(N,2↑(7-int(r4*8))))→E$(r3+8,r3+8)
61: char(ior(num(E$(r5+8,r5+8)),2↑(7-int(r6*8))))→E$(r5+8,r5+8)
62: if int(Q)=M;char(1)→E$(40,40);char(252)→E$(41,41);M+5→M
63: wtb 701,E$
64: char(0)→E$(r3+8,r3+8)→E$(r5+8,r5+8);char(32)→E$(41,41)
65: 0→N
66: if int(Q)=M-4;0→P
67: ret

```

#### File 4

Lines 0-22: Routine for setting the 59309A H/P clock.

```
0: "CLOCK DATE/TIME SET-UP 59309-16002 rev A":
1: dim D[12],T#[20]
2: 0+D[1];31+D[2];59+D[3];90+D[4];120+D[5];151+D[6]
3: 181+D[7];212+D[8];243+D[9];273+D[10];304+D[11];334+D[12]
4: 704+C;1+M+D+H+N;0+S
5: 731+B
6: dsp "MONTH",M;ent "",M
7: dsp "DAY",D;ent "",D
8: dsp "HOUR",H;ent "",H
9: dsp "MINUTES",N;ent "",N
10: dsp "SECONDS",S;ent "",S
11:
12: cmd C,"RP"
13: for I=1 to D[M];wtb B,68;next I
14: for I=1 to D-1;wtb B,68;next I
15: for I=1 to H;wtb B,72;next I
16: for I=1 to N;wtb B,77;next I
17: for I=1 to S;wtb B,83;next I
18: dsp "PRESS CONTINUE TO START CLOCK";stp
19: cmd C,"T"
20: fmt ;red C,T#
21: dsp "THE TIME IS ",T#
22: gto -2
```

#### File 5

File 5 is used to redefine characters for printing.

```
0: wtb 701,27,"&n92c30g16h16j48k16L",13,10
1: wtb 701,27,"&n94c8f28g42h8i8j8k8L",13,10
2: wtb 701,27,"&n125c8g4h62i4j8K",13,10
3: ldp 1
```

### A3. COMPUTER DEVICE CODES AND THEIR FUNCTIONS

<u>Device Code</u>	<u>Function</u>
9	Real-time clock: H/P Model 98035A
10	Miniterm: Computer Devices Mod 1202
701	Printer: H/P Model 9876A
703	Counter: H/P Model 5370A
704	Clock: H/P Model 59309A
723	Voltmeter: (Measures pressure) H/P Model 3438A



#### A4. SPECIAL FUNCTION KEYS

f0: \*fxd3;dsp'g=', G[3], " s.d. =", G[4], I  
f1: \*dsp's.e.=', G[4]/rI  
f2: \*cont15  
f3: \*fxd0;dspD\$, " ", intU\*100+frU\*60;fxd3  
f4: \*dsp'tide co rr=', G[5]  
f5: \*flt1;dsp'P=', r30\*1e-7;fxd3  
f6: \*list#10  
f7: \*wti0,10;wti6,3  
f8: \*cont'time9'  
f9: \*cont'summary'  
f10: \*cont'time"  
f11: \*list#701

#### A5. SPECIAL KEY FUNCTIONS

f0: Displays current g value and standard deviation and number of drops in the current set.  
f1: Displays standard error in the currently stored sets.  
f2: Continue at line 15 - restarts program without destroying current values.  
f3: Display date and time of last drop.  
f4: Display tide correction for last drop.  
f5: Display pressure in mm of Hg.  
f6: List on computer terminal.  
f7: Initialize  
f8: Read clock (9) [real time clock located on back of 9825] and display continuously (line 134 of main program).  
f9: Perform summary of all data taken since last summary (may be less than 15 sets).  
f10: Read clock (separate H-P clock with visual read out). Display current time.  
f11: List on 9876A printer.

## Appendix B

### Set-up Procedure

The set-up procedures include references to figures and/or diagrams (Figures B1 through B37) as aids in the procedure. In cases where more than one reference is given, the standard used is: the first referenced figure is the general location of the part in the system, the bracketed numeral refers to the legend (where in the figure the part can be found) and the subsequent figure(s) is a more detailed photograph/diagram of the part in question. For example, Figure B1(5), B6(1), B7(2) means, the location of the dropped object can be seen in its operating position inside the vacuum chamber in Figure B1, legend location 5 and a close-up view can be seen in Figure B6, legend location 1 and another view is shown in Figure B7, legend location 2.

The following procedures apply to the system after being shipped from the main laboratory to another site. Although the set-up procedure remains the same there are certain steps peculiar to field operation. Upon arrival at a site, close attention should be paid to the condition of the equipment boxes. This could be a key factor in diagnosing damaged equipment, especially internal damage. Holes, dents, or gouges in the shipping containers usually indicate rough handling during shipment. Containers in this condition should be opened and the content evaluated as soon as possible. If a problem exists it can usually be remedied early enough upon arrival at the site to ensure that hours or even days do not pass before it is discovered. Again, pay close attention to the condition of the shipping containers as they are packed for shipment and when they are received upon arrival at each location.

After the equipment has arrived and after opening the shipping containers and inspecting their contents (and it is concluded that everything appears to be operational), the procedures for assembly should be followed. Although the following steps are listed for ease of assembly it is not imperative that they be followed in the exact sequence as listed. It is suggested the laser (119), rubidium frequency standard, and the VAC ION pump be turned on as soon as practical to ensure stabilization.

1. Remove the covers from the electronic racks at this time and position them in the general location of where the measurement will be made. Pay close attention to cable length and access to power outlets. A convenient set-up is shown in Figure B1.

2. Remove the laser head (Spectra Physics 119) from its shipping crate and connect the cable to the Spectra Physics 256 Power Supply Exciter located in rack 2 as seen in Figure B4(17). Turn on for warm up.

3. Open the box containing the vacuum chamber and connect the cable from the Varian ION pump power-supply to the VAC ION pump located at the base of the chamber. Turn the control switch to 6 kV [refer to Figure B5(9) for control location] place the START/PROTECT switch in Start position. (When this switch is in START position, the circuit breaker is by-passed, allowing a higher than normal current flow. In the PROTECT position a circuit breaker trips, shutting the power supply off if excessive current is being drawn. If the breaker trips, the system will shut down and the OVERLOAD light will come on.) Turn the power switch on.

Since the system is normally shipped under vacuum and the ION pump is gated off from the main chamber, by a gate valve (Figure B21(1)), it should start almost immediately. While the pump is pumping on itself (gate valve closed) continue to the next step, but occasionally check to ensure the pump's analog meter gradually moves up scale (right to left), indicating a decrease in pressure.

- 4(a). Remove and place the optics box close to the desired station marker. Remove the end plate from the optics box at the laser end (Figure B17). Slide the moveable turning mirror to its rearmost position, by use of the positioning rod as shown in Figure B19(2). Position the optics box over the desired mark by looking down through the near center hole in the top of the box, through the beam-splitter, and through the bottom hole to the marker on the floor. Refer to Figure B15(2) for the location of the top hole in optics box. Figure B17(12), B18(1) shows beamsplitter. Adjust the entire box as necessary to position the center of the mark over the desired measurement point.

- 4(b). Level the optics box by placing the two levels, orthogonally, on the optics box and adjusting the three leveling screws shown in Figure B25. For best

results adjust the two leveling screws at the rear of the box first and then the single screw at the front of the box.

5. Remove the vacuum chamber from its box and install it on the isolation tripod as shown in Figure B1(4)(16), B6(14). Correct orientation is accomplished by lining up the marks (as pointed out in Figure B6(15)) on the tripod and chamber. Bolt the chamber to the tripod. Note: Tripod orientation is always accomplished with the Vac ION pump positioned over the single adjusting screw of the tripod. Note: Scribe marks are used throughout the assembly procedures. This, along with experience, should eliminate any confusion during assembly.

6(a). By now the Vac ION pump supply should read on scale. If it does not, go to the Maintenance Section. If the analog meter is on scale, continue monitoring the system until a reading of at least  $2 \times 10^{-6}$  Torr is obtained and the back surface of the pump (Figure B21) is reasonably cool. Now, begin opening the gate valve to the main chamber. Remember the main chamber was also shipped under vacuum, but it is possible that outgassing or leaking may have occurred during shipment. If there is reason to believe that the chamber is at atmospheric pressure, proceed to next step. If not, be cautious and deliberate while opening the gate valve. As soon as the analog meter deflects to the right stop turning. If the meter continues to the right close the valve slightly. (This gives the ION pump a chance to recover from the higher pressure in the main chamber and will eventually equalize.) If you are unable to equalize the system by opening and closing the gate valve after a period of 30 min, close the gate valve and let the ION pump recover to at least  $2 \times 10^{-6}$  Torr. If during this procedure the ION pump has become hot (too hot to touch), cool the pump with a bag of ice and/or by circulating air around the pump using a fan.

6(b). The main concern at this point is to determine if there is a leak in the chamber. Do this by connecting the thermocouple gauge TC#1 to the appropriate receptacle as shown in Figure B23(2). Turn on the Varian 845 gauge controller and check to see if the meter moves from right to left. If the meter reading is 50 mTorr or less, there probably is no leak in the system. Any reading above 50 mTorr, especially if the meter is completely off scale (to the right), indicates a definite leak and will require further maintenance as described in the Maintenance Section. For meter readings of 50 mTorr or less simply perform the following procedures to evacuate to the desired 5 mTorr or less:

- 7(a). Connect roughing pump to chamber as shown in Figure B1(8)(15).
- 7(b). Turn on pump. DO NOT open valve to vacuum chamber.
- 7(c). Connect vacuum gages (ION gage and thermocouple (TC) gages - TC#1 to roughing pump hose and TC#2 to the vacuum chamber).

7(d). When TC#1 shows a vacuum below 10 on the scale, Open the valve between the vacuum chamber and the roughing pump (valve is shown in

Figure B1(8)). If the pressure does not go below 10 within approximately 15 min, it indicates there is a leak in the hose/connections between the roughing pump and vacuum chamber. Repair before proceeding.

7(e). After determining that no leak exists the pump will now evacuate the main chamber and will probably require a period of 30 to 60 min before 5 mTorr or less is reached.

8. When TC#2 shows a vacuum of 5 mTorr or less proceed with the following steps:

a. Check the meter reading on the ION pump power supply. The pressure should be on the order of  $10^{-7}$  (meter switch in PRESSURE position).

Note: Do not turn off roughing pump.

b. Place ION pump switch to 6 kV and START-PROTECT to START.

c. Slowly open the gate valve to the ION pump (gate valve is shown in Figure B6(6), B21(1)). The analog readout on the ION pump power-supply should be closely monitored during this phase. The meter may peg (all the way to the right). If after 10 min the meter needle has not gone to the left slightly, close the ION pump valve, wait 1/2 hr and slowly open the valve. The pump may get warm. If it gets hot (to the touch) close the valve again. If a fan is available, circulate air across pump. Keep close watch on all gages. Repeat until the meter moves to the left to a reading of about 3 kV. Slowly open the ION pump valve, paying close attention to the gages. It may be necessary to run the pump with the valve barely open for an hour or so. After the analog reading is on scale with switch in PRESSURE position, turn the ION gauge switch on for the digital ION gauge readout. Close roughing pump valve (leave pump on); if the pressure starts to rise open the valve and continue rough pumping while ION pump is on. When pressure drops, close the roughing pump valve and repeat until pressure stays down after closing valve. Do not shut off roughing pump until satisfied that pressure will continue to drop without it. The digital readout should read  $10^{-4}$  or lower. Check the temperature of the ION pump (with your hand); make sure it is not too hot to the touch. (Keep checking the temperature in this manner until satisfied that the pump is OK.) If the temperature does not stabilize (feel cool) partially close the ION pump gate valve. As the pump cools down open the valve slightly until fully open (making sure meter reading is on scale).

d. Turn START-PROTECT switch to PROTECT.

e. Remove the roughing pump from the system.

9. Install the laser head in the optics box (if shipped separately). Bolt laser head with the two screws — do not overtighten since this can cause the head (consequently, the laser cavity) to twist. Refer to Figure B17(7) for correct positioning of laser head.

10. Slide the turning mirror [see Figure B19(2)] to the full forward position (all the way to the mechanical stops).

11(a). Install the microscope [Figure B1(10), B15(1)] in its hole, aligning the pellicle [Figure B18(4), B27(4)] such that the pinhole of the spatial filter is observable through the microscope. The laser spot should be visible — if it is not, loosen the laser-head retaining bolts and adjust the laser until it is observable, then retighten the screws.

11(b). Observing through the microscope, adjust mirrors  $M_1$  and  $M_2$  (Figure B34) until the laser spot disappears through the pinhole (some of the light will be visible around the pinhole).

11(c). Looking down through one of the cube corner exit apertures in the top of the optics box [Figure B15(2)] back along the laser optical path, continue to adjust mirrors  $M_1$  and  $M_2$ . The laser spot will brighten/dim as these adjustments are made. When the beam is going through the pinhole on axis of the collimator, it will be too bright to view in this manner.

Caution: Do not stare at any laser beam on axis. Eye damage will not result with this system (the power at this point is about  $10 \mu\text{W}/\text{cm}^2$ ), but it can cause discomfort and, possibly, seeing spots for a period of time if prolonged exposure is encountered.

When the beam comes through, it is a reflex to remove the eye from the brightness of the light. Do not look down the axis of the beam for the rest of the alignment. During this portion of the alignment, it may be necessary to alternate between steps 11(b) and (c). If successful with steps 11(b) and (c), go to step 11(e).

11(d). Complete readjustment: Complete readjustment is not normally required, but, in extreme cases such as parts coming loose or other severe damage during shipment, it may be necessary to perform this more extensive (basic) adjustment.

- (1) Remove the optics-box top cover.
- (2) Referring to Figure B34, measure/mark the height of the center of the front lens of the collimator to the optics box base ( $h_1$ ) and the distance from the center of the collimator lens to the optics-box sidewall ( $h_3$ ).
- (3) Remove the beam expander (Figure B18(5)).
- (4) Adjust mirror  $M_1$  (Figure B34), such that it strikes (after reflection)  $M_2$  at the height/distance measured ( $h_1$ ) in step (2).
- (5) Adjust mirror  $M_2$  (Figure B34), such that the height ( $h_2$ ) is the same as  $h_1$ .
- (6) Adjust mirrors  $M_1$  and  $M_2$  for the measured distance ( $h_3$ ) in the same way.

(7) Replace the collimator so that the center of both the input and output lenses are the same as distance  $h_3$ .

Note: All of the optical components have scribed marks at their respective tiedown points. These marks are for reference only and not to be taken as absolute position marks — mirror positioning adjustments are used to compensate for the small errors in component placement.

(8) Return to steps 11(b) and (c).

11(e). Place a white card at the exit hole into the central chamber (Figure B17(5)). Continue to adjust mirrors  $M_1$  and  $M_2$  until a bright round spot appears on the card.

Note: Since the light is collimated, the spot will dim and then disappear as  $M_1$  and/or  $M_2$  are adjusted.

The collimation of the laser can be quickly checked by observing the spot size at the card vs the size at a distance: the sizes should be the same. A sufficient distance is to observe the spot on the ceiling after it is reflected from one of the turning mirrors [Figure B17(12), (13)] (an exit path through one of the holes in the top of the optics box). The collimator lenses should be adjusted if the size of the spot changes with distance (exclusive of the diffraction limit).

11(f). If not done so previously, replace/secure optics-box top. Recheck the spot with the white card [step 11(e)] and adjust mirrors  $M_1$  and  $M_2$  if necessary.

12(a). Position the tripod/vacuum chamber over the optics box such that the entrance/exit aperture in the bottom of the vacuum chamber is centered over the exit/entrance hole in the top of the optics box. Precise location will be performed later.

12(b). Level the system by adjusting the leveling screws on the three feet of the tripod and observing the level bubbles affixed to the top of the chamber. Final level will be accomplished later in the procedure.

13(a). Mount the drive motor on the tripod base with four mounting bolts [Figure B20(5)].

13(b). Slide the drive solenoid magnet onto the magnetic pickup drive shaft [Figure B20(4)].

13(c). Place the solenoid in its place on top of the vacuum chamber [Figure B1(2), B24(4)], connect its wires, and adjust the solenoid power supply to 1.6 V (no current should be flowing).

13(d). Install the drive belt connecting the drive motor and the magnetic pickup and adjust for proper tension following these steps:

- (1) Place the motor control switch in AUTO position [Figure B4(9)].
- (2) Place the power supply control switch to LOW [Figure B4(2)].
- (3) The pick-up mechanism (robot) should start to move [Figure B1(7), B6(3)].

(4) When the robot reaches the top of the chamber it should position the balls, located on the dropped object [Figure B13(7)] into the V grooves, located on the underside of the top cover [Figure B13(3)] in such a way that at no time should there be slippage of the drive belt.

14(a). When satisfied with the belt tension, cycle the robot until it positions the dropped object at the top of the chamber.

14(b). Turn the controller power switch off before the solenoid turns the magnet on.

14(c). Remove the end plate from the photomultiplier end of the optics box (if not previously done) (Figure B18).

15. To precisely position the chamber over the optics box the following procedures should be followed. The object of this procedure is to correctly position the cube corner (located in the underside of the dropped object [Figure B11(1)], so that the incoming light beam is correctly oriented with respect to the cube corner. This is also a preliminary step in the verticality alignment.

a. Place a white piece of paper (target screen) approximately 6 in. from the opening in the optics box where the photomultiplier is inserted.

Note: For this procedure the photomultiplier is not in position.

b. The background lights should be dimmed so that the returned beam can be viewed on the target screen.

c. Move the tripod backward and/or forward until the laser beam strikes the forward position of the cube corner and is laterally centered. Evidence of an incorrectly positioned beam is indicated by a wildly oscillating needle on the laser power supply that is caused by feedback into the laser. This is caused by the incoming light beam striking a portion of the apex of the cube corner.

16. After the positioning procedures are completed, leave the dropped object (cube corner) positioned at the top of the chamber. Make sure the front entrance/exit aperture Figure B16(3) is clear, not blocked, so that the laser beam can be viewed, via an optical mirror, on a target screen for verticality alignment. During this alignment process refer to Figure B35 for clarity of relationships between the reflected beam, through beam, mirrors ( $M_3$ ,  $M_4$ ), and the various other optical components.

a. Slide the turning mirror Figure B19(2) to the rear-most position (this opens entrance/exit aperture to the mercury pool).



b. Position the mercury pool underneath the optics box so that the complete return beam from the dropped object (cube corner) strikes the pool. (This can be accomplished easiest with a piece of white paper as a reference as the pool is being positioned.)

c. Slide the turning mirror to its full forward position (closed).

d. Mount an angular mirror at the front entrance/exit aperture and position it so the through beam Figure B35 can be seen on a target screen (white piece of paper). The through beam at this point should be a full field spot. (If it is not, recheck the beams path starting at the collimator.)

e. Partially block the through window [Figure B17(5)] so that approximately one-half the beam is viewed on the target screen. (This allows for a full spot to be viewed when the through beam (one-half) and the (Hg) reflected beam (one-half) are correctly positioned for verticality.)

f. While viewing the through beam on the target screen slide the turning mirror to its rearmost position (open). [This procedure should be done with as little background light as possible as the reflected (Hg) beam is usually quite dim, therefore difficult to see on the target screen.]

g. Adjust mirrors  $M_3$  and  $M_4$  until the reflected (Hg) beam is positioned, as shown in Figure B35, on the screen.

Caution: These mirrors have single multiadjustment screws; it is suggested that the fine adjustment screw be used whenever practical. It is very easy to overadjust, using the course screw, and not see the reflected (Hg) beam.

h. Look through the microscope to precisely position the two beams for verticality. Adjust mirrors  $M_3$  and  $M_4$  until a small bright shimmering spot from the (Hg) pool is seen. It may be necessary to glance at the target screen occasionally during this procedure for beam orientation.

i. Once verticality procedures are completed, it is usually not necessary for further adjustments unless the optics box is disturbed or the laser beam becomes misaligned.

17. Optical alignment of the Michelson interferometer is a procedure for obtaining light fringes necessary for the wavelength standard used in calculating the acceleration of the dropped object due to gravity during its free-fall:

a. Position the dropped object into the V grooves at the top of the chamber by cycling the robot [Figure B13(3)].

b. Install the reference reflector in the rear entrance/exit aperture retaining ring.

c. Position, rotate, and move the reference reflector until the through beam and the return beam from the dropped object cube corner coincide and are viewed on the target screen as interference fringes. Precise positioning is achieved when a single fringe is obtained.

d. Secure the reference reflector by tightening the four securing screws located on the retaining ring [Figure B16(2)].

e. Recheck fringe pattern.

18(a). Remove the target screen and install the photomultiplier in the optics box as shown in Figure B17(4).

18(b). Connect all cables from the power supply to the photomultiplier and adjust the power supply to approximately 1600 V.

18(c). Connect the remaining video out cable from the photomultiplier to the input of the oscilloscope with a sensitivity setting of 0.2 V/cm.

18(d). Let the robot cycle several times while adjusting the photomultiplier for maximum signal (amplitude) as viewed on the oscilloscope. When satisfied that maximum signal is achieved, without distortion, disconnect the signal cable from the oscilloscope and connect it to the input of the quad discriminator [Figure B3(6)].

19. This section is for final leveling adjustment of the tripod and falling object:

a. Place the solenoid in its place on top of the vacuum chamber [Figure B1(2), B24(4)], connect its wires, turn solenoid power supply on, [Figure B4(11)], and adjust to 1.6 V (no current should be flowing). Place the motor control in AUTO position and turn the control on. The pick up mechanism (the robot) should start. (For detailed description of the robot see Section 6, DESCRIPTION OF ORIGINAL EQUIPMENT.) Observe how the dropped object falls. If the bounce does not have a nice sounding twang (rather than a clunk), adjust the leveling screws. The correct sound will only become evident with experience. (As with many mechanical devices - it does not sound right is valuable information.)

b. Set up the external laser on top of the vacuum chamber (as shown in Figure B24) and direct the laser beam down through the top window by adjusting elevation/azimuth screws on the mount and adjusting the beamsplitter in/out, rotating it to direct the beam onto the mirror located on top of the dropped object.

Caution: Avoid eye exposure to the direct laser beam. Keep the through-beam cap on the beamsplitter mount to avoid the eye-level laser beam from entering eyes. Using the robot, run the dropped object up and down while adjusting the laser beam. While observing the reflected spot on the ceiling allow the object to drop. The

spot should exhibit a minimum of movement. (The amount of movement allowed is dependent on ceiling height: a 10-cm movement for a ceiling 1 m above the apparatus has been found to be acceptable.) The amount of movement (the rotation of the dropped object during its fall) can be changed by (1) rotating the solenoid (thereby rotating the soft iron inside the internal sleeve) and (2) sliding the internal sleeve in or out of the solenoid [the sleeve is shown in Figure B28(3), B29(1)]. These are trial and error adjustments and one's own judgment comes into play.

Note: Do not be confused by the results of a tilted mirror, which will cause the spot to move on the ceiling while the object is actually falling correctly as shown in the diagram below:

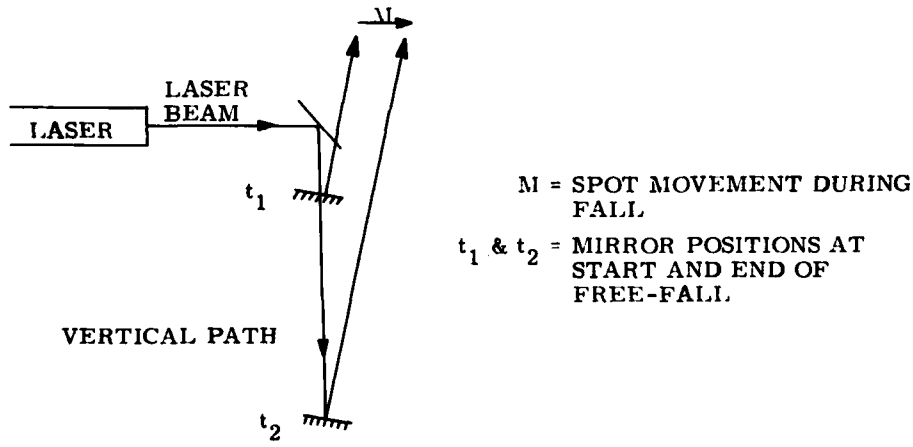


DIAGRAM OF CORRECTLY FALLING OBJECT WITH A  
TILTED MIRROR

If the tilt becomes so gross that this is a limiting factor in determining rotation, the mirror should be removed and the orientation corrected. If adjustment is necessary, removal of dropped object is accomplished by following Section 2 in Maintenance Section.

Generally, the observed spot on the ceiling will move slowly with a smooth movement indicating a tilted mirror while the movement will be sudden if the object is falling badly. If adjustment of the soft iron located in the sleeve (see above), or adjusting the leveling screws outlined above does not remedy the bad

free-fall (either optically or mechanically) it generally means that (1) the balls on the dropped object are sticking in the V grooves, (2) the robot positioning fingers are not out of the way, or (3) it is rubbing elsewhere mechanically.

The fingers' [see Figure B6(2), B7(5), B11(3), B14(1)] position can be observed through the glass enclosure, while the object is held in the V grooves by the solenoid. The object can be held in place by turning the AUTO - OFF - ON switch to ON [see Figure B4(2)]. This switches the solenoid on continuously.

Caution: Do not leave in this position more than 1 min at a time because the solenoid will heat up quickly. If the fingers are not out of the way, the chamber will have to be opened for repairs. See Maintenance Section for opening chamber.

LEGEND FOR FIGURE B1

1. FALLING BODY ALIGNMENT LASER
2. SOLENOID
3. ORTHOGONAL LEVELS
4. VACUUM CHAMBER
5. DROPPED OBJECT
6. ALIGNMENT LASER POWER SUPPLY
7. CARRIAGE RETURN - "ROBOT"
8. ROUGHING PUMP CONNECTOR/VALVE
9. ELECTRONICS RACKS/SHIPPING CRATES [3 EA]
10. ALIGNMENT MICROSCOPE
11. ION PUMP GATE VALVE
12. ION PUMP HIGH-VOLTAGE CONNECTOR
13. TRIPOD LEVELING SCREWS ON SHOCK MOUNTS
14. REFERENCE REFLECTOR
15. ROUGHING PUMP
16. VACUUM CHAMBER/ISOLATION TRIPOD
17. ION PUMP
18. OPTICS BOX
19. LASER BEAM ALIGNMENT SCREWS



Figure B1. Overview of Absolute-gravity Measurement Equipment

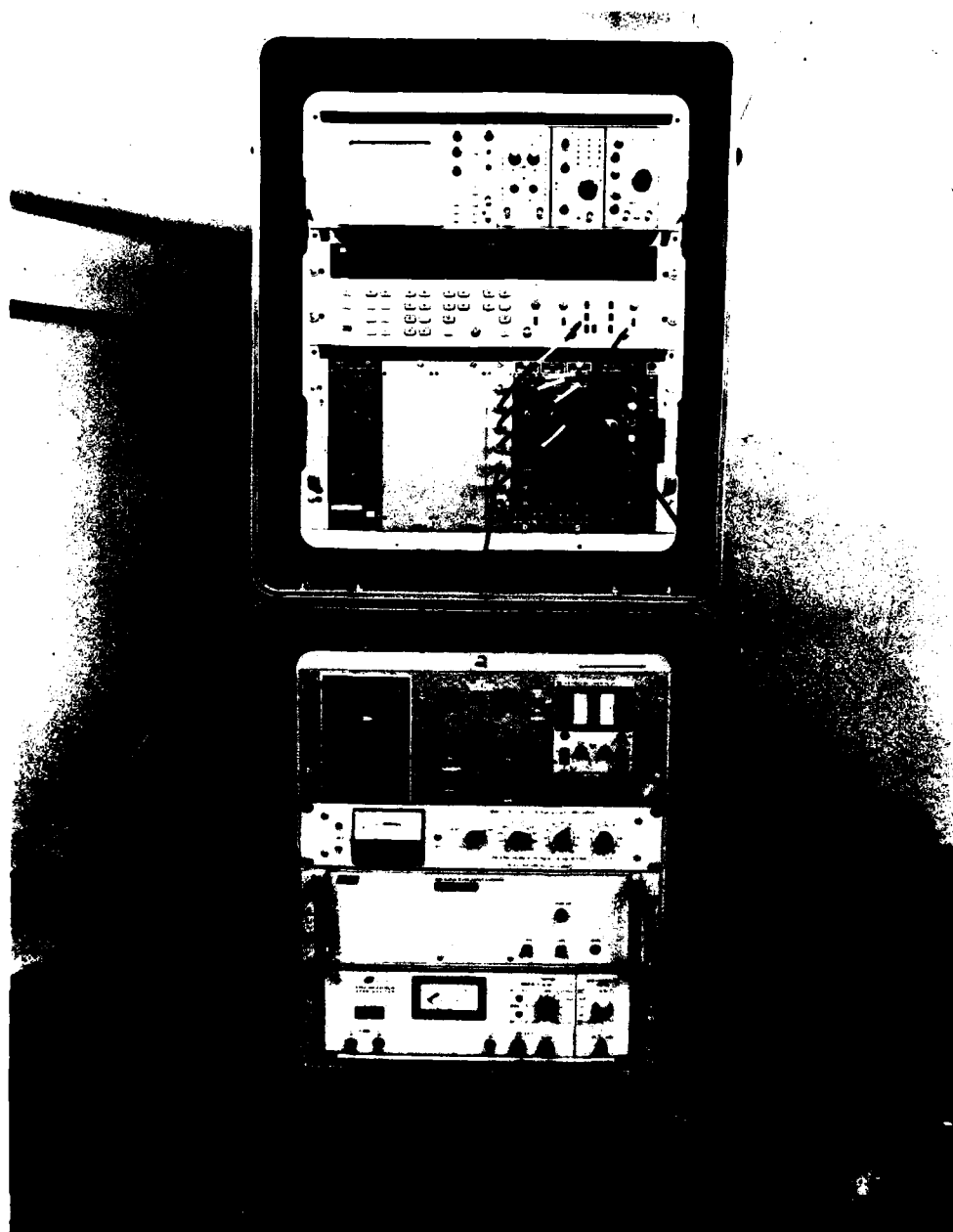


Figure B2. Overview of Electronics Racks Nos. 1 and 2

LEGEND FOR FIGURE B3

1. OSCILLOSCOPE, TECTRONIX MODEL 7903
2. INTERVAL TIME COUNTER H/P MODEL 5370A
3. SPARE DISCRIMINATOR - EG&G MODEL T140/N
4. DISTRIBUTION/WAVE SHAPE CONDITIONER PANEL
5. DUAL DIVIDE BY 10 PRESCALERS (3 EACH, DUAL)  
(ONE SECTION MODIFIED TO DIVIDE BY 4)
6. QUAD DISCRIMINATOR, EG&G MODEL T140/N
7. POWER/SIGNAL DISTRIBUTION CRATE



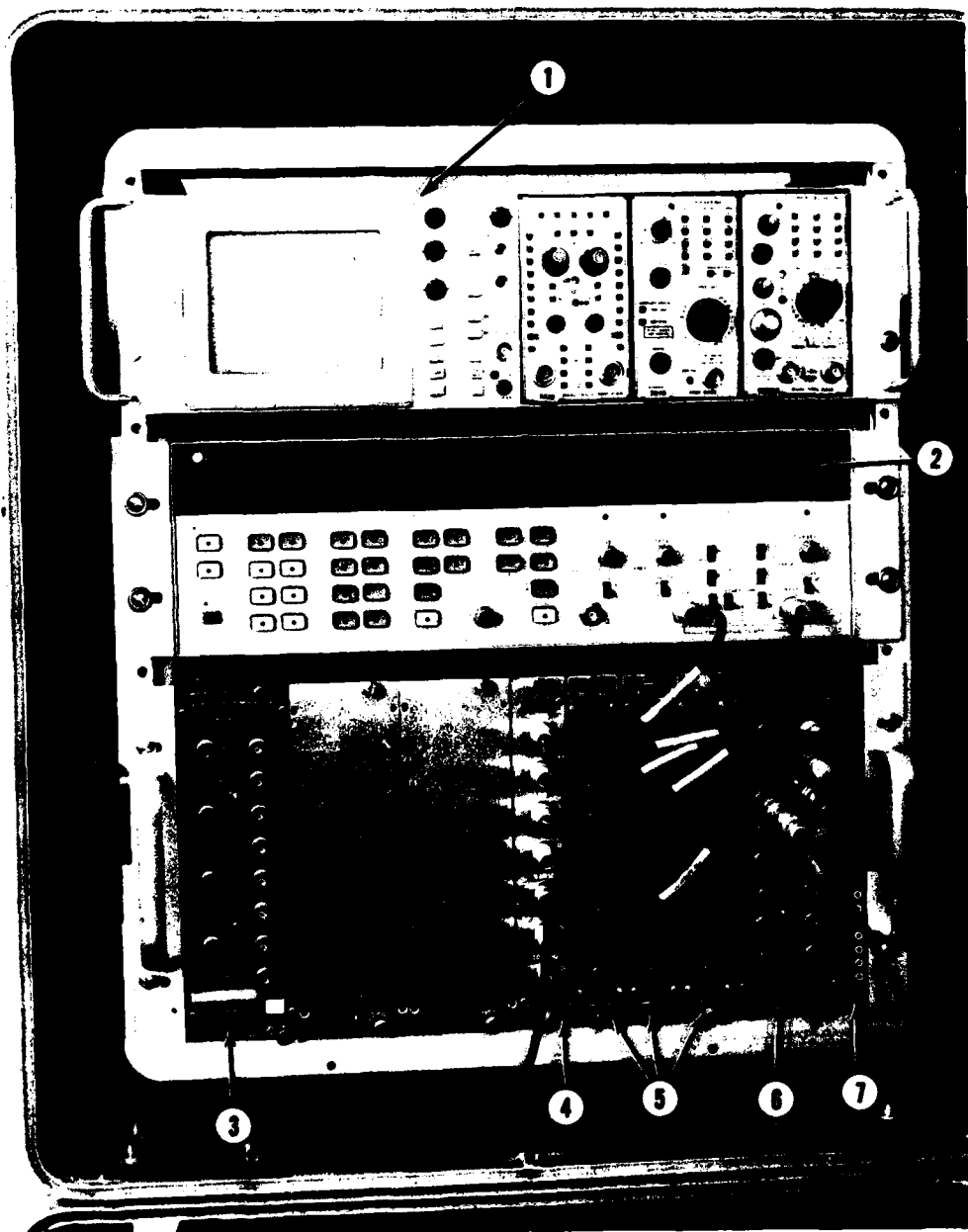


Figure B3. Electronics Rack No. 1

LEGEND FOR FIGURE B4

1. CARRIAGE/ROBOT CONTROL UNIT
2. POWER/RANGE CONTROL
3. CARRIAGE ROBOT SPEED CONTROL
4. MANUAL DIRECTION (FORWARD/REVERSE/BRAKE) CONTROL

NOTE: 5 THROUGH 8 ARE ROBOT MOTOR SPEED/MAGNET ON/OFF TIME

5.  $T_1$  - TIME DELAY FROM TOP TO SOLENOID TURN ON
6.  $T_2$  - MAGNET ON TIME
7.  $T_3$  - TIMING DELAY FOR TIME FROM SOLENOID OFF TO START OF ROBOT TO RETURN TO BOTTOM TO PICK UP DROPPED OBJECT
8.  $T_4$  - MOTOR ON TIME FROM MAGNET ON TO BACK-OFF - (BACK-OFF FOR FINGERS TO BE REMOVED FROM PATH OF FREE FALLING OBJECT)
9. AUTO/MANUAL CONTROL
10. SLOW. MOTOR SLOW-DOWN NEAR TOP OF ROBOT TRAVEL
11. SOLENOID POWER SUPPLY
12. (a) VOLTMETER  
(b) VOLTAGE CONTROL
13. (a) AMPMETER  
(b) CURRENT CONTROL
14. SOLENOID POWER SWITCH
15. PHOTOMULTIPLIER POWER SUPPLY
16. RUBIDIUM FREQUENCY STANDARD
17. FREQUENCY STABILIZED LASER POWER SUPPLY
18. LASER POWER FUNCTION SWITCH
19. AUTO WAVELENGTH ( $\lambda$ ) CONTROL
20. LASER FREQUENCY LOCK CONTROL

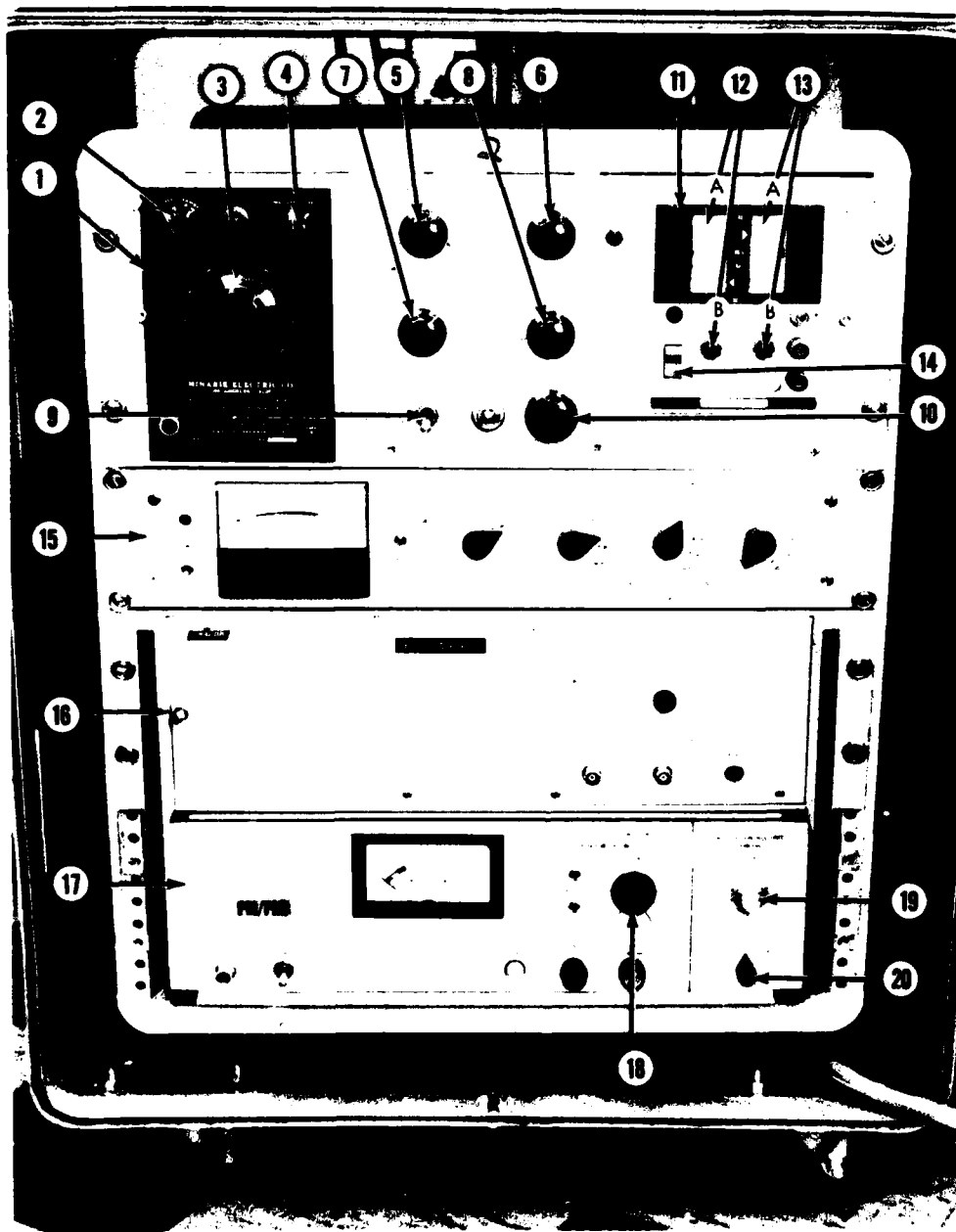


Figure B4. Electronics Rack No. 2

# LEGEND FOR FIGURE B5

- |             |   |
|-------------|---|
|             | 1. ON-LINE COMPUTER TERMINAL                                      |
|             | 2. DATA PRINTOUT TERMINAL   |
|             | 3. PRESSURE READOUT/INTERFACE                                     |
|             | 4. COMPUTER TERMINAL SHIPPING COMPARTMENT                         |
| ONE<br>UNIT | 5. THERMOCOUPLE (TC1 AND TC2) ANALOG READOUT GAUGES               |
|             | 6. ION GAUGE DIGITAL READOUT                                      |
|             | 7. ION GAUGE CONTROLS<br>PUSHBUTTON SWITCHES (FROM LEFT TO RIGHT) |
|             | 7(a) (GREEN) E.M.   |
|             | 7(b) (YELLOW) ION GAUGE TUBE - OFF                                |
|             | 7(c) (GREEN) ION GAUGE TUBE - ON                                  |
|             | 7(d) (YELLOW) ION GAUGE - DEGAS                                   |
|             | 7(e) (GREEN) ION GAUGE MAIN POWER - ON/OFF                        |
| ONE<br>UNIT | 8. ION PUMP POWER SUPPLY ANALOG READOUT                           |
|             | 9. ION CONTROL METER FUNCTION SWITCH                              |
|             | 10. ION PUMP CONTROL SWITCH - <u>ON/OFF</u>                       |
|             | 11. ION PUMP POWER SUPPLY CIRCUIT BREAKER <u>RESET</u>            |
|             | 12. ION PUMP <u>START/PROJECT</u> SWITCH                          |
|             | 13. DIGITAL CLOCK   |
|             | 14. STORAGE DRAWER  |

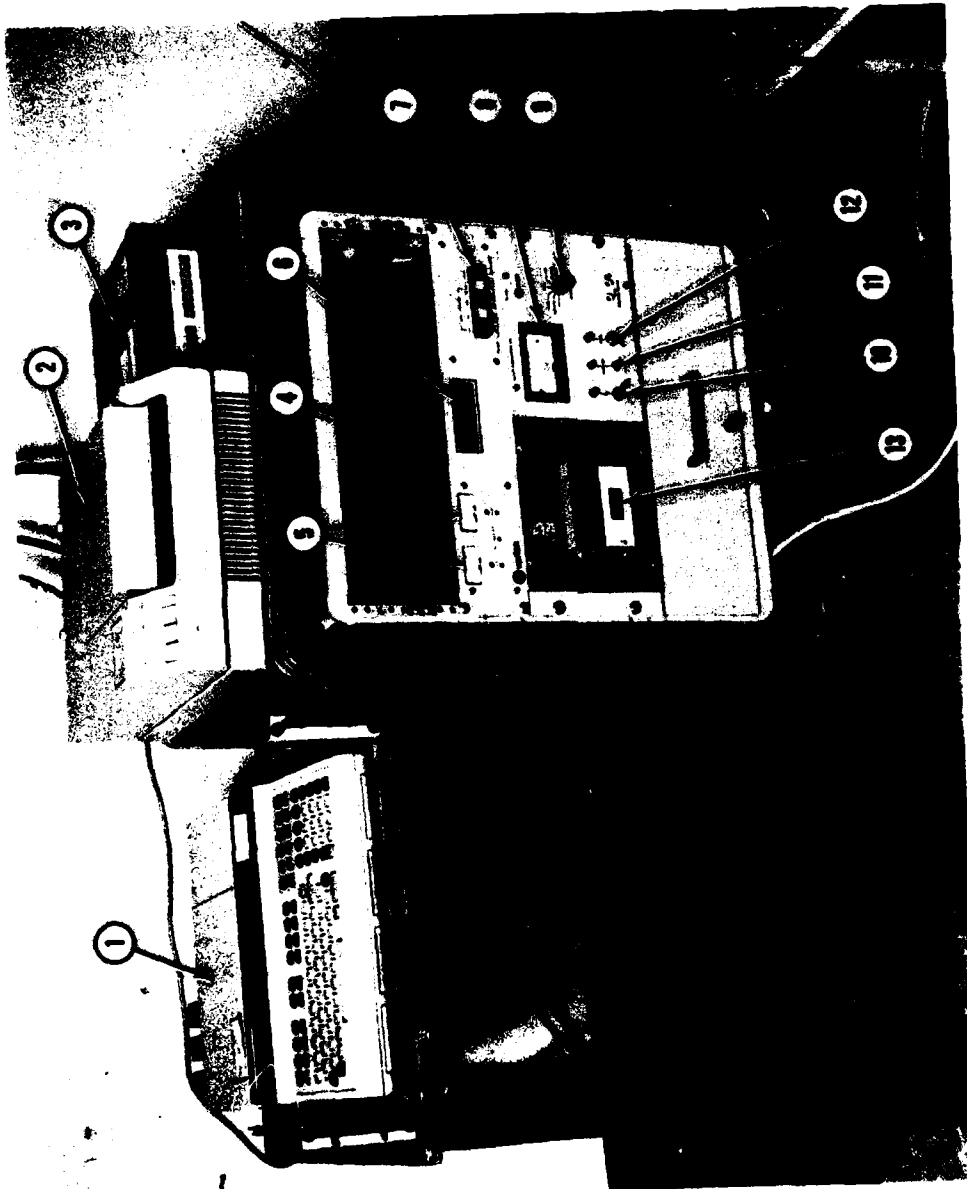
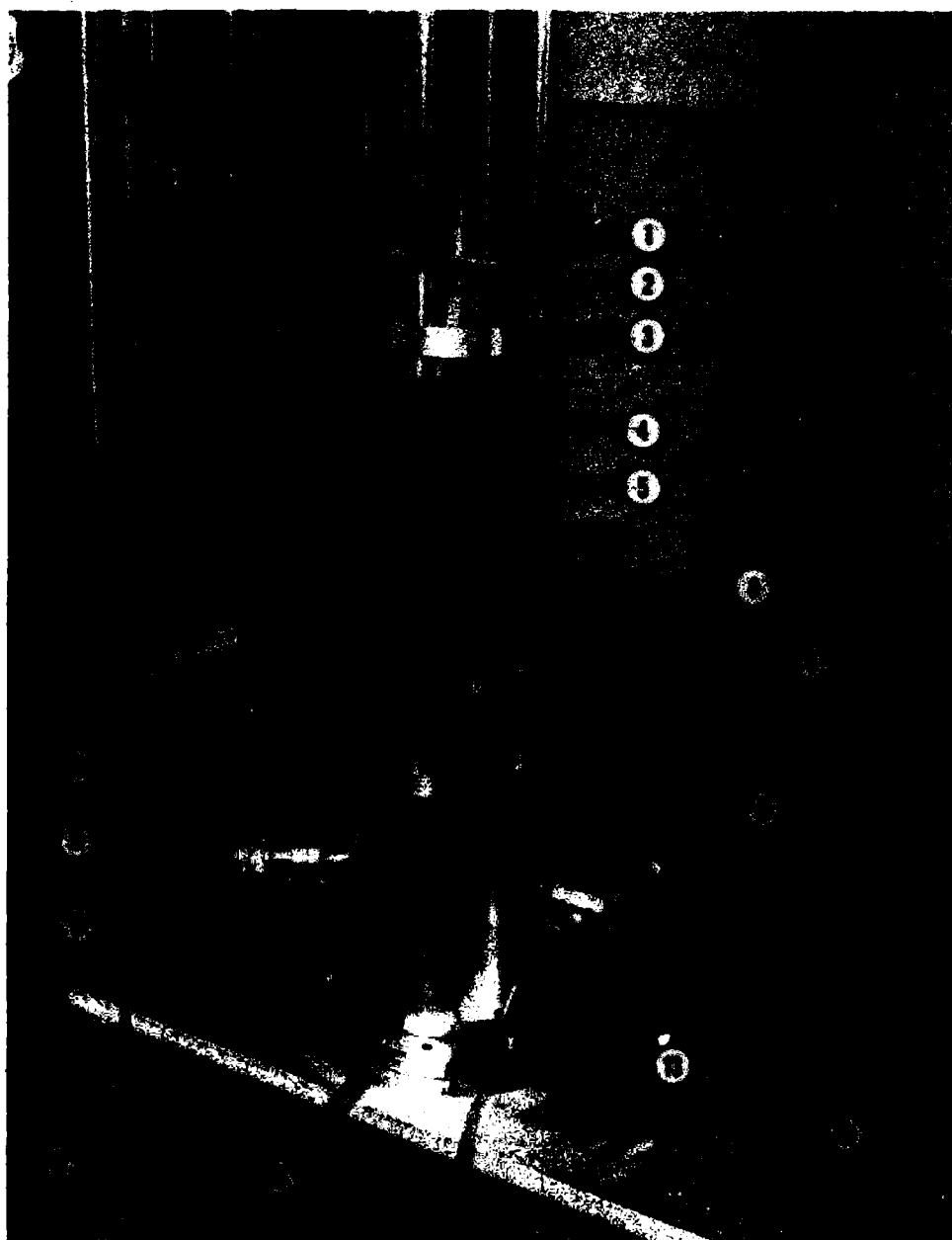


Figure B5. Electronics Rack No. 3 Plus Peripherals

LEGEND FOR FIGURE B6

1. DROPPED OBJECT
2. ROBOT POSITIONING FINGER (1 OF 3)
3. CARRIAGE RETURN - ROBOT
4. DROPPED OBJECT GUIDEPOST (3 EA)
5. SUPPORT/ROBOT GUIDEPOST (3 EA)
6. ION PUMP GATE VALVE
7. ION PUMP HIGH VOLTAGE CONNECTOR
8. ION GAUGE CONNECTOR
9. ELECTRICAL FEEDTHROUGH (FOR ROBOT)
10. MAGNETIC PULLEY FEEDTHROUGH
11. ROBOT CONTROL MOTOR
12. LASER COVER PLATE
13. THERMOCOUPLE GAUGE CONNECTORS (2 EA)
14. VACUUM CHAMBER/ISOLATION TRIPOD
15. ORIENTATION MARKS



**Figure B6. View of Chamber With Vacuum Sleeve Removed**

LEGEND FOR FIGURE B7

1. DROPPED OBJECT MIRROR FOR ROTATION CHECK
2. DROPPED OBJECT PACKAGE
3. GUIDEPOST -(1 OF 3)
4. SUPPORT/ROBOT GUIDEPOST -(1 OF 3)
5. ROBOT FINGERS -(1 OF 3)
6. POSITIONING BALL -(1 OF 3)
7. FINGER RELEASE/DAMPING SPRING - (1 OF 3)



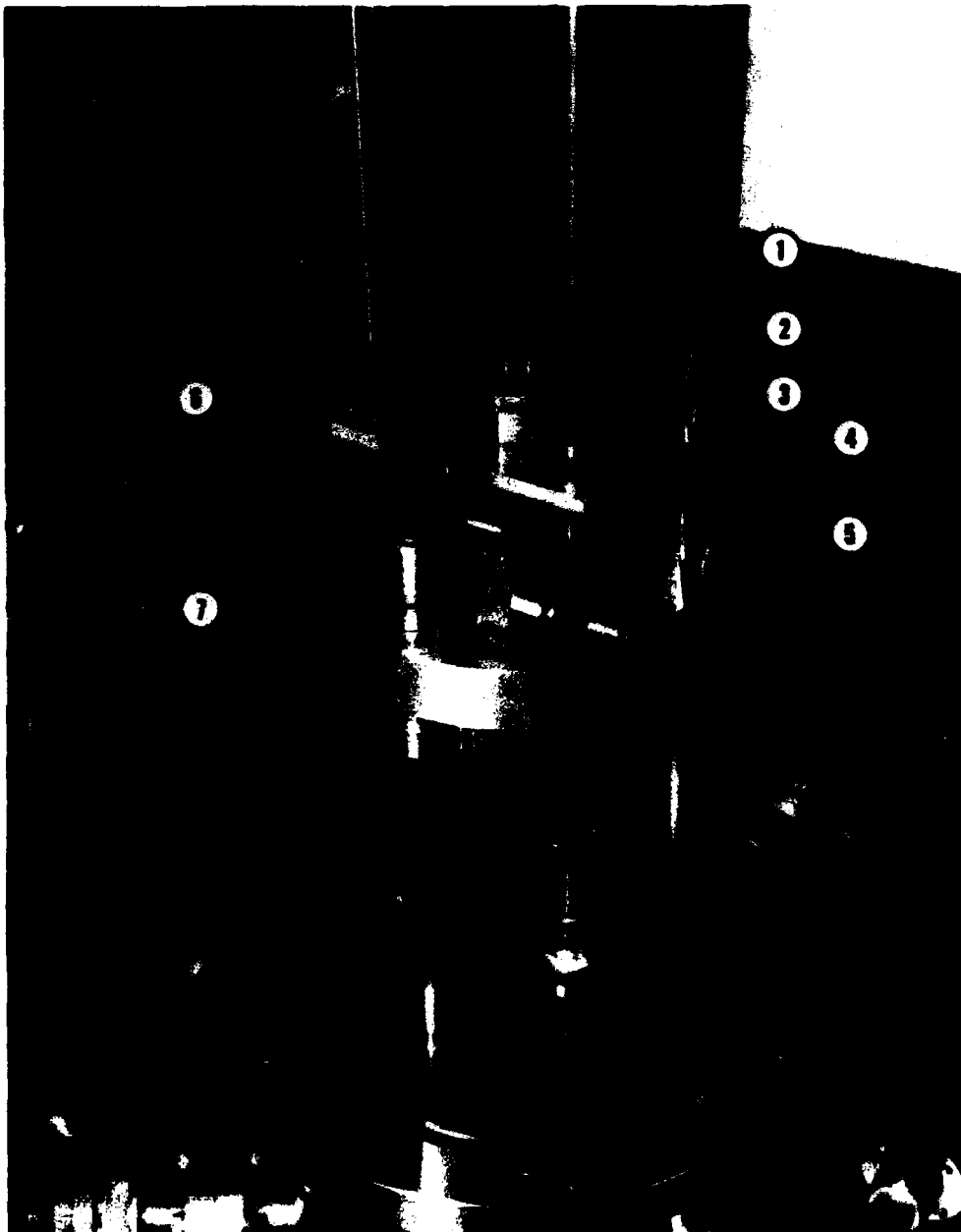


Figure B7. Close-up View of Dropped Object and Robot

LEGEND FOR FIGURE B8

1. DROPPED-OBJECT GUIDEPOST (3 EA)
2. SUPPORT/ROBOT GUIDEPOST (3 EA)
3. DROPPED-OBJECT CATCHING CONES (3 EA)
4. DROPPED-OBJECT CATCH SPRINGS (3 EA)

AD-A147 853 THE AFGL (AIR FORCE GEOPHYSICS LABORATORY) ABSOLUTE GRAVITY MEASURING SYS. (U) AIR FORCE GEOPHYSICS LAB HANSCOM AFB MA R L ILIFF ET AL. 28 OCT 83 540 241

AD-A147 853 THE AFGL (AIR FORCE GEOPHYSICS LABORATORY) ABSOLUTE GRAVITY MEASURING SYS. (U) AIR FORCE GEOPHYSICS LAB HANSCOM AFB MA R L ILIFF ET AL. 28 OCT 83 540 241

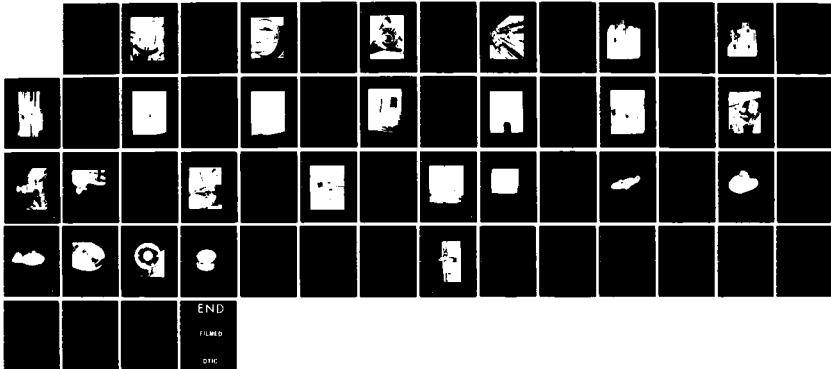
AD-A147 853	THE AFGL (AIR FORCE GEOPHYSICS LABORATORY) ABSOLUTE GRAVITY MEASURING SYS. (U) AIR FORCE GEOPHYSICS LAB HANSCOM AFB MA R L ILIFF ET AL. 28 OCT 83	2/2
-------------	---	-----

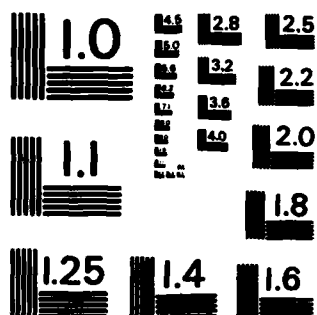
UNCLASSIFIED AFGL-TR-83-0297

UNCLASSIFIED AFGL-TR-83-0297

UNCLASSIFIED AFGL-TR-83-0297 F/G 8/5

UNCLASSIFIED AFGL-TR-83-0297 F/G 8/5 NL





MICROCOPY RESOLUTION TEST CHART  
NATIONAL BUREAU OF STANDARDS-1963-A

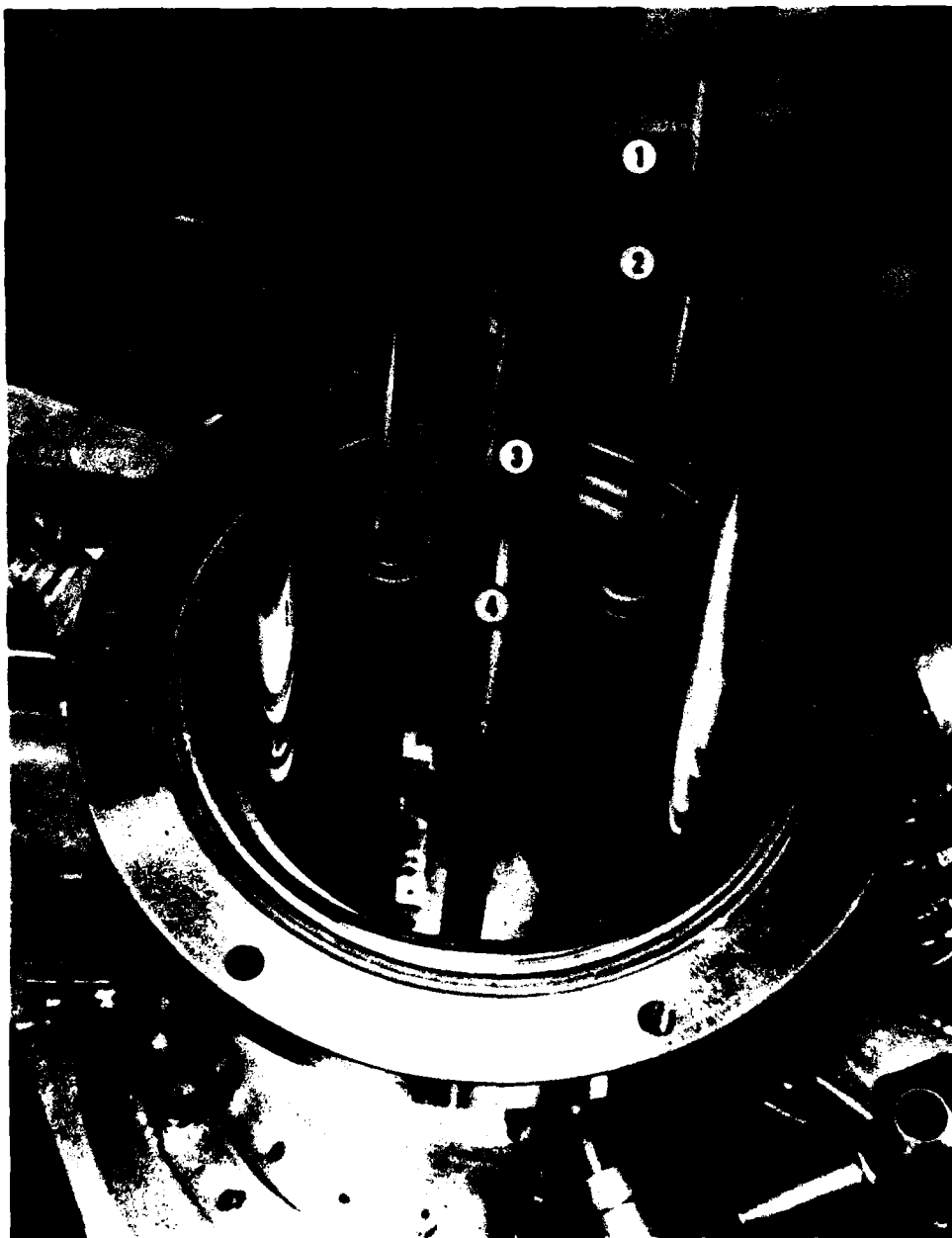


Figure B8. Guides and Catching Mechanism

LEGEND FOR FIGURE B9

1. ELECTRICAL FEEDTHROUGH
2. ROBOT CHAIN GUIDE
3. LOWER CHAIN-SPROCKET AND HOUSING



Figure B9. Lower Structure

LEGEND FOR FIGURE B10

1. SUPPORT/ROBOT GUIDEPOST WITH ALIGNMENT/  
ORIENTATION NUMBERS (3 EA)
2. TOP CHAIN-SPROCKET HOUSING SCREW
3. DROPPED-OBJECT GUIDEPOST (3 EA)



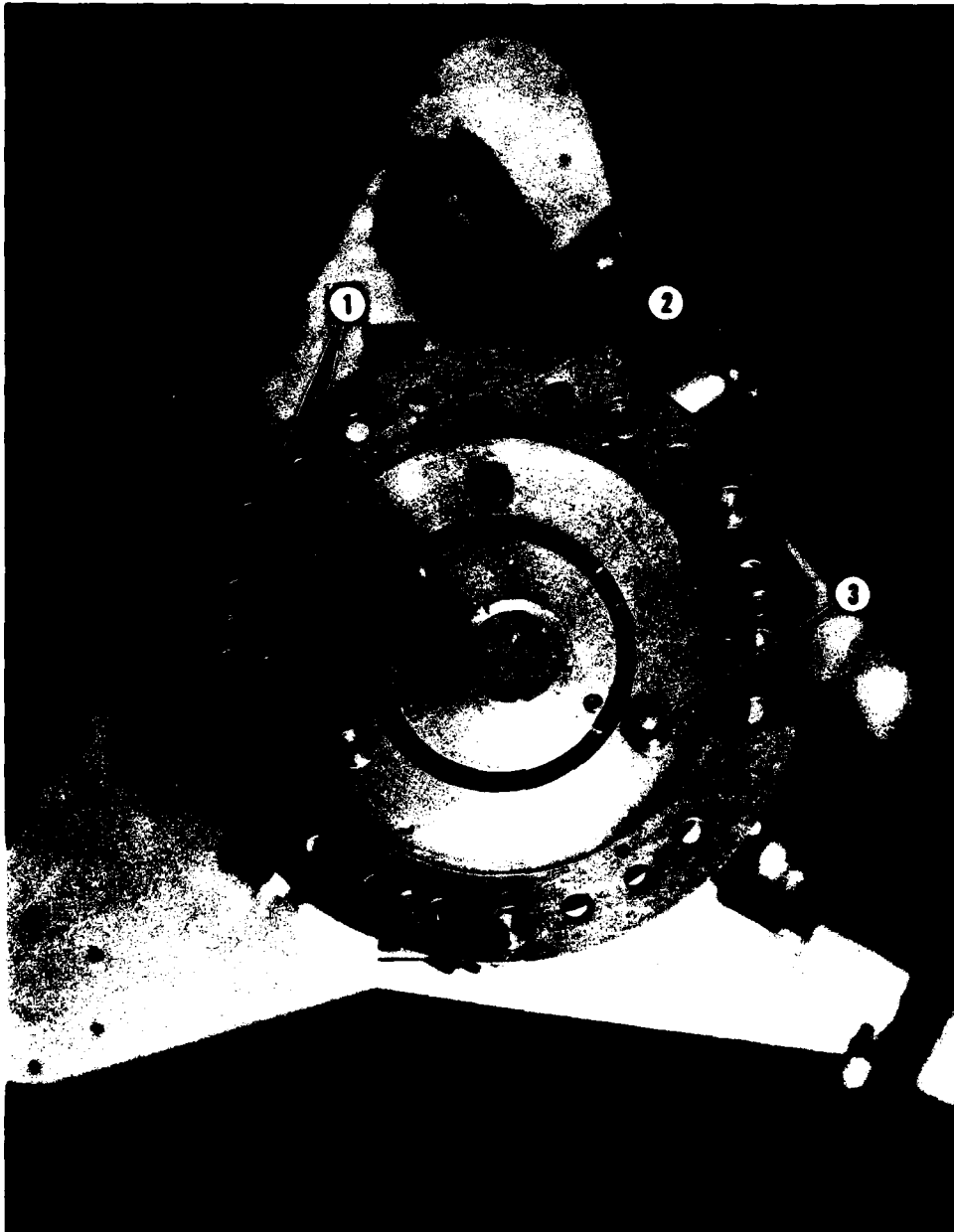


Figure B10. Top View of Inner Hat

**LEGEND FOR FIGURE B11**

- 1. DROPPED CUBE CORNER**
- 2. UPPER CHAIN SPROCKET AND HOUSING**
- 3. ROBOT POSITIONING FINGERS**

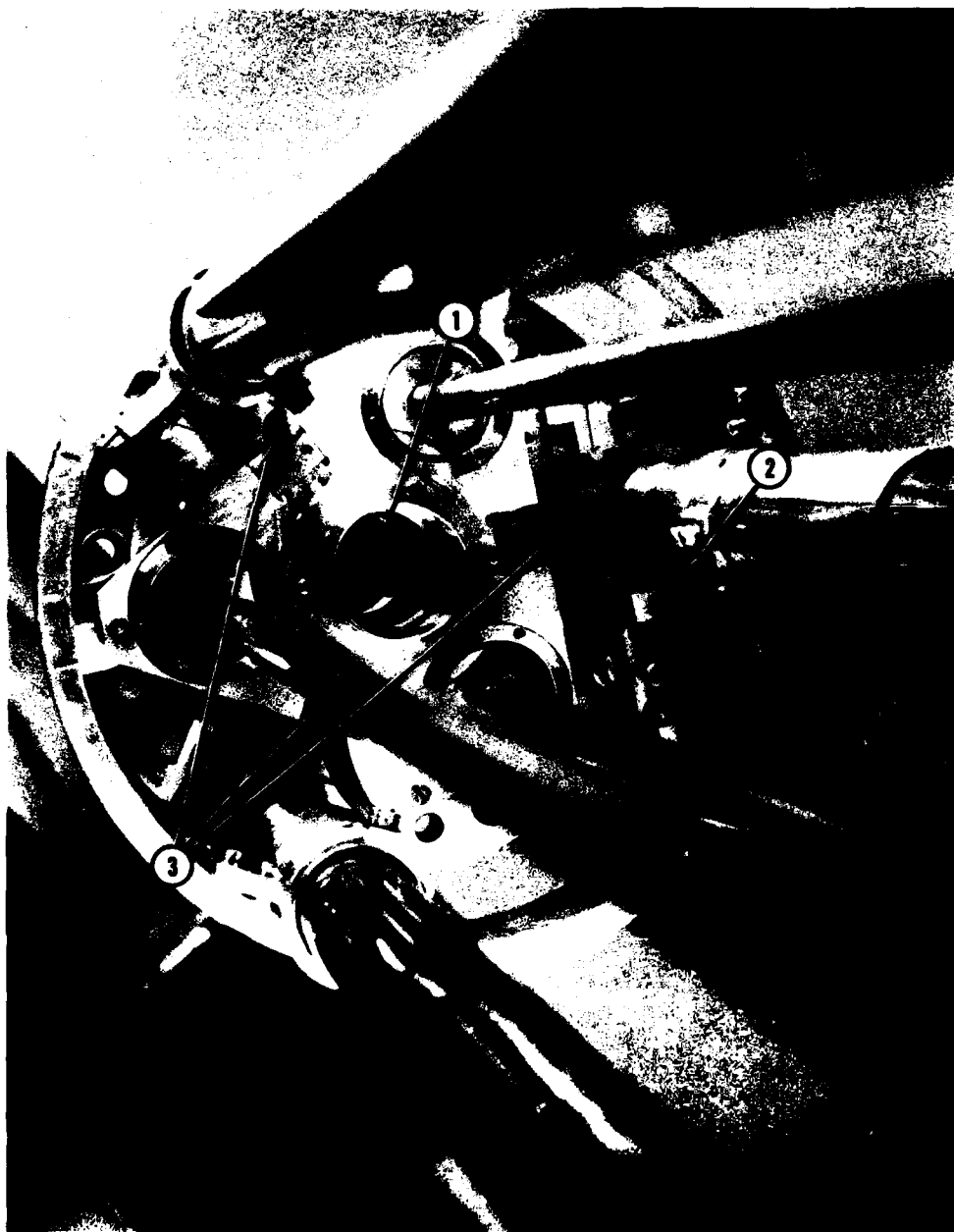


Figure B11. View of Dropped Object in Uppermost Position

**LEGEND FOR FIGURE B12**

- 1. FINGER RELEASE/DAMPING SPRING**
- 2. SUPPORT/ROBOT GUIDEPOST SET SCREW**
- 3. DROPPED-OBJECT ALIGNMENT/ROTATION MIRROR SET SCREW**

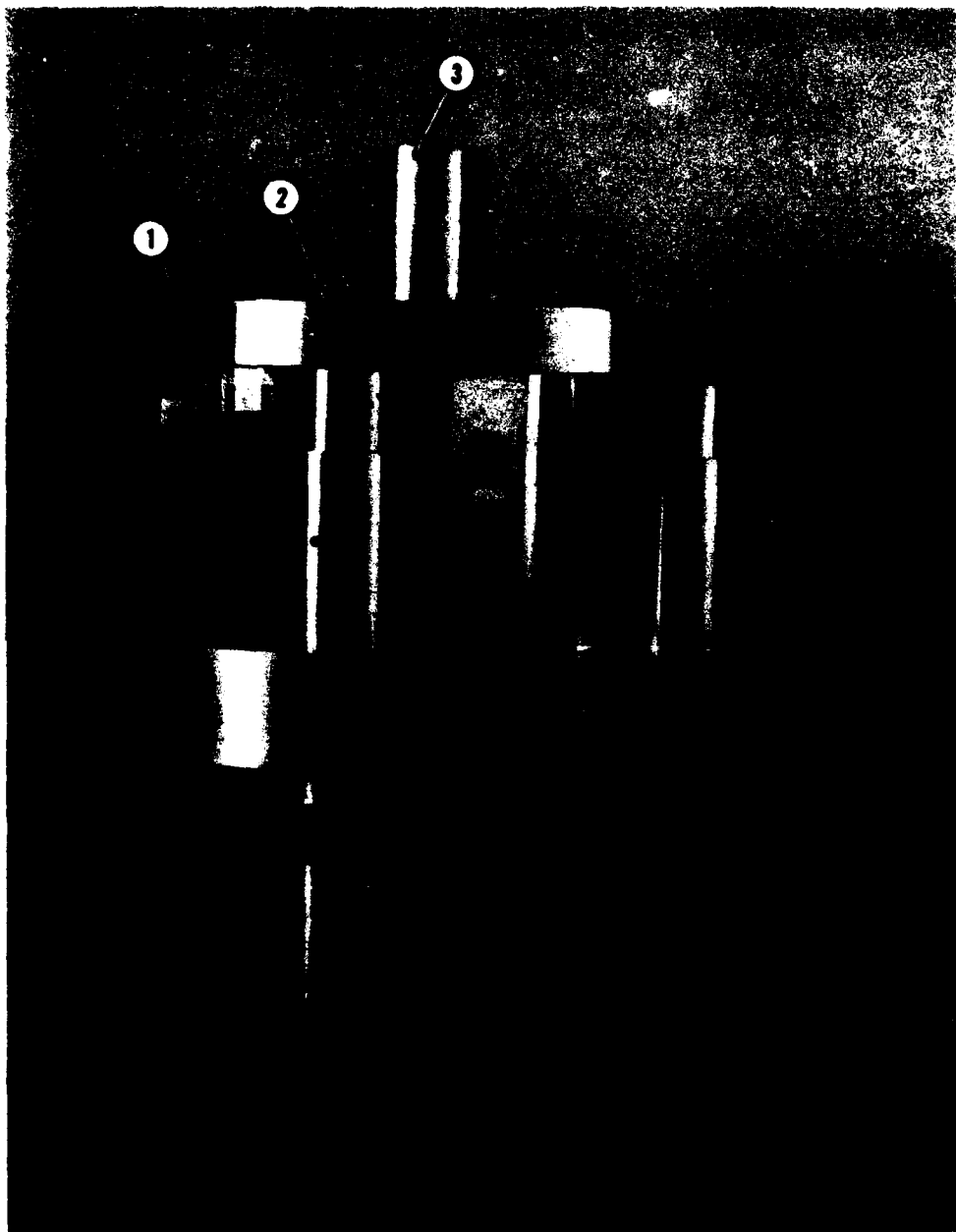


Figure B12. View of Robot in Uppermost Position

LEGEND FOR FIGURE B13

1. UPPER CHAIN SPROCKET HOUSING
2. SUPPORT/ROBOT GUIDEPOST SET SCREW (3 EA)
3. POSITIONING "V" GROOVE
4. SOFT IRON SET SCREW
5. DROPPED OBJECT ALIGNMENT/ROTATION MIRROR SET SCREW (3 EA)
6. DROPPED-OBJECT GUIDEPOST SET SCREW (3 EA)
7. DROPPED-OBJECT POSITIONING BALLS (3 EA)

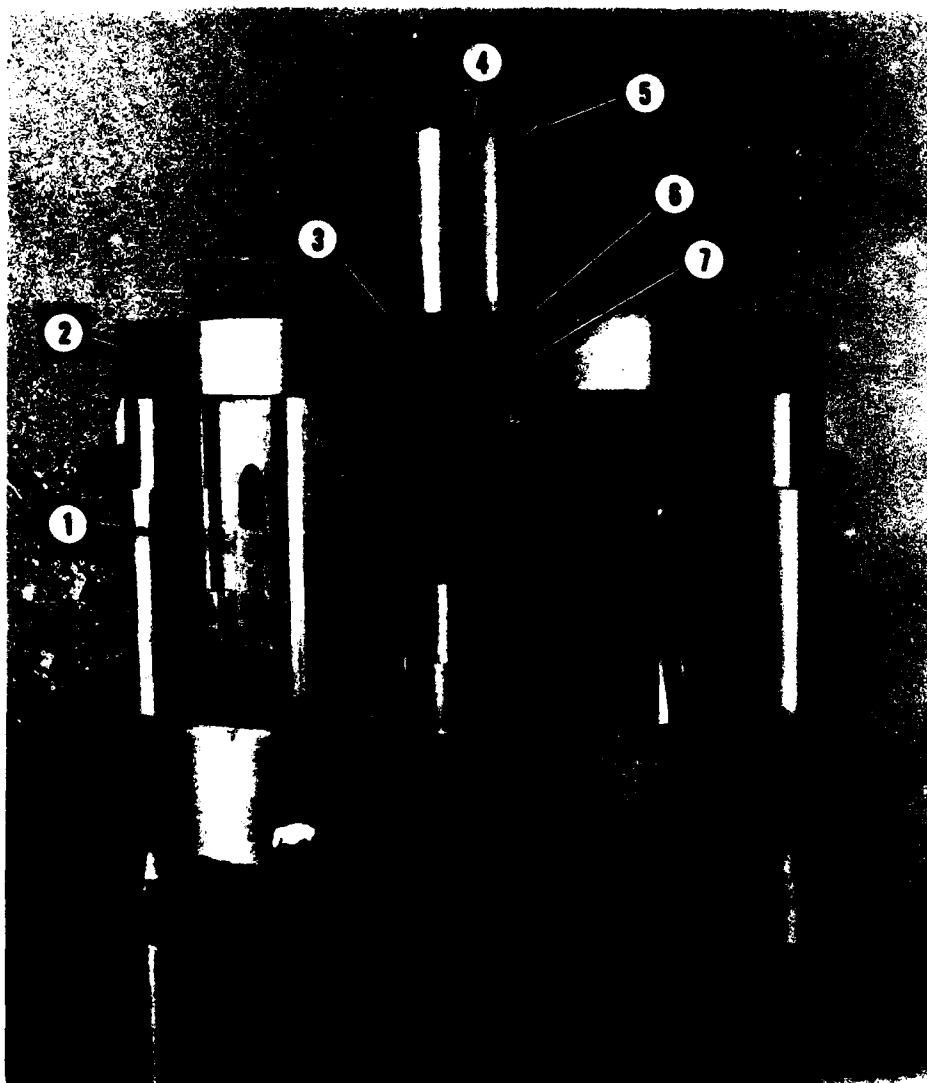


Figure B13. View of Robot and Dropped Object Package in Near Seated Position

LEGEND FOR FIGURE B14

1. POSITIONING FINGERS (2 OF 3 SHOWN)
2. SUPPORT/ROBOT GUIDEPOST (3 EA)
3. ROBOT GUIDE SLAVE (3 EA)
4. DAMPING SPRINGS



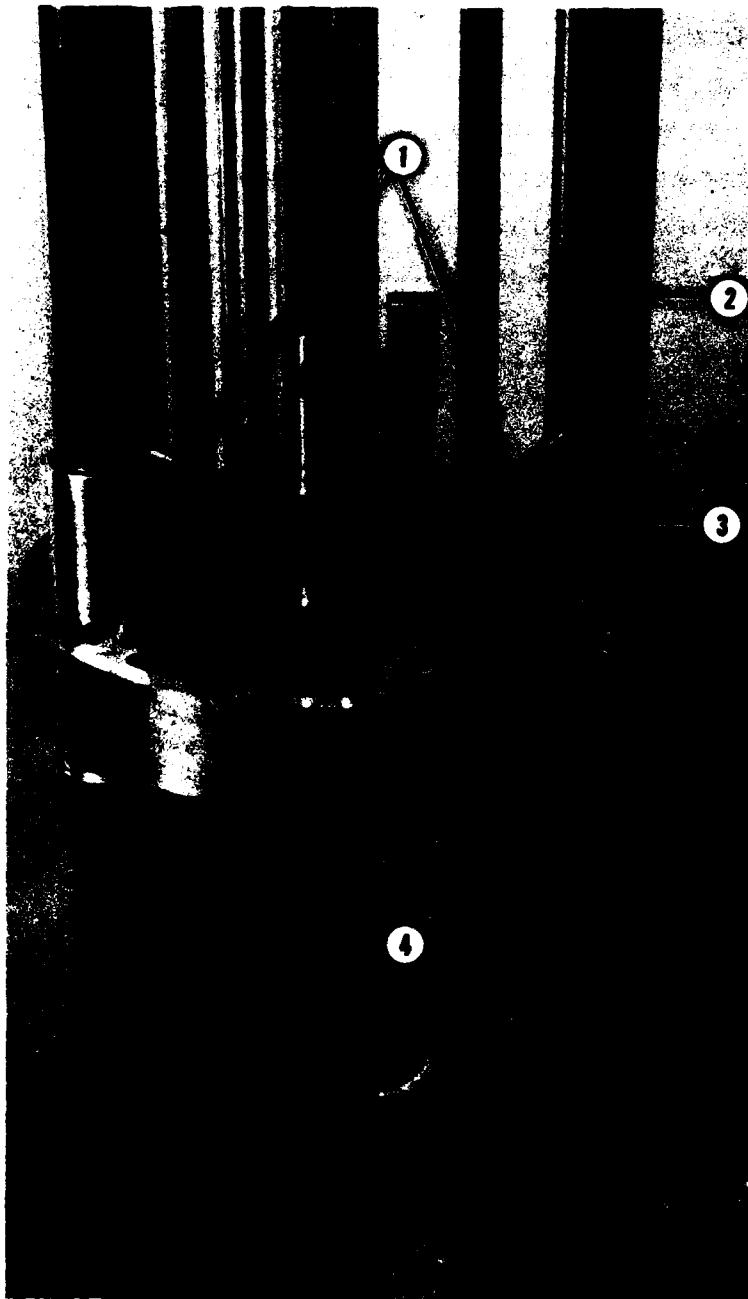


Figure B14. View of Robot

LEGEND FOR FIGURE B15

1. ALIGNMENT MICROSCOPE
2. OPTICS BOX/VACUUM CHAMBER LASER EXIT/ENTRANCE HOLE
3. REFERENCE-CUBE CORNER REFLECTOR
4. LASER-BEAM ANGLE ADJUSTMENT CONTROL KNOBS
5. LASER-BEAM POSITION ADJUSTMENT CONTROL KNOBS

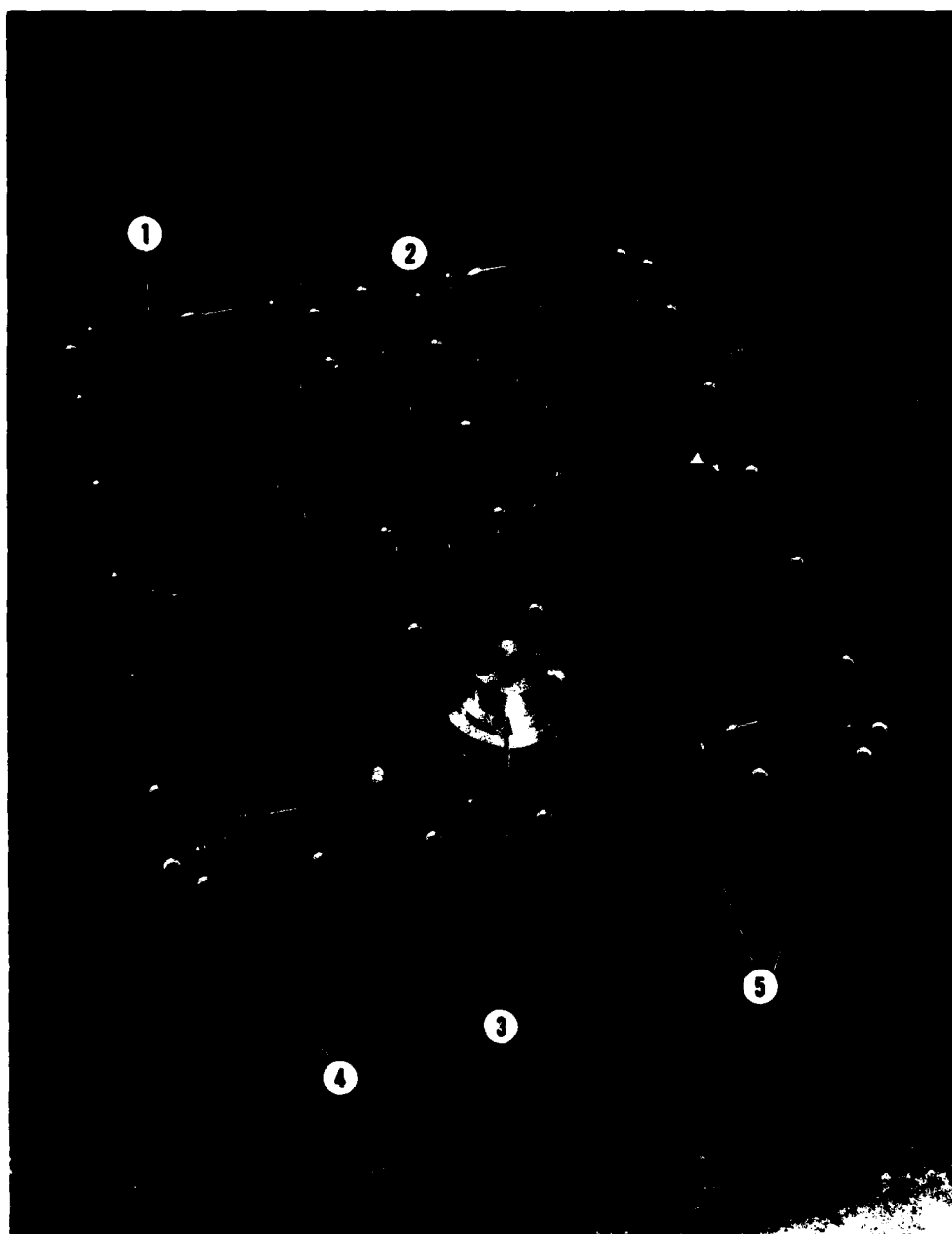


Figure B15. Optics Box

LEGEND FOR FIGURE B16

1. REFERENCE REFLECTOR WITH HOUSING
2. REFERENCE-REFLECTOR POSITIONING SCREWS
3. REFERENCE ENTRANCE/EXIT HOLE

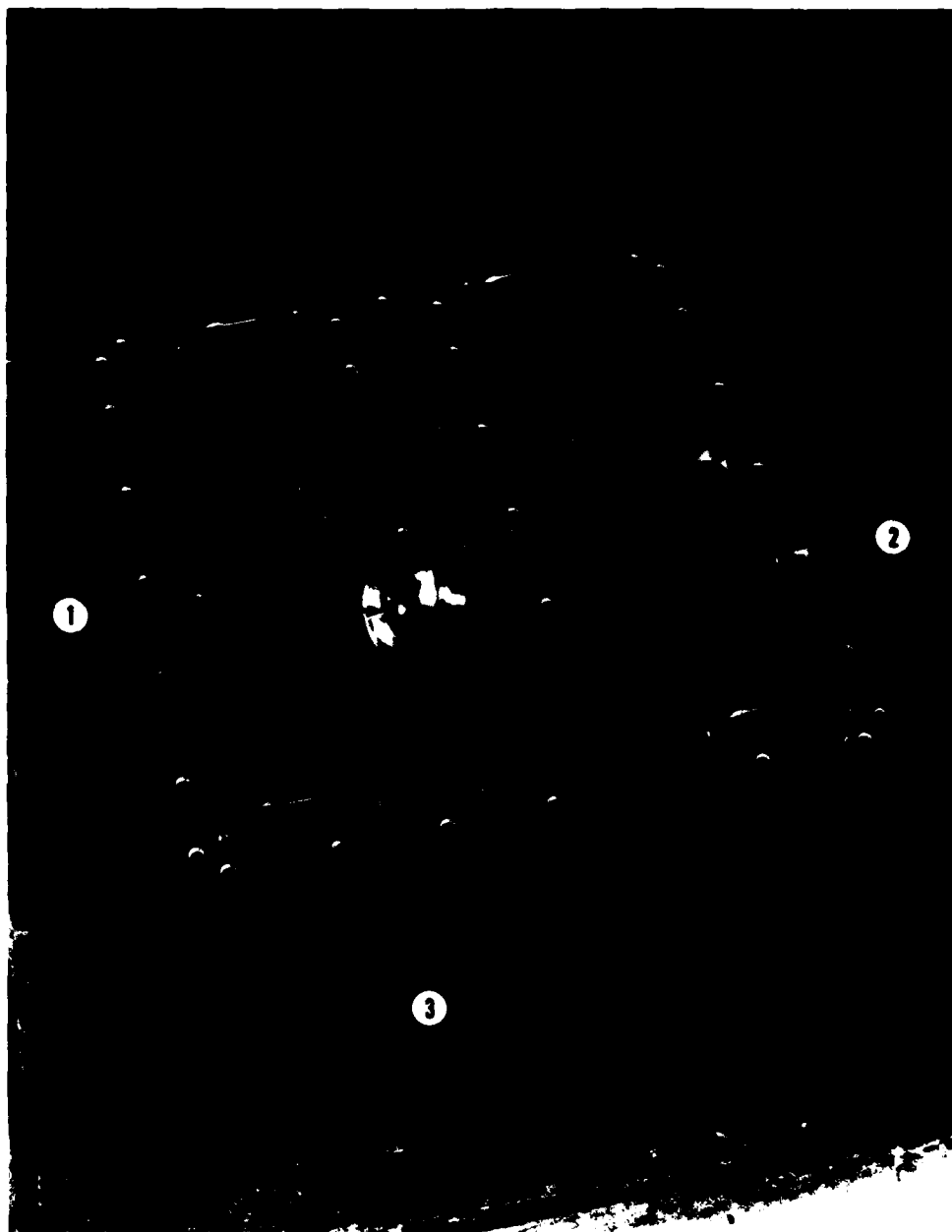


Figure B16. Optics Box With Reference Reflector Removed

# LEGEND FOR FIGURE B17

1. ALIGNMENT MICROSCOPE ON ALIGNMENT JIG
2. BEAM EXPANDER/COLLIMATOR/SPATIAL FILTER COMBINATION
3. TURNING MIRROR/ADJUSTMENT MOUNT
4. PHOTOMULTIPLIER
5. EXIT HOLE TO CENTRAL CHAMBER
6. TURNING MIRROR/ADJUSTMENT MOUNT
7. LASER
8. TURNING MIRROR
9. TURNING MIRROR
10. LASER-BEAM ANGLE ADJUSTMENT MOUNT
11. LASER-BEAM ANGLE ADJUSTMENT CONTROL KNOBS
12. BEAMSPLITTER
13. TURNING MIRROR
14. LASER-BEAM POSITION ADJUSTMENT MOUNT
15. LASER-BEAM POSITIONING ADJUSTMENT CONTROL KNOBS

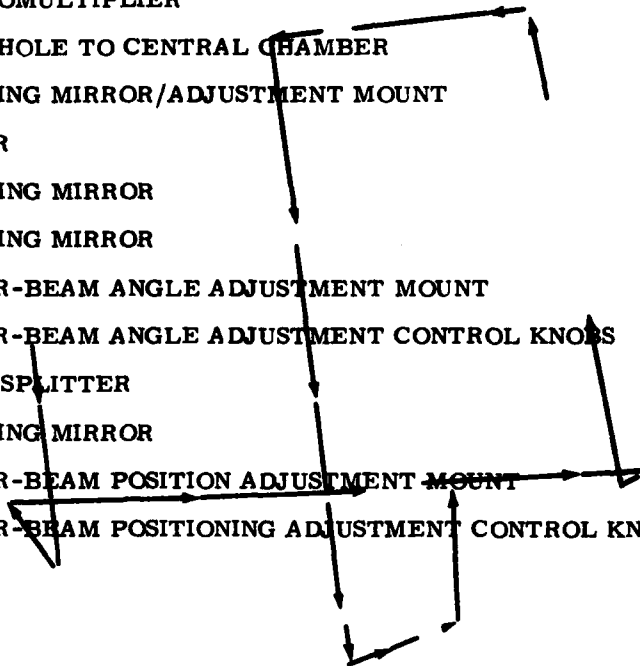




Figure B17. Interior View of Optics Box

**LEGEND FOR FIGURE B18**

- 1. BEAMSPLITTERS**
- 2. PHOTOMULTIPLIER**
- 3. ALIGNMENT MICROSCOPE**
- 4. MICROSCOPE PELLICLE**
- 5. BEAM EXPANDER/COLLIMATOR/SPATIAL FILTER**
- 6. TURNING MIRROR-MOUNT ADJUSTMENT SCREWS**



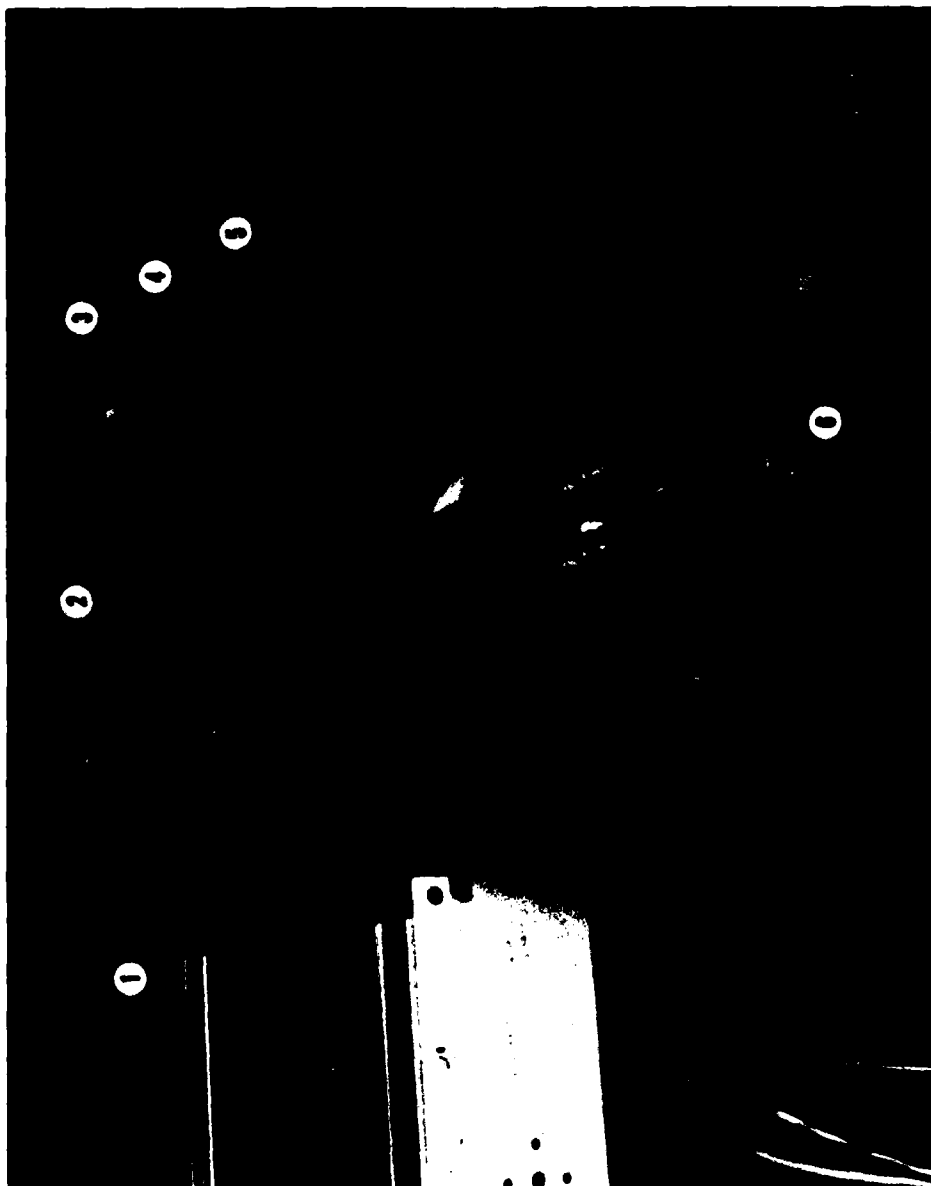


Figure B18. Interior View of Optics Box

LEGEND FOR FIGURE B19

1. MOVEABLE MIRROR AND MOUNT
2. MOVEABLE-MIRROR ACCESS ROD



**Figure B19. Moveable Turning Mirror**

LEGEND FOR FIGURE B20

1. VACUUM CHAMBER BASE
2. VACUUM ELECTRICAL FEEDTHROUGH
3. ROBOT CONTROL ELECTRICAL CONNECTOR
4. MAGNETIC PULLEY
5. REVERSIBLE DC MOTOR

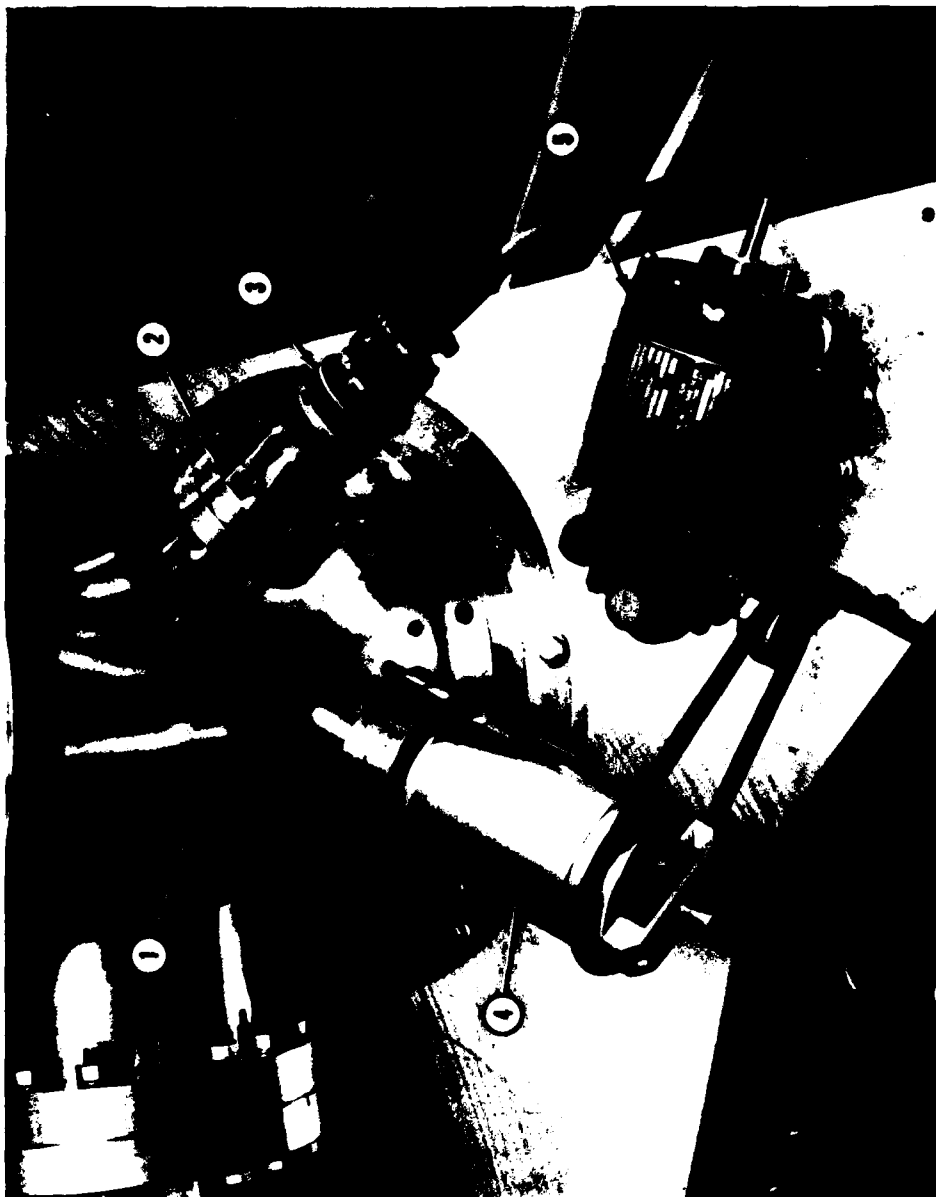


Figure B20. Robot Controls

LEGEND FOR FIGURE B21

1. ION PUMP GATE VALVE CONTROL
2. GATE VALVE HOUSING
3. ION PUMP
4. ION PUMP HIGH-VOLTAGE CONNECTOR

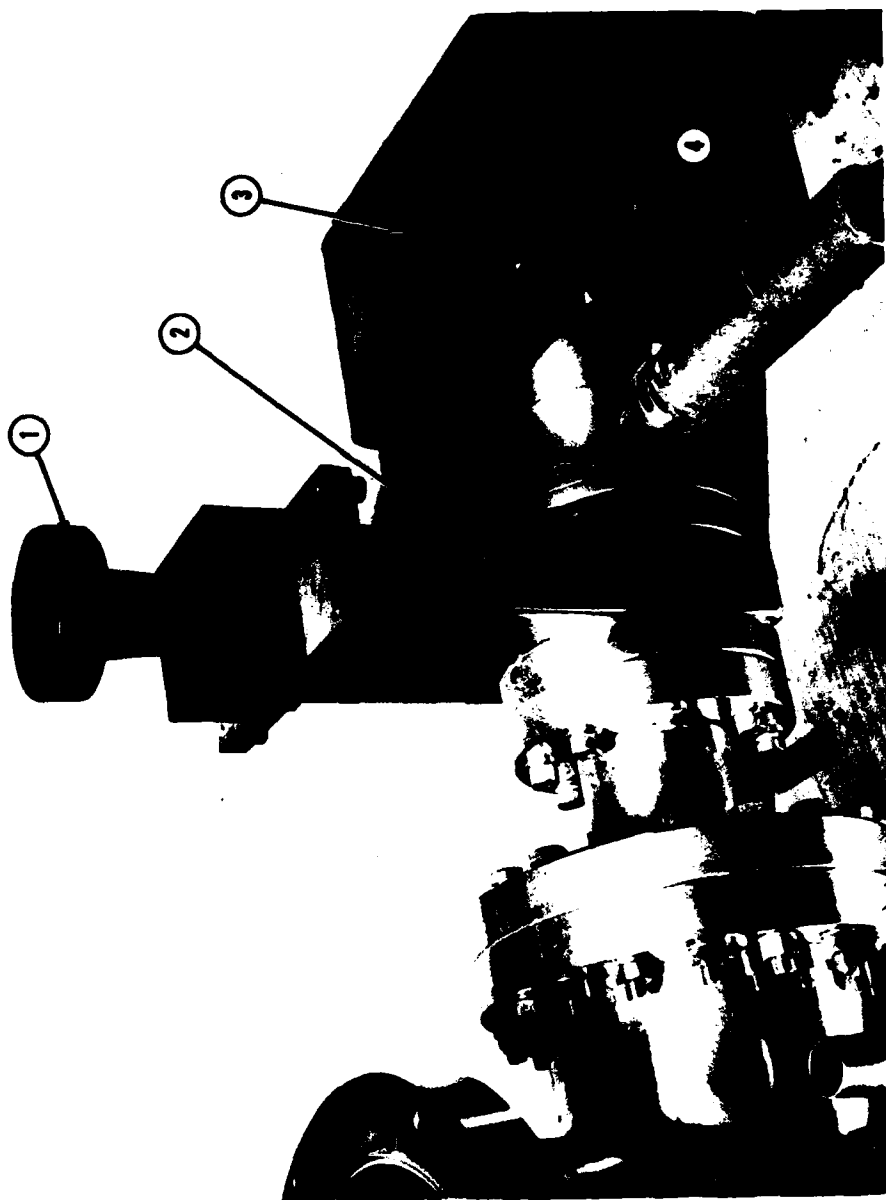


Figure B21. ION Pump

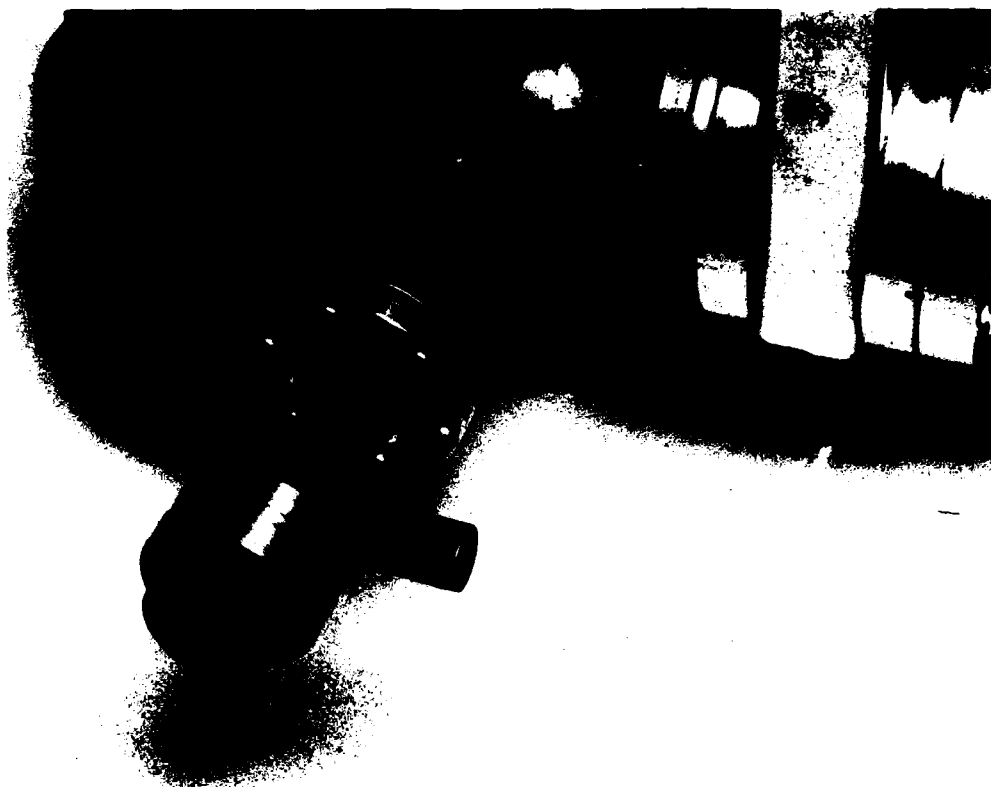


Figure B22. ION Pump External Evacuation Port and Shutoff Valve



LEGEND FOR FIGURE B23

1. VACUUM CHAMBER BASE
2. THERMOCOUPLE [TC #1] AND CONNECTOR
3. ROUGHING PUMP INPUT PART
4. ROUGHING PUMP VALVE CONTROL
5. ION GAUGE CONNECTOR

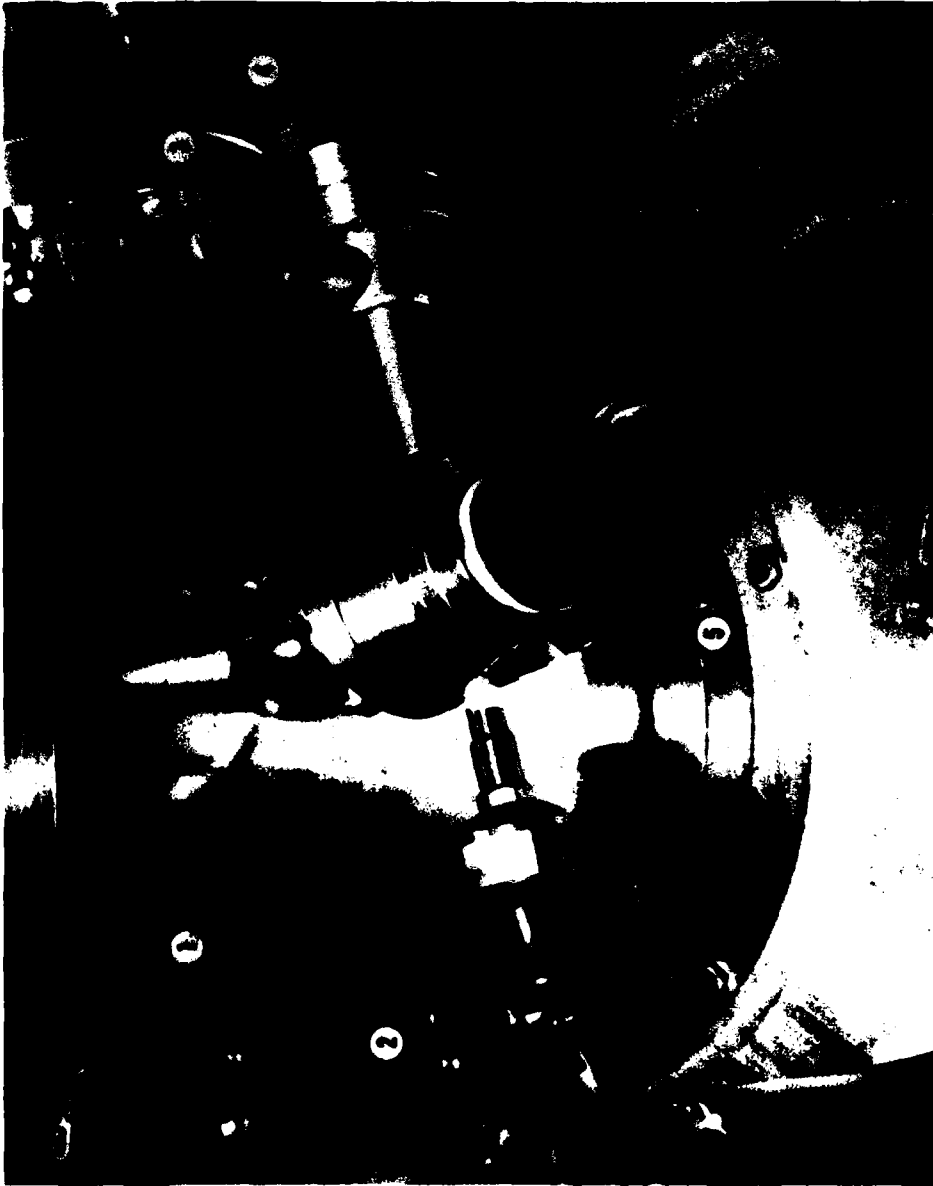


Figure B23. Vacuum Gauges and Roughing Pump Connector Value

LEGEND FOR FIGURE B24

1. HeNe ALIGNMENT LASER
2. LASER MOUNT ADJUSTMENT SCREW (2 EA)
3. BEAMSPLITTER CUBE
4. SOLENOID
5. LASER MOUNTING BLOCK

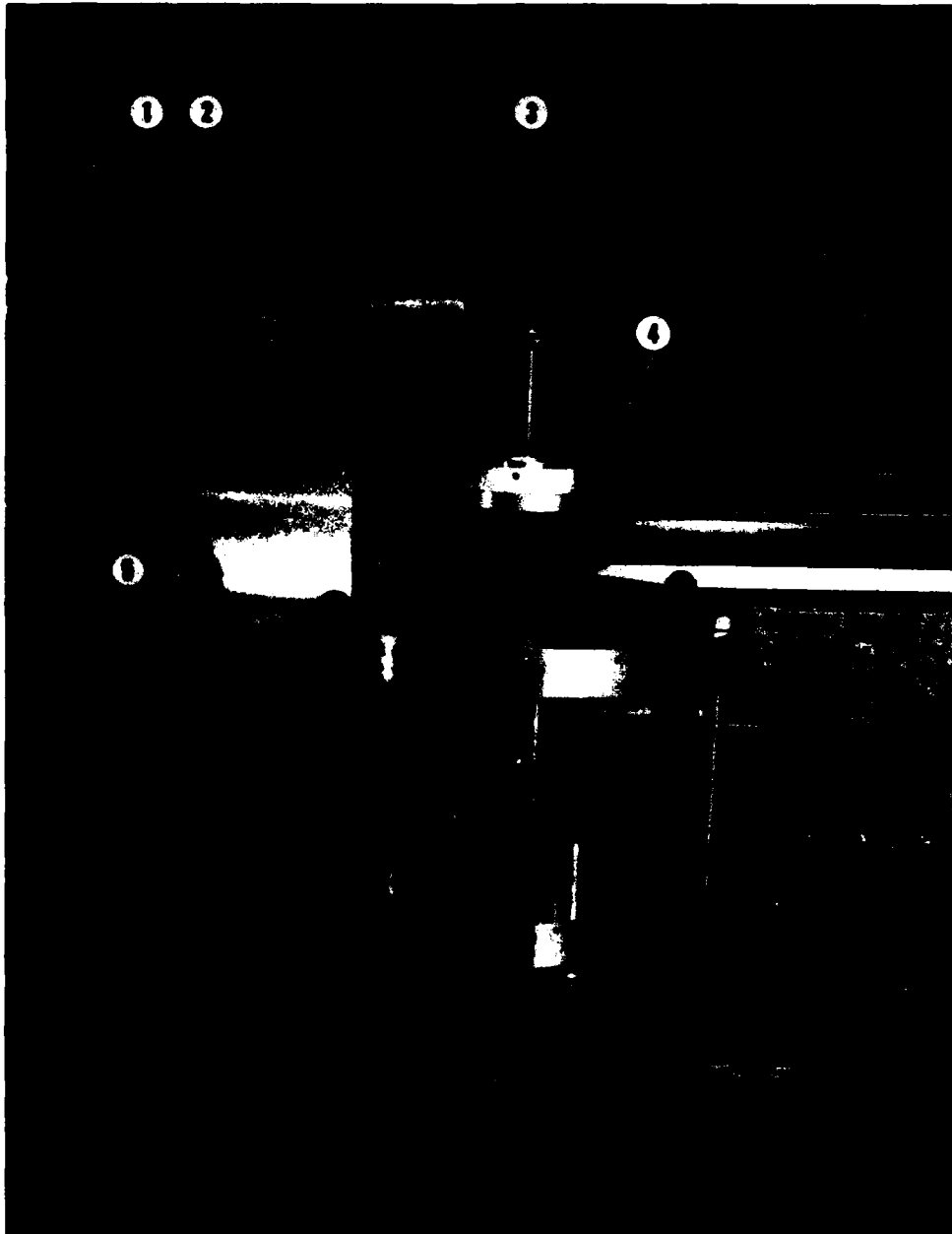


Figure B24. External Alignment Laser

LEGEND FOR FIGURE B25

1. LEVELING SCREW LOCK NUT
2. LEVELING SCREW ADJUSTMENT NUT
3. "V" GROOVED LEVELING BLOCK

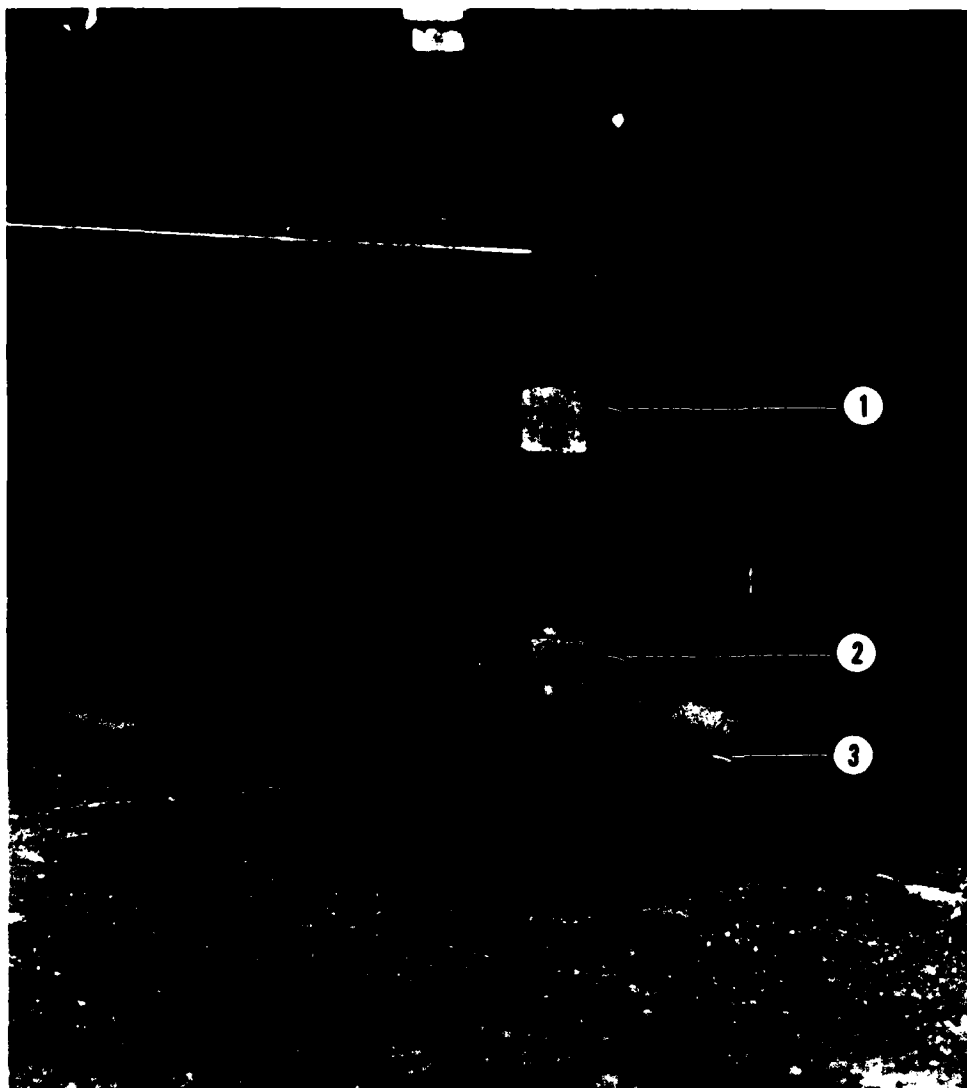
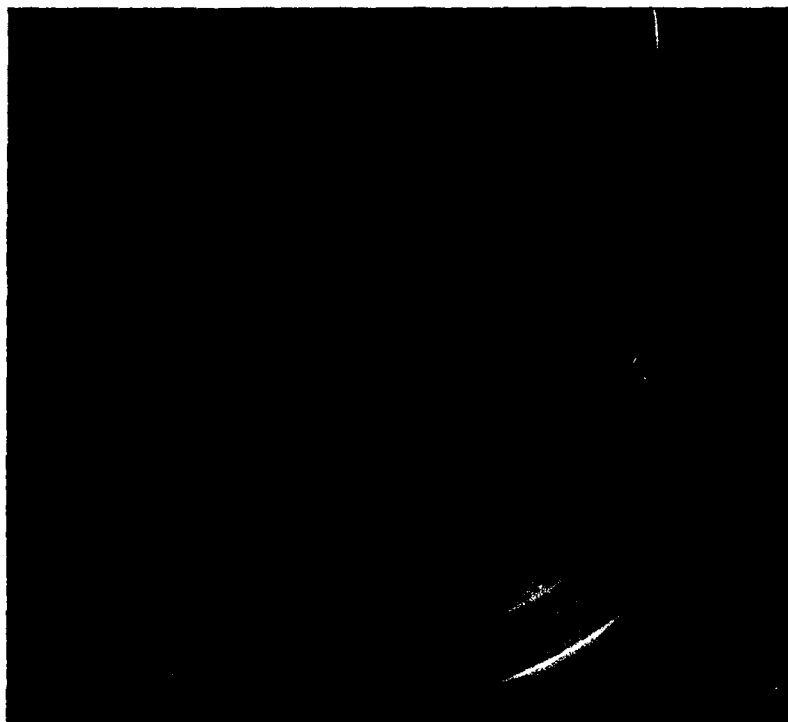


Figure B25. Optics-box Leveling Screw



**Figure B26. Reference Reflector in Mounting**

**LEGEND FOR FIGURE B27**

- 1. EYEPiece**
- 2. ADJUSTABLE BALL MOUNT**
- 3. MICROSCOPE HOUSING TUBE**
- 4. PELLICLE BEAMSPLITTER**



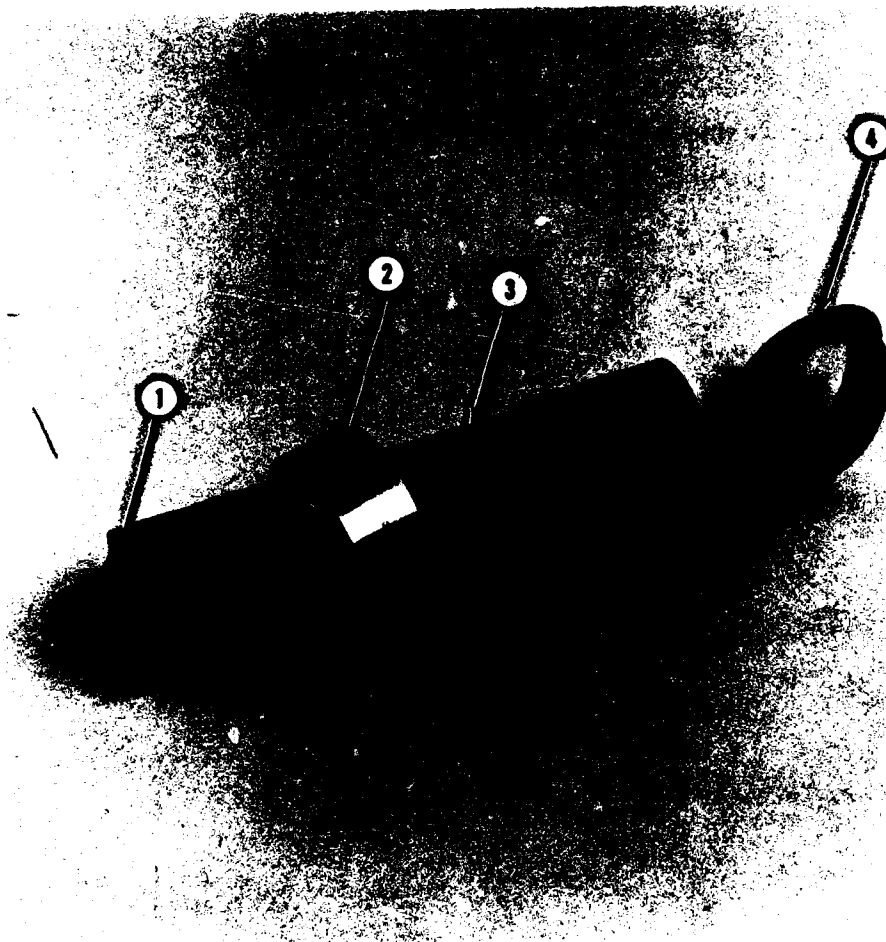


Figure B27. Alignment Microscope

**LEGEND FOR FIGURE B28**

- 1. CHAMBER LEVELS**
- 2. SOLENOID**
- 3. SOLENOID INTERNAL SLEEVE WITH SOFT IRON**
- 4. SOLENOID ELECTRICAL CONNECTORS**

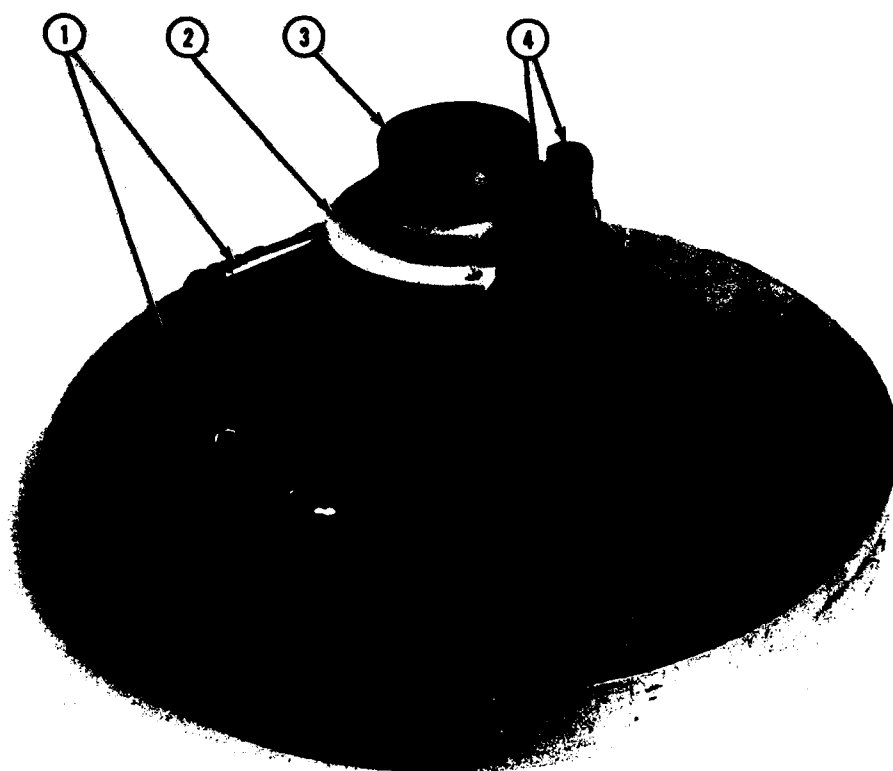


Figure B28. Vacuum Chamber Top Hat

LEGEND FOR FIGURE B29

1. SOLENOID INTERNAL SLEEVE
2. SOLENOID
3. VIEWING WINDOW IN TOP HAT

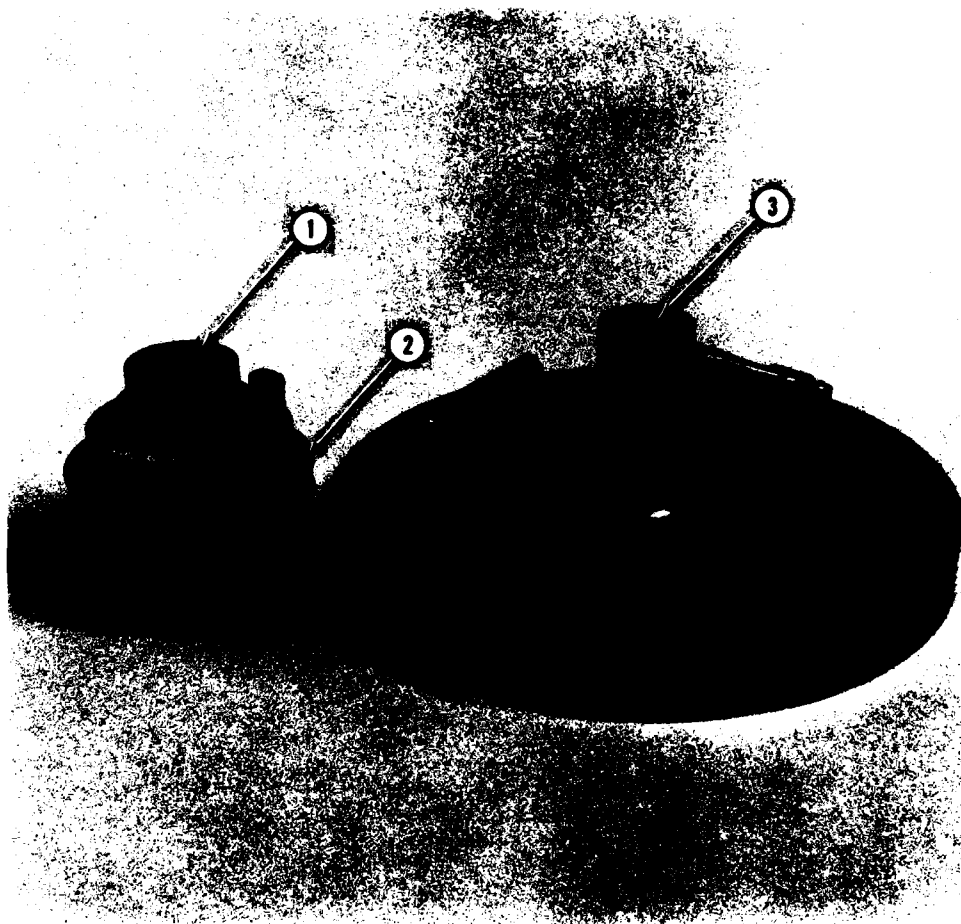


Figure B29. View of Vacuum Chamber Top Hat With Solenoid Removed

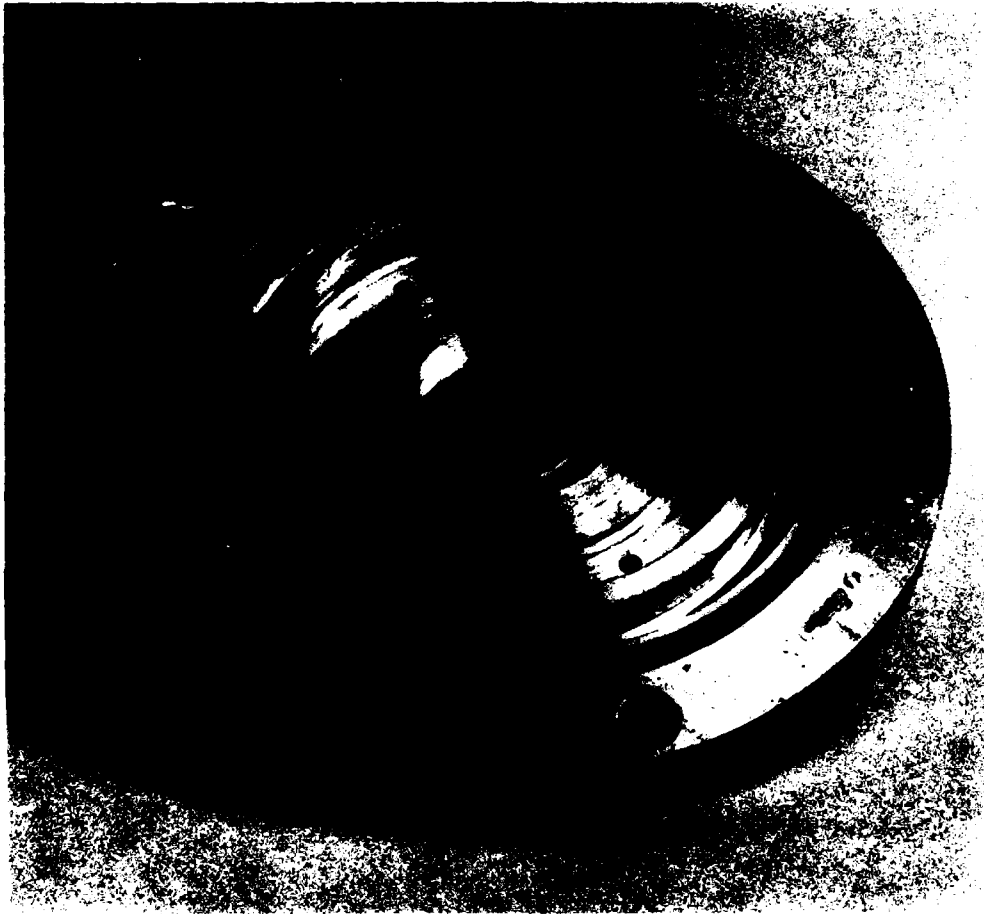


Figure B30. Bottom View of Top Hat



Figure B31. View of Vacuum Chamber Optical Entrance/Exit Window



Figure B32. Mercury Pool



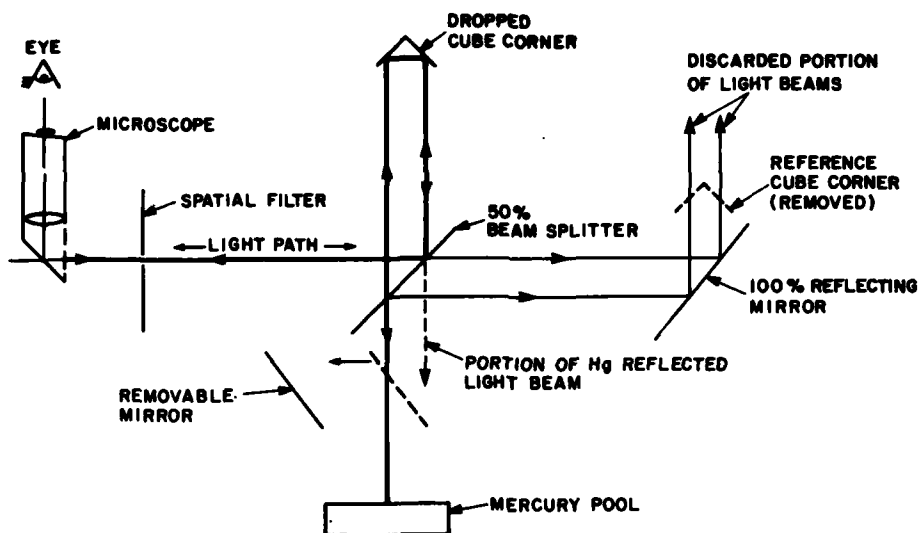
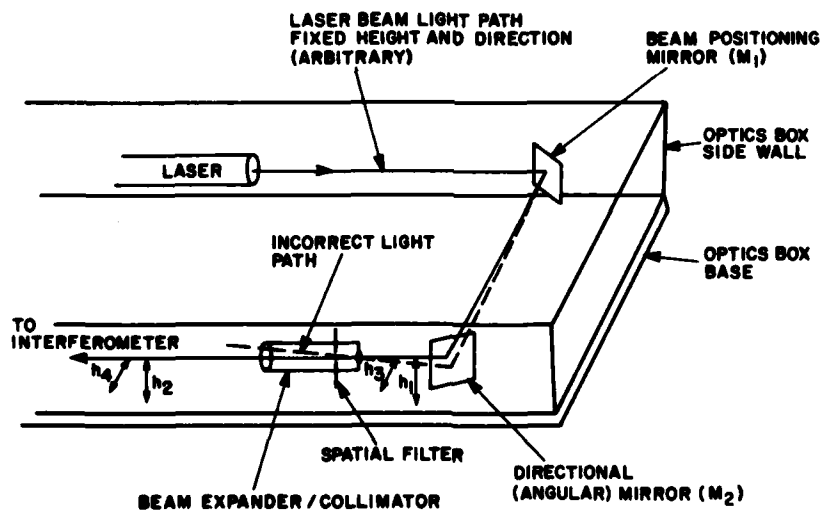


Figure B33. Simplified Diagram of the Light Path for Verticality



NOTE:  $h_1 = h_2$  AND  $h_3 = h_4$  BY ADJUSTING  $M_1$  AND  $M_2$

Figure B34. Simplified Diagram of Beam Position and Angle Adjusting Optics

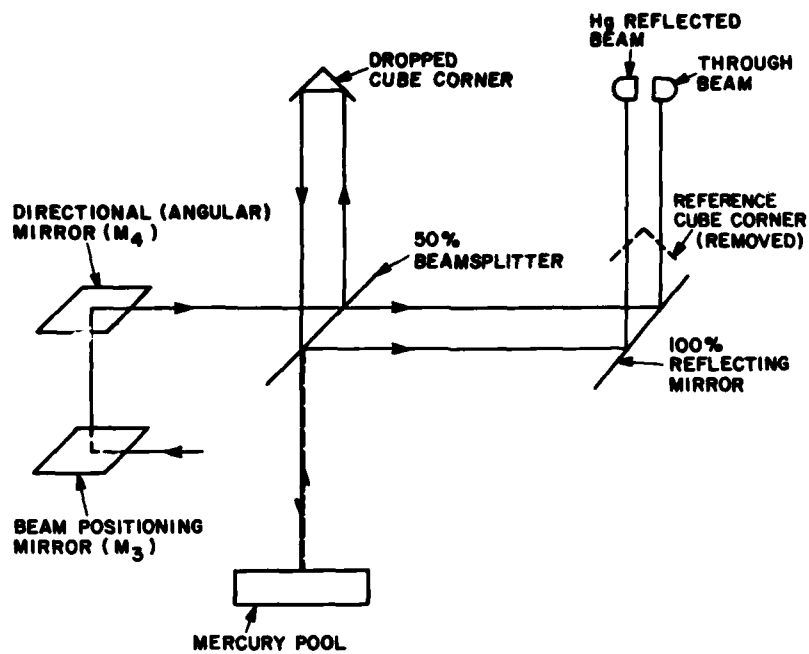


Figure B35. Simplified Diagram of Verticality and Beam Positioning

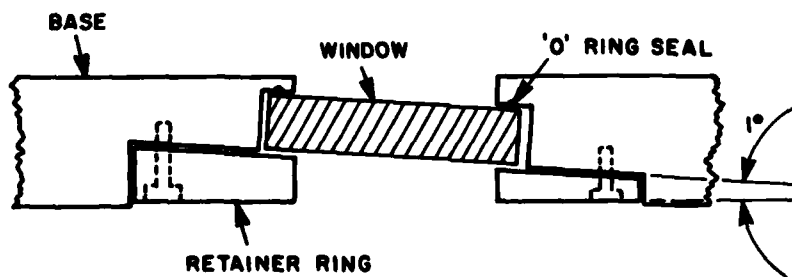


Figure B36. Diagram of Vacuum Chamber Window Tilt (Exaggerated)

**LEGEND FOR FIGURE B37**

- 1. HeNe LASER LIGHT SOURCE**
- 2. BEAM BROADENING LENS**
- 3. REFERENCE-CUBE CORNER REFLECTOR**
- 4. BEAMSPLITTER CUBE**
- 5. AXIS OF ROTATION**
- 6. DROPPED OBJECT PACKAGE**

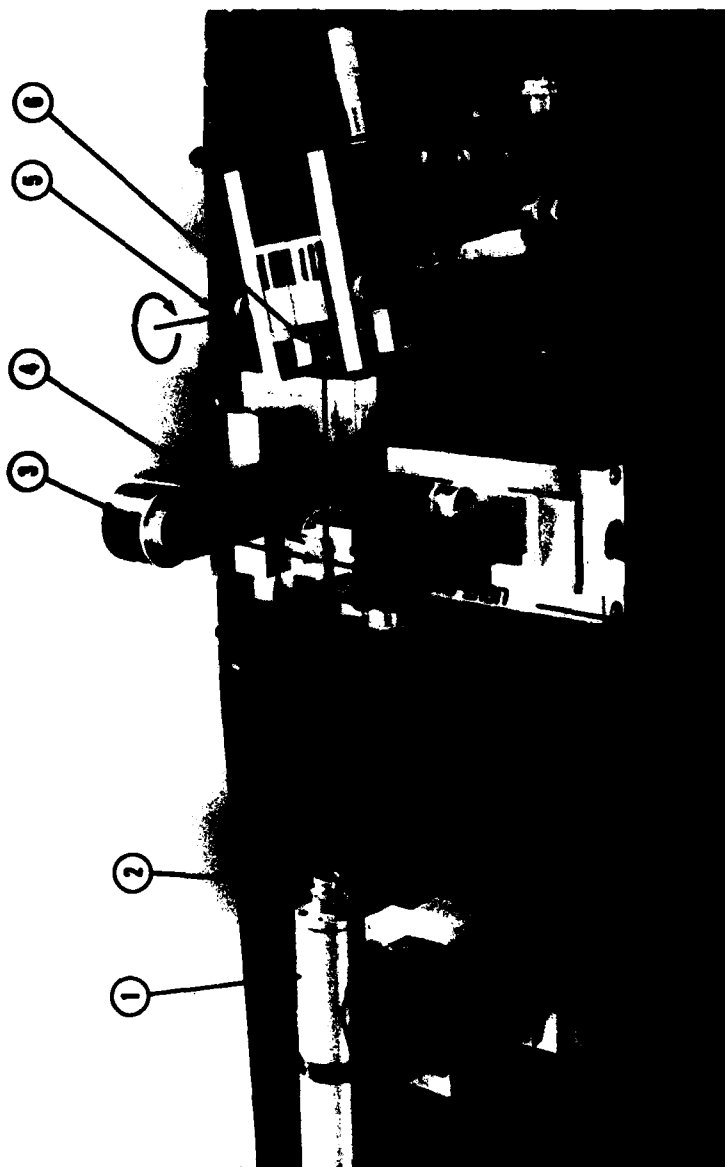


Figure B37. Center-of-mass Optical Center Alignment Set-up

## Appendix C

### Maintenance Procedures

#### C1. VAC-ION PUMP MAINTENANCE

Normally Vac-ION pumps are very dependable and require little or no maintenance. If the pump is opened to atmospheric pressure or a leak develops at a seal, it will be necessary to rough pump the ION pump before trying to start it. The procedures for doing this are:

- a. Connect TC#1 to its receptacle on the roughing pump valve as shown in Figure B23(2).
- b. Start the roughing pump and monitor the TC#1 meter until the needle falls below 10 mTorr.
- c. Turn START/PROTECT switch to START position, turn the ION pump power supply on, and partially close the roughing pump valve. (Allow ample time for the ION pump to outgas.)
- d. When the meter reading stabilizes, close the roughing pump valve completely off. (Leave the roughing pump running.)
- e. After 10 to 15 min of pumping on itself, the pump's analog meter should read on scale (move to the left). If this does not happen, feel the backside of the pump. If it is hot to the touch, apply a bag of ice or cool it with a circulating fan. (This reduces the pump temperature and improves pumping efficiency.) Open the roughing pump valve (slightly) allowing gases to flow to the roughing pump while the pump is cooling down.

- f. When the pump has had time to outgas (approximately 30 min), close the roughing pump valve again and monitor the analog meter as in step e.
- g. Once the meter reading is on scale, shut off and disconnect the roughing pump.
- h. Turn the START/PROTECT switch to PROTECT as soon as possible.

Note: Before trying to open the Vac-ION pump to the main chamber, make sure it is cool to the touch and the meter reading is at least  $2 \times 10^{-6}$  or below.

## C2. OPENING THE VACUUM CHAMBER

Caution: Since opening the chamber involves high risk of damage to the glass enclosure and mechanical parts and loss of time due to evacuating the system, the extra time required to insure that difficulties with the system do not exist outside the chamber can be well worth the effort and time involved. Also permanent damage to the ION gauge and ION pump may result if the procedure is not followed. Care must also be taken throughout the procedure to ensure that mechanical damage does not occur.

- a. Close ION pump gate valve [see Figure B1(11), B21(1) for location of the gate valve]. Note: This is a multiturn control and must be screwed completely in (in a clockwise direction).
- b. Turn the ION gauge switch off [see Figure B5(7e)]. As a precautionary measure, remove the cable from the ION gauge tube at the vacuum chamber [see Figure B23(5)].
- c. Remove dust, lint, and other foreign particles from the roughing pump (main chamber) valve orifice by blowing air into it (this can be done by mouth) to prevent foreign material from being sucked into the chamber.
- d. Remove the alignment laser [see Figure B24(1)] and the solenoid coil [see Figure B24(4)] from the top of the vacuum chamber and secure in a safe place.
- e. Remove the (long) bolts securing the top of the chamber (hat).
- f. Slowly open the main chamber vacuum valve to the atmosphere; a sudden inrush of air could cause mechanical damage.
- g. Carefully remove the hat; the hat must be removed by pulling straight up to prevent chipping of the glass tube.
- h. Remove the plastic safety tube surrounding the chamber glass tube.
- i. Caution: The dropped object and the robot must be at the bottom of the chamber before removing the glass tubing. Carefully remove (preferably with two people) the glass tube by lifting straight up, making every effort not to touch/scrape the tube on the metal parts of the inner chamber. The inside of the

chamber is now accessible and the extent of further system breakdown is dependent on the nature of the problem. The maintenance personnel must use their own judgment as to the necessity and extent of further breakdown and determine which of the following procedures is necessary, based on their assessment of required repairs.

### **C3. REMOVING THE INNER TOP**

- a. Remove the screw retaining the upper chain pulley [pointed out in Figure B10(2)].
- b. Loosen (removal is not necessary or even desirable) the three set screws located on the support/robot guideposts (one on each guidepost) as shown in Figure B12(2) and the three dropped-object guidepost set screws located inside the three V grooves (one at each V groove) as shown in Figure B13(6).
- c. Remove the top by pulling straight up. The guideposts are very precisely fitted and may require careful tapping (with a nonmetal mallet) around the periphery of the top. For reassembly, note the scribed numbers on top of the guideposts and matching numbers on the top plate [see Figure B10(1)].

### **CA. REMOVING THE CHAMBER OPTICS WINDOW**

- a. The chamber optics window is located at the base of the chamber (Figure B31) and is removed from the underside of the chamber.
- b. Removal of the window may become necessary if:
  - (1) The window is broken, cracked, or chipped.
  - (2) The window needs cleaning that cannot be accomplished while installed.
  - (3) A vacuum leak develops in the chamber and cannot be located elsewhere.
  - (4) The intensity of the laser beam diminishes and no other obvious obstruction is the cause, the optics window should be checked.

**Caution:** During removal and installation keep in mind that the window is slightly tilted (approximately  $1^\circ$ ) and if the retainer rings are not positioned correctly before tightening the screws, damage will result to the glass window (Figure B36).

### C5. CENTER-OF-MASS OPTICAL CENTER ALIGNMENT

The dropped object package [Figure B7(2)] is configured so that the center-of-mass can be adjusted to facilitate placing the optical center of the cube corner at the center of mass of the package. This coincidence is necessary as explained in the text. An interferometer is used to check this alignment and to adjust the center-of-mass to coincide with the optical center. The dropped object package is mounted [see Figure B37(6)] in an adjustable yoke and is pivoted about a horizontal axis [Figure B37(5)].

The simple Michelson interferometer is made up with the HeNe laser illuminator, Figure B37(1), with beam-broadening lens [Figure B37(2)] to give a broad (but bright) monochromatic illumination; the light is sent to the reference reflector [Figure B37(3)] and the dropped-object cube corner [Figure B37(6)] by the beamsplitter cube (Figure B37(4)). The dropped object package is positioned in the yoke such that the optical center is on the pivot axis. This is adjusted/checked until the circular fringes, as seen on the target screen, do not pulsate in and out or move up and down when the yoke is rocked  $\pm 10^\circ$  about the pivot axis. Rotation in excess of  $10^\circ$  will cause movement of the fringes (because of optical considerations) in excess of the rotation expected (or even accepted) for the free-falling reflector. When this is achieved, the mass distribution of the package is then adjusted for mechanical balance, completing the coincidence of the optical/mechanical center of rotation. Depending on the perseverance and care taken, this procedure results in the center-of-mass and optical center of the cube corner being well within 1 mm of each other.



## **Appendix D**

### **Commercial Equipment**

#### **Equipment Rack #1: (Figure B3)**

1. Oscilloscope  
Tectronix Model 7903  
with plug ins: 7A12 Dual Trace Amplifier  
7B70 Time Base  
7B92A Dual Time Base
2. Time Interval Counter  
Hewlett-Packard Model 5370A
3. Nim Bin Crate  
Ortec Model 401A with standard units:
  - a. Quad Discriminator  
EG&G Model T140/N with 1 spare
  - b. Pre-Scaler, Dual  $\div 10$   
Ortec Model 9310 (3 each)  
(1 section modified to divide by 4)

#### **Equipment Rack #2: (Figure B4)**

1. Robot Controller (unit Lab built with commercial Power Supply) -  
Power Supply - KEPCO  
Model JQE 0-75V-0-1.5A

2. Photomultiplier Power Supply  
Pacific Photometric Instruments  
Model 204; 0-2 KV
3. Rubidium Frequency Standard  
TRACOR Model 304A
4. Laser Power Supply  
Spectra Physics Model 259B Exciter

**Equipment Rack #3: (Figure B5)**

1. Top space is storage for shipping of the Hewlett-Packard  
Model 9825 Terminal
2. Vacuum IONIZATION Gauge Power Supply and Control Unit  
Varian Model 845
3. Vac ION Pump Power Supply and Control Unit  
Varian Model 921-0062

**Also shown in Figure B5, but not in the rack:**

1. Printer, Hewlett-Packard Model 9876A, which is used in conjunction  
with the H/P 9825 computer (see 1., Equipment Rack #3).
2. Digital Multimeter  
Hewlett-Packard Model 3438A

The following commercial equipment are not in racks and can be identified with the aid of Figure B1 and (legend number).

1. Figure B1(1, 6), HeNe Laser and Power Supply Hughes Model 3225H-PC  
and 3599-H
2. Figure B1(15), Roughing Vacuum Pump  
Sargent-Welch/Direct Torr Model 6610
3. Figure B1(17), ION Pump  
Varian Model 911-5032

Typical Shipping List

<u>FSN</u>	<u>Noun</u>	<u>Box No.</u>	<u>Model</u>	<u>S/N</u>	<u>Doc No.</u>	<u>Price (\$)</u>	<u>Qty (ea)</u>
4310P8816-B	Vacuum pump	6	Varian	N/A	1153	827.18	1
5180P0538602835	Tool kit	6	Jensen	N/A	1121	221.40	1
5821P0544102835	Prescaler	1	EG&G 9310	N/A	1145	441.50	4
5860L0411932835	Laser inter-ferometer	2,5,7,&8	System	N/A	0949	30,000.00	1
5860P3225-HPC	Laser Helium/neon	10	Hughes	1827	1151	603.90	1
5860P Model 119	Laser	10	119	3592461	1078	6,255.00	1
5885P5391A	Freq hline acq. system	1-10	5391A	N/A	1163	17,685.00	1
6130P204-2KV	Power supply	2	204	410	1120	428.97	1
6130L0347612835	Power supply	10	H/P 620	N/A	0563	197.31	1
6625003215176	Counter	10	5306A	N/A	1187	627.80	1
6625004780595	Plug in	1	7A12	B115971	0948	1,396.00	1
6625010079171	Recorder	4	H/P 7132A	02600	1160	2,681.52	1
6625P260-4P	Voltmeter	10	260	7632	0555	72.43	1
6625010186361	Counter	10	Opt 001 TCX0	1824A08661	1137	485.40	1
6625010270265	Plug in	1	7B92A	B088094	1139	1,490.00	1
6625010405758	Counter	10	5305B	1652A01318	1136	980.63	1
6645010215491	Clock	3	59309A	538115	1174	1,042.00	1
6645PHP5370A	Counter	1	5370A	1936A00591	1170	6,500.00	1
7025P9876A	Printer	4	9876A	1834A01324	1173	3,500.00	1
6625P3438A	Multimeter	10	3438A	1717A02812	1181	888.08	1
6625P Model 7903	Oscilloscope	1	7903	B181158	1180	6,000.00	1
7420001768947	Calculator	3	9825A	1622A11766	1057	6,930.00	1

**Appendix E**  
**Typical Shipping List**

# Supplies

<u>Noun</u>	<u>Model</u>	<u>Box No.</u>
Mechanical controller	Lab-built	2
Electrical wire	Various assortment	6
Electrical components	Resistors, capacitors, etc.	10
Mechanical super spring plus controller	Lab-built	9 4
Optical supplies	Lenses, mirrors, etc.	10
Cables	Power, HP-IB, etc.	5
Manuals	TO's, operating, etc.	5
Test and repair items	Soldering iron, etc.	10

**END**

**FILMED**

**1-85**

**DTIC**